Master Thesis
submitted within the UNIGIS MSc programme
Interfaculty Department of Geoinformatics - Z_GIS
University of Salzburg

Analysing Vienna’s Underground

by

Mag. phil. Mag. phil. Kira Lappé
104896, UNIGIS MSc 2017

A thesis submitted in partial fulfilment of the requirements of the degree of
Master of Science (Geographical Information Science & Systems) – MSc (GIS)

Advisor:

Dr. Robert Marschallinger

Vienna, 28.02.2020

matri carissimae

ve beni en çok destekleğen eşim için – en iyi arkadaşımsın

Acknowledgements

The development of a scientific work, from the idea to the completion, is a long and tedious process in which many people participate. I would like to take this opportunity to thank them.

First and foremost, I would like to thank my mother for her support during the whole period of my studies and especially during the time of writing my thesis. Like all my academic work, this one is dedicated to her with all my heart.

Beneficial to any scientific work is a fascinating subject to which one can and wants to devote longer periods of time. I would like to thank Michael Wagreich and Katrin Hornek for the idea and submission of the project "The Anthropocene Surge", in which this thesis is embedded, and especially Michael Wagreich for the confidence in my skills. I am very pleased to be able to continue working on this topic in my future scientific work.

I would like to thank the cooperation partners of our project, especially Christine Jawecki (MA 29) and Martin Mosser (Stadtarchäologie Wien) for the generous provision of data and for their time and availability whenever I had questions or needed information.

Furthermore, I am thankful to the whole UNIGIS team for their support during the whole study, for always answering any question quickly, but especially for putting me in touch with my supervisor Robert Marschallinger, who took away my fear of geostatistics with his friendly and helpful manner and who was available almost any time during the time of writing and took a lot of time for my questions. Without him this thesis could not have been done in this form.

I would like to thank my legendary Viennese GIS regulars' table (Clotar, Harald, Klaus, Roman and Thomas) for the cosy get-together, friendly exchange and GIS-related discussions across all disciplines. Hopefully our tradition will continue beyond the end of our UNIGIS studies.

I am grateful to the Vienna Employment Promotion Fund (WAFF) for its generous support, which made it easier for me to take up this study.

Finally, I thank my partner from the bottom of my heart for his selfless support during numerous late and weekend shifts during my studies, his enthusiasm for my work and his tireless willingness to discuss the Viennese underground.

Science Pledge

By my signature below, I certify that my thesis is entirely the result of my own work. I have cited all sources I have used in my thesis and I have always indicated their origin.

Signiert von:	Kira Lappe
Datum:	28.02.2020 18:43

www.handy-signatur.at

Dieses mit einer qualifizierten elektronischen Signatur versehene Dokument hat gemäß Art. 25 Abs. 2 der Verordnung (EU) Nr. 910/2014 vom 23. Juli 2014 ("eIDas-VO") die gleiche Rechtswirkung wie ein handschriftlich unterschriebenes Dokument.

Dieses Dokument ist digital signiert!

Prüfinformation:
Informationen zur Prüfung der elektronischen Signatur finden Sie unter:
www.handy-signatur.at

TRUST einfach sicher

Vienna, 28.02.2020 Kira Lappé

Place, Date Signature

Abstract

Anthropogenic, i.e. human-made sediments as results of the human impact on the Earth's surface are globally widespread and can be detected almost everywhere – yet, in urban environments, these deposits of anthropogenic origin are especially massive. In Vienna, a city with more than 2,000 years of history, almost 10,000 well core drillings and 70 excavation sites help to throw light on the underground of the city centre. Aim is the creation of an interpolation of the Boundary A, the boundary between the "natural ground", untouched by humans, and the anthropogenic deposits. This interpolation is used to produce figures on the current thickness as well as volume of the anthropogenic sediments. By this, the human impact on the underground of a modern, but long-lived city can be visualised and quantified.

A study area of 12.25 m^2, covering the Inner City and parts of the neighbouring districts, is selected because of its high density of data available and historical importance, being the centre of settlement from Prehistory to Modern times. Statistical analysis of well core logs and archaeological data makes figures on the thickness of anthropogenic sediments in the study area available for the first time. Using Universal Kriging, an interpolation of the lower boundary of anthropogenic sediments is achieved, allowing to map the thickness of artificially modified ground (AMG) and to calculate the volume of anthropogenic deposits (~ 46.5 million m^3). The distribution of AMG in the study area is directly reflecting historical and natural reasons relevant to the study area. Comparison with the results of a study conducted on two districts of London shows similar, but somewhat higher accumulations of anthropogenic deposits in Vienna.

Table of Contents

List of figures

List of tables

1. Introduction

Living in a city, one comes across the human impact on Earth practically on every street corner. Skyscrapers, bridges, streets and building complexes – almost every centimetre of urban areas has been transformed and built over. Even parks and green areas are no exceptions, with asphalted pavements and cemented benches. This has become normal to us and it does not attract our attention anymore. Yet, hardly anyone realises that the same applies to the underground. Two to three cellar levels, underground parking garages and the underground railway are everyday spaces of use through which humans have begun to conquer the subsurface of the cities.

Yet, these are not recent developments. Since the sedentism of humans and the building of permanent structures, humans have left an imprint on Earth and its sediments. By digging ditches for foundations, by levelling the terrain for construction works, by demolishing a building and erecting a new one on top – all of these actions result in what is called in this study "anthropogenic sediments" or "artificially modified ground" (AMG), i.e. sediments that have been transformed, removed or deposited by human activity. To investigate the anthropogenic sediments underneath the city of Vienna, accumulated over 2,000 years of history, is in the focus of this study.

This study is embedded in an interdisciplinary research project based at the University of Vienna and the University of Applied Art Vienna and funded by the Vienna Science and Technology Fund ("The Anthropocene Surge", WWTF ESR17-040). In the focus of this project is the investigation of Vienna's subsurface from a geological-stratigraphic, geochemical, archaeological, geoinformatics and artistic perspective, including a look at the Anthropocene, estimating human's influence on the city's (under)ground. This study shall represent a pilot study to this project, by testing methods for the project restricted to a smaller study area in the centre of the city.

2. Archaeosphere and Boundary A

In the focus of this study are sediments that are referred to as "artificial ground" in the field of Geology. These deposits, which are, by definition, products of human action, have been included in geological maps as standard since the 1990s (Edgeworth 2014), although a few considerably earlier examples of recognising anthropogenic sediments exist (e.g. Suess 1862; Suess 1897). In the Lexicon of Named Rock Units of the British Geological Survey, five main categories of artificial ground are listed: worked ground, made ground, infilled ground, landscaped ground and disturbed ground (Ford et al. 2010; Ford et al. 2014; cf. also Terrington et al. 2018; Edgeworth 2014; Edgeworth et al. 2015) (cf. fig. 1).

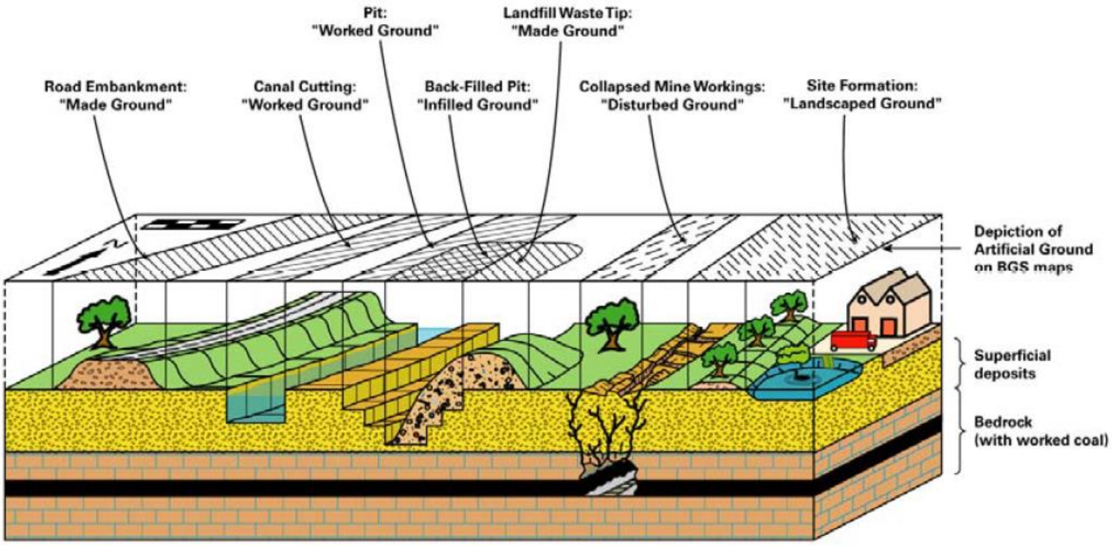

Figure 1: Examples of the main types of artificial ground (Source: Ford et al. 2010)

In the field of archaeology, deposits declared as "artificial ground" by a geologist are referred to as "archaeological stratigraphy" (Edgeworth 2014). This stratigraphy is recorded using tools as the Harris matrix, which documents the sequence in which the archaeological layers have been formed, the so-called stratigraphic sequence, and produces a stratigraphical relation between the individual layers (Harris 1989; Edgeworth 2014).

Differences between those two scientific fields exist on which part of the anthropogenic layers is focused on. In archaeology, layers of the last 200 years are often neglected, declassified as "modern disturbances", whereas for geologists, these more recent deposits are often of greater importance and interest concerning the suitability of land for developments. As another difference, layers are dated and correlated in geology by "type-fossils", whereas in archaeology human artefacts as pottery etc. are used (Edgeworth 2014).

In this study, the archaeological as well as the geological point of view are taken and so datasets from both disciplines are combined. Edgeworth (2014), an archaeologist working since many years in the geological field, has coined the term "archaeosphere" for the combination of geological "artificial ground" and archaeological stratigraphy. Structures as building foundations, cellars, pipelines, underground railways, underground car garages and other infrastructural and architectural elements which occupy space in the ground are included as part of the archaeosphere (Edgeworth et al. 2015).

Moreover, Edgeworth (2014) has defined the term "Boundary A", referring to the "base of archaeological stratigraphy", for the boundary between "natural", i.e. undisturbed geological ground and the “occupational debris”, i.e. archaeological deposits or archaeosphere, marking the earliest surviving trace of human activity on the landscape at any given location (cf. Edgeworth et al. 2015).[1] However, this only holds true if earlier layers are not removed by later human actions, by which the new Boundary A would be of later date. This already shows that the Boundary A is diachronous, i.e. of different date at different locations, even on the same site (Edgeworth 2014). Already Edward Harris has highlighted this horizon between natural and archaeological layers, seeing it as “revolution in stratigraphical processes” when cultural forces represented by humankind were coming into effect for the first time (Harris 1989; Edgeworth 2014).

Regarding the other, i.e. the upper boundary of the archaeosphere, Edgeworth (2014) points out that this stratum of the archaeosphere is “still in the process of formation” and can be transformed, covered or even removed by later activities.

3. Aim and objectives

> *“With regard to its manifestation on terrestrial surfaces of the Earth, the archaeosphere can be conceptualized as a kind of giant carpet covering large areas, on which the furniture of the human world (its buildings, bridges, monuments, pylons, oil-rigs, telegraph poles, roads, railway viaducts, cities, shanty towns, parks, airports) stands and is supported, and into which it will eventually crumble. Deep-layered in places, threadbare and patchy in others, this carpet of near-global extent provides the surface on which people carry out their lives. Like a carpet, it is so well-used it is taken almost totally for granted […].” (Edgeworth 2014)*

Edgeworth (2014) has claimed one characteristic of the archaeosphere that it first existed as small individual and patchy areas, growing in extent, frequency and thickness over time and due to the increasing human population. Aim of this study is to analyse this “carpet” in the heart of Vienna, which are the anthropogenic sediments accumulated underneath the study area during its more than 2,000 years of history. As output, an interpolation of the boundary between

[1] This boundary is known by Japanese geologists as the “Jinji unconformity” or “discontinuity”, from “Jin” for “human being” and “Ji” for “natural” (Nirei et al. 2012). – This lower boundary is generally referred to by archaeologists and often marks the end and downward extent of an excavation. Field archaeologists refer to it informally as “the surface of the natural” (cf. Edgeworth et al. 2015) – in German: “bis zur Geologie”.

the “natural ground”, untouched by humans, and the anthropogenic deposits, of the so-called Boundary A, is sought to create. This interpolation is used to calculate the current thickness of AMG (artificially made ground) as well as the actual volume of the anthropogenic sediments. Objective is to develop a workflow for a small study area that can later be extended to the whole city area and might be applied to other cities as well, allowing comparison between urban areas with different histories and even on different continents.

This study combines different data sets available for this task, which are well core logs as well as data from archaeological excavations. The data mainly used are provided by the cooperation partners of the project mentioned above, which are the Municipal Department for Bridge Construction and Foundation Engineering (MA 29 Brückenbau und Grundbau, Stadt Wien), and the Department of Urban Archaeology (Stadtarchäologie Wien, Wien Museum). The results of this study will hopefully be of value also for the data providers: Through the careful analysis of the data, errors in the well core data set can be detected and reported back to the MA 29 in order to correct the data and, by this, enhance the quality of the well core database. For the Department of Urban Archaeology, the gridding result of Boundary A is of interest. This interpolation could help the archaeologists to estimate the expected workload for an excavation site in advance and thus can improve their position in negotiations on the duration of an excavation with developers of planned construction projects.

Two general considerations regarding the limits of this study should be mentioned: well cores are usually drilled before construction measures, aiming at examining the ground concerning civil engineering reasons. This means that although the information on anthropogenic soils that I am working with in this study derives from these well cores, more has changed and probably more anthropogenic soils have been accumulated by the building activities following the drilling. As examples can be given the foundations and cellars of a newly erected building complex or the installation of an underground railway. Even the ground level at the drilling site has probably changed by the subsequent development.[2]

Another thought worth mentioning is that, unlike geological or stratigraphical processes, human interaction with the ground is not following predictable rules but is rather chaotic. If a Roman was building his house at a specific place or 3 m to the left or right is by chance, and so is if the well core drilling touches these archaeological layers or not.

Considering this, a scientifically exact interpolation is neither possible nor in the scope of this study. More, the focus is on getting an approximation of the human imprint on the ground in a

[2] Cf. on this thought also Terrington et al. 2018.

modern, but long-lived city. And to get, by this, a glimpse at a reality that is usually hidden from our eyes, under the subsurface of Vienna.

4. State of research

Using geostatistical methods to interpolate layer boundaries from well cores are common practice in geological studies. Considerably fewer studies have dealt with the human impact on the ground and anthropogenic sediments in urban areas.[3]

In previous projects, the use of well cores has in some cases proved problematic, as these are often irregularly distributed and too small in number to produce a model of high accuracy (Chesnaux et al. 2017; Luberti 2018). The methods used for interpolation range in these studies from TIN (Chesnaux et al. 2017; Balasubramani and Dodagoudar 2018) to Inverse Distance Weighting (IDW) (Chesnaux et al. 2017; Balasubramani and Dodagoudar 2018; Rufo et al, 2017) and Spline Interpolation (Rufo et al., 2017) up to Ordinary Kriging (Chesnaux et al., 2017; Balasubramani and Dodagoudar, 2018; Rufo et al., 2017).

A different approach to estimate the thickness of AMG was used by Luberti (2018), who was investigating the modern anthropogenic-deposit thickness of the North-Eastern part of Rome. Using historic maps from the 19th and 20th century, he interpolated digital terrain models (DTM) and calculated the change-in-elevation, in topographic rise and lowering.

The present study will use a similar approach as has been applied in a recent investigation focusing on two boroughs of the modern city centre of London, City of London and Tower Hamlets (Terrington et al. 2018). The aim of this study was to quantify thickness, volume, mass and accretion of artificial (anthropogenic) deposits and additional volume and mass of buildings in these two districts. This study relies mainly on well core records obtained from the British Geological Survey (BGS) borehole geology database. From the well core records held in the database, 49% and 45%, respectively, of the two districts' well cores have artificially modified ground (AMG) described. In total, 1,738 and 6,353 boreholes, respectively, have been drilled in the City of London and Tower Hamlets (total: 8,091). The AMG thickness obtained from the borehole records is interpolated using kriging. No continuous surface has been produced, yet the elevation information has been connected to the European Urban Atlas areas. By this, thickness and volume could be directly compared to various parameters, as land use, building heights, age of buildings etc. By including anthropogenic materials mentioned in the

[3] This topic has only moved to the centre of interest in recent years, which can be seen from the increasing numbers of publications: e.g. Chesnaux et al. 2017; Rufo et al. 2017; Luberti 2018, Balasubramani and Dodagoudar 2018; Terrington et al. 2018 etc.

descriptions of the borehole records, pre- and post-World War II layers were distinguished, calculating the distinct volumes and accretion rates. The mass of AMG was estimated by multiplying the total volume by 1.5 t per m³, which is the approximate density of sand and gravel, crushed rock or soil (Terrington et al. 2018, cf. Edgeworth et al. 2015). As stated by Terrington et al. (2018), an implementation of the elevation data of archaeological finds would have been a significant attribution to the study. In the present study, information on the anthropogenic sediments by archaeological excavations will be implemented.

Studies on anthropogenic sediments in urban environments are often limited by the data sets available. The insufficient input data in a specific study area is one of the reasons why this kind of research is relatively rarely undertaken – the interpolation process is affected by the missing availability of well core data and might result in imprecise outputs. For the London study, only a total of 8,091 well cores were used, not even half of them included anthropogenic sediments in the documentation of the well core logs.

Additionally, a striking fact is that archaeological data is used in some cases for the overall interpretation of results (e.g. Terrington et al. 2018), but the digitised excavation data, that is the digitised outlines of the single archaeological layers, are not implemented in the study itself.

5. Materials and methods

This study uses remote techniques including well core logs, digital excavation data and a modern digital terrain model (DTM) to obtain the ground level elevation values to assess the human impact on the ground underneath a modern city with a long history of urban development. As this study serves as a pilot study, the methodology shall be tested in a study area, that first has to be determined.

The workflow applied in this study is displayed in Figure 2. For estimating the thickness of anthropogenic sediments in Vienna, the boundaries of the artificially modified ground (AMG) have to be determined. The lower boundary, i.e. the so-called Boundary A of Edgeworth (2014), is the transition from artificial to natural layers. As upper boundary, the modern surface retrieved by a DTM is used. Regarding the data, different classes are applied to differentiate between certain and probable information. The information on Boundary A by the well cores is complemented by archaeological data. The obtained data points showing the thickness at specific locations are then analysed by an Explorative Spatial Data Analysis (ESDA) and thereafter interpolated to receive a map of Boundary A of the study area. This grid is an important outcome helpful e.g. for the Department of Urban Archaeology, as it can be used to estimate the duration of archaeological excavations at specific locations. To obtain a reliable result, two different variograms are produced, considering the anisotropy of the data set, and the gridded outcomes using kriging are compared. The outcome is validated by different values of the cross validation. The map displaying Boundary A is used to calculate the negative and positive volume of the anthropogenic sediments underneath the study area. By subtracting the interpolated map of Boundary A from the modern DTM, a map of the thickness of AMG is received, which can be analysed against the background of the historical development of the city. Finally, the results are compared to the outcomes of the London study, contrasting two modern cities with more than 2,000 years of urban development.

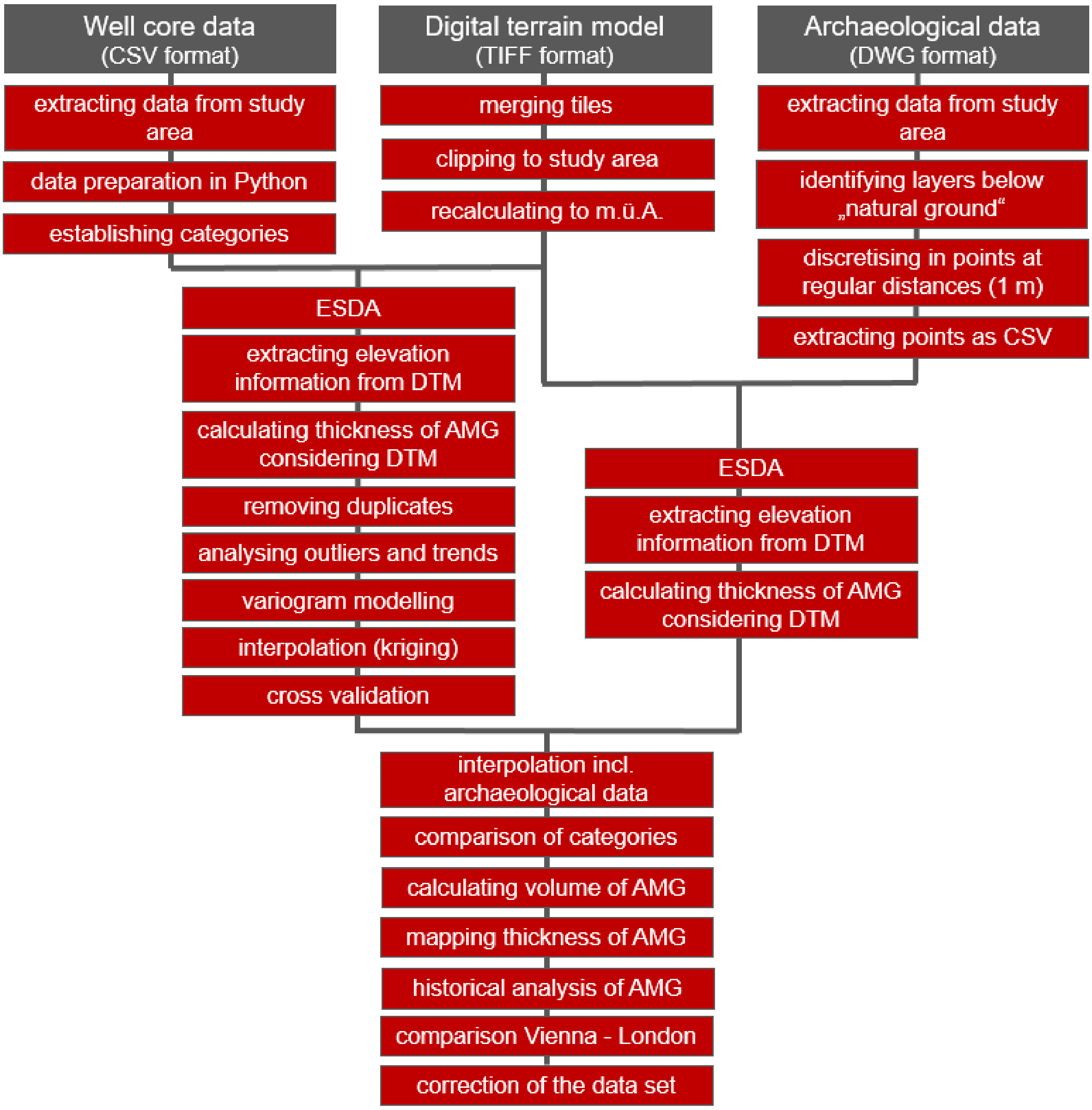

Figure 2: Workflow applied in this study

5.1 Software

The whole data preparation processing is carried out in Python, a programming language created and first released in 1991. In 2008, Python 3.0 was released, which is the version used in this study. Python is complemented by different modules that have been contributed by the community of Python developers, which count at the moment more than 218,000 modules.[4] The module used most in this study is pandas, an open source library for data manipulation and analysis, particularly offering operations for manipulating numerical tables (McKinney et al. 2020).

For visualisation purposes and mapping the data, the proprietary GIS software ArcGIS Pro by ESRI was used. The descriptive statistics and the ESDA were done with ArcGIS Pro and R, which is a free software environment for statistical computing. The geostatistical tasks were performed in the proprietary software Surfer v. 17.1.288, a surface and contour mapping program by Golden Software LLC.

5.2 Study area

In the present thesis, the workflow and methods shall be tested in small area before being transferred to the whole city area in future research. Therefore, a study area in the centre of the city of Vienna was chosen, covering an area of 12,25 km², 3.5 x 3.5 km and enclosing the first district of Vienna and parts of its surrounding districts (fig. 3). This area was chosen because of the data availability – being the historic city centre covering more than 2,000 years of history and therefore providing the highest density of excavation and well core data of the city area.

The coordinates for the study area are the following:

Table 1: Bounding box of the study area

Ymin	339 300 m
Ymax	342 800 m
Xmin	1 100 m
Xmax	4 600 m

[4] 220,158 moduls in the Python Package Index (PyPI) on the 28th of February 2020 with an addition of 157 new modules per day, cf. http://www.modulecounts.com/# (accessed February 28, 2020).

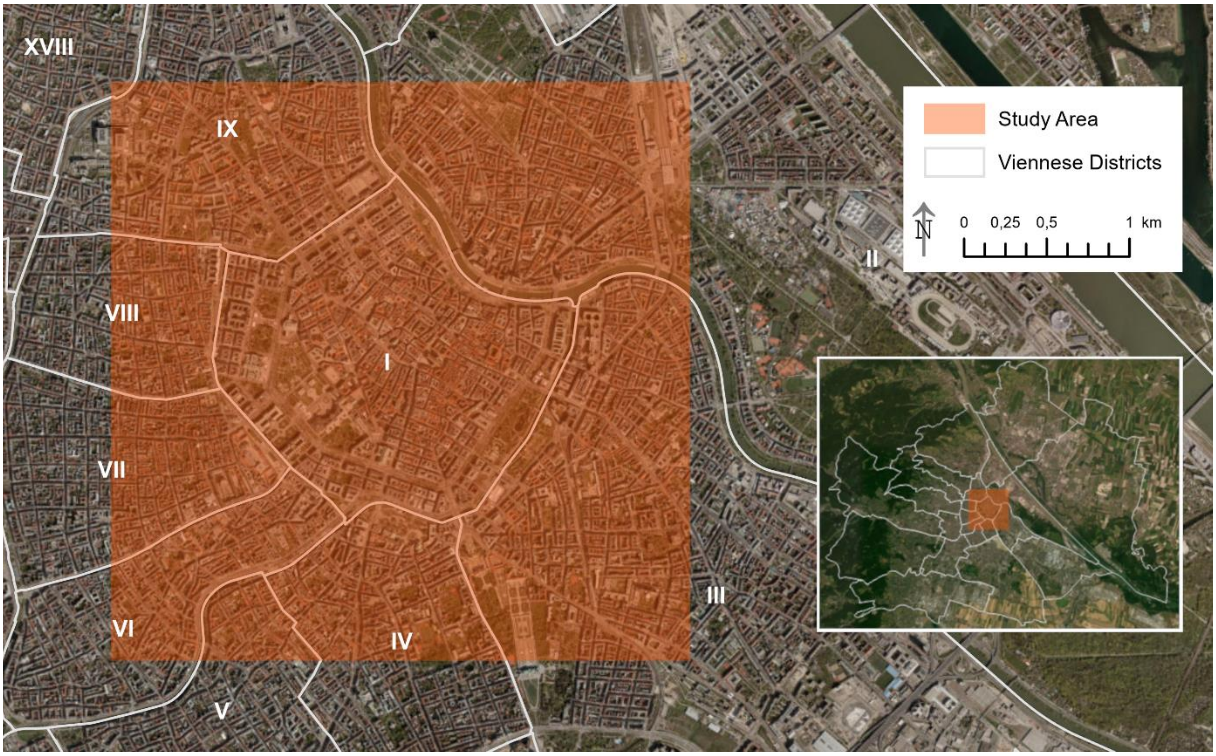

Figure 3: Study area

5.3 Data

The available datasets for this study cover mainly well core data, provided by the Municipal Department for Bridge Construction and Foundation Engineering (MA 29 Brückenbau und Grundbau, Stadt Wien), and data from archaeological excavations, provided by the Department of Urban Archaeology (Stadtarchäologie Wien, Wien Museum). Besides this, the digital terrain model (DTM) used stem from the Municipal Department for Surveying and Mapping (MA 41 Stadtvermessung Wien, Stadt Wien).

All data use the projected coordinate system MGI Austria GK East / Mag Wien (Spatial Reference: 31256), which will further be used for this study.

Heights are provided in "Metres above the Adriatic" ("*m.ü.A.*"), which uses the gauging station in the Port of Trieste that was established in the year 1875 ("*Pegel Triest 1875*"). Some data (as the data provided by the Municipal Department for Surveying and Mapping and most of the excavation data) is using the "*Wiener Null*", which is the datum level for urban surveys in the city area of Vienna.[5] This specific height reference system has been defined at the end of the 19th century by the mean tide water of the Danube Canal gauge at the Schwedenbrücke. The

[5] https://www.wien.gv.at/stadtentwicklung/stadtvermessung/geodaten/festpunkt.html (accessed February 28, 2020).

Wiener Null is referring to a gauge value of 4 m above the gauge zero of 152.68 metres above the Adriatic (*m.ü.A.*). Therefore, the *Wiener Null* corresponds to 156.68 m.ü.A.

5.3.1 Well core data

The well core data are extracted from the well core database of the City of Vienna, the so-called "*Wiener Baugrundkataster*". This database includes more than 63,000 well cores[6], which are not only from the city area, but are sporadically stemming also from different construction works in other states of Austria.[7] Most of the well cores were drilled for building projects of the City of Vienna, so covering public works as public buildings and infrastructure. Yet, as a smaller portion, well cores on account of private developers are included in the database, too.[8]

The well core data cover a time span of more than 170 years, starting with the first well core in 1844 until today. After the drilling, the well cores are described by the drilling foreman and documented in the so-called well logs (fig. 4). The well logs are entered in the database "*Wiener Baugrundkataster*", which is in the responsibility of the Municipal Department for Bridge Construction and Foundation Engineering (MA 29 Brückenbau und Grundbau, Stadt Wien).

Of interest for this study is the impact of human activity on the ground. Anthropogenic sediments are highlighted in red in the Viennese well logs (cf. fig. 4) and depicted by the letter "A", which stands for "*Anschüttung*", i.e. the anthropogenically modified ground.[9] Besides "A", two other types are used for anthropogenic impact in the layer descriptions relevant for this study, which are "A?" and "Bw" (cf. fig. 5). "A?" stands for "probable anthropogenic modified ground", which means that no artefacts or ingredients (as tiles, charcoal etc.) gave a clear indication to the drilling foreman that this layer does not stem from natural processes. However, by their experience, these sediments seem to differ from natural sediments, and therefore they were classified as "A?".[10] Yet, it depends on the person in charge, when and how often layers are classified as "A?".[11] So, sediments documented as "A?" do not only appear as the lowest layers of the *Anschüttung*, as borders to the natural sediments, but sometimes "A?"

---

[6] 63,436 as at the 22nd of August 2019.
[7] As the Vienna Mountain Spring Pipeline or highway and railway constructions (personal comment by Christine Jawecki, MA 29, on 31st of January 2020).
[8] Well core drillings done by private developers might be a maximum 20 % of total (personal comment by Christine Jawecki, MA 29, on 31st of January 2020).
[9] On the terms „anthropogenically modified ground" etc. see Ford et al. 2014, cf. Terrington et al. 2018, Edgeworth et al. 2015.
[10] The reason for this can be visual differences, differences during the drilling process (e.g. harder to drill), does not fit the stratigraphy, hints by the terrain or the building history etc. (personal comment by Christine Jawecki, MA 29, on 31st of January 2020).
[11] These varieties can be explained by the fact that there is no official definition of "A?" (personal comment by Christine Jawecki, MA 29, on 31st of January 2020).

layers are documented as the uppermost layers or in the middle between two or more layers of *Anschüttung*. For this study, only the classification of the lowest layers as "A?" are respected, as these make a difference for the depth and thickness of anthropogenic ground at this position. The third type is "Bw", which stands for "*Bauwerk*", which is German for structure or construction. This label is used for (intact) structures hit by the drilling, which are cellars, wells or masonry in general.

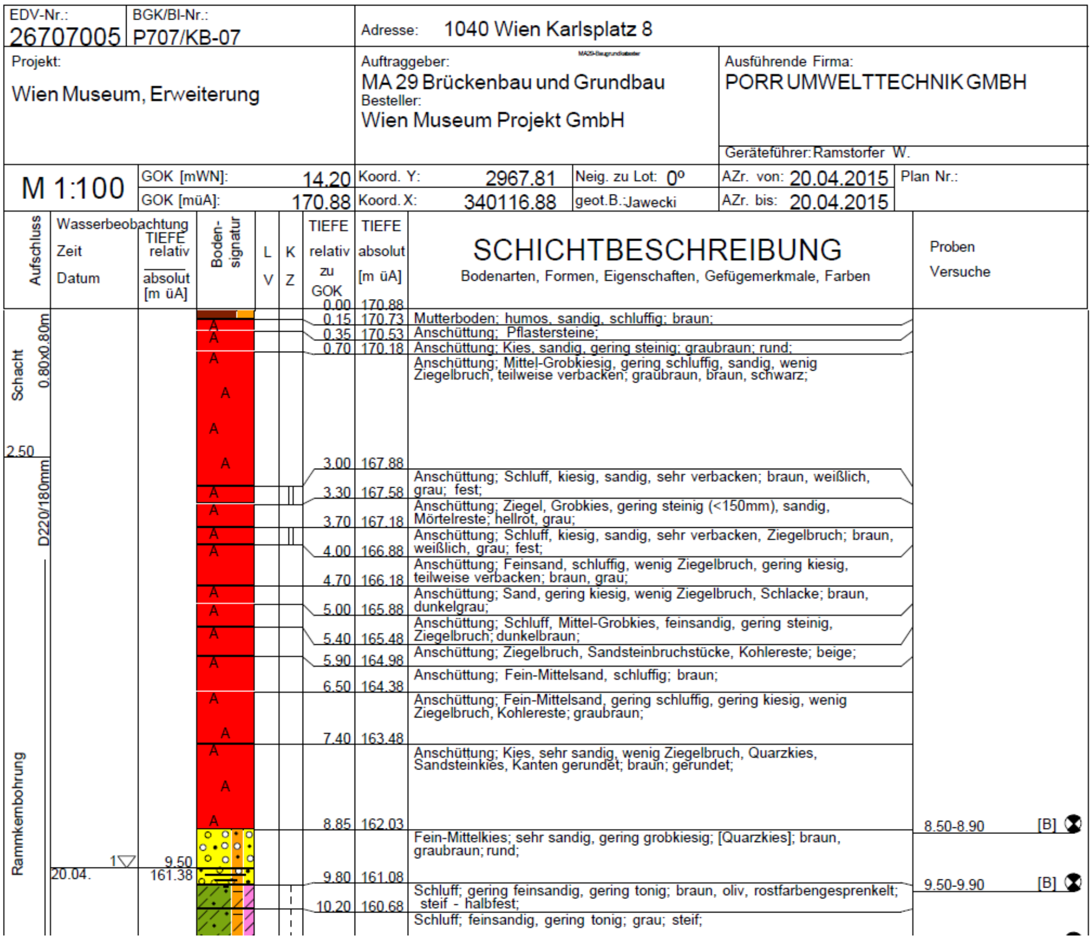

Figure 4: Example for a well log from the Viennese "*Baugrundkataster*" (Source: MA 29)

Regarding these labels, it has to be pointed out that these categories do not seem to be strictly followed by the persons in charge of documenting the well cores. Checking the annexed layer descriptions revealed that e.g. "asphalt" and "concrete" can be labelled as "Bw" or as "A".[12] Especially well logs of earlier dates show greater varieties in the use of the categories. This must be considered particularly concerning the category "A?". Although most layers in this

[12] Unlike the other two categories, "Bw" has been introduced about 20 years ago. This explains, why sometimes walls are assigned to "A" instead of "Bw" (personal comment by Christine Jawecki, MA 29, on 31st of January 2020).

category seem to be correctly assigned, some entries with bricks in the layer description are classified as “A?” as well.

Due to the amount of well core data, inconsistencies in the data material cannot be completely corrected for this thesis. The preceding paragraph should point out the inconsistencies detected in the well logs, indicating that those might be reflected in the results.

5.3.1.1 Well core data of the study area

The well logs used in this study were directly extracted from the well core database and delivered by the MA 29 as CSV-tables (fig. 5). The information included covers the ID of each well core (“EDVNR”), the coordinates (“X”, “Y”), the elevation (“GOK”) and the date of the drilling using the format DD.MM.YYYY (“ERSTELLT_VON”).

Those well logs covering the layers of anthropogenic sediments or structures (“A”, “A?” or “Bw”) give additional information. Each layer fills a row in the CSV-table, giving information on the well core it stems from (“EDVNR”, “X”, “Y”, “GOK”), adding the category (“HAUPTANTEIL_SCHICHT_1”, which are the categories “A”, “A?” and “Bw” mentioned above), the upper boundary of the layer (“TEUFE_VON”, measured from the elevation “GOK”) as well as the lower boundary of the layer (“TEUFE_BIS”, measured from the elevation “GOK”). For each layer, a detailed description of its texture, colour, material or artefacts found within etc. is included (“ERGAENZUNG_SCHICHT”). Besides that, the type of drilling (“AUFSCHLUSSART”) and the date (“ERSTELLT_VON”) are documented.

1	EDVNR	X	Y	GOK	HAUPTANTEIL_SCHICHT_1	TEUFE_VON	TEUFE_BIS	ERGAENZUNG_SCHICHT	AUFSCHLUSSART	ERSTELLT_VON
182	26893006	334440,34	4594,03	211,88	A	0,5	0,7	Kies, feinsandig, schluffig	24	30.10.2017
183	26893007	334376,1	4589,27	208,16	A	0,4	0,6	Schluff, sehr feinsandig, kiesig, Wurzelreste	24	16.11.2017
184	26894006	335743,17	12779,34	155,36	A?	0,3	1	Sand, schluffig, kiesig, Wurzelreste	24	16.11.2017
185	26894007	335724,36	12772,47	155,8	A?	0,3	1	Feinsand, gering schluffig, Wurzelreste	24	16.11.2017
186	26894007	335724,36	12772,47	155,8	A?	1	1,5	Feinsand, schluffig, Wurzelreste	24	16.11.2017
187	26894011	335745,33	12824,1	155,4	A?	0,3	1,4	Feinsand, sehr kiesig, gering schluffig	24	16.11.2017
188	26894011	335745,33	12824,1	155,4	A?	1,4	2	Kies, sehr mittelsandig, feinsandig, schluffig	24	16.11.2017
189	26894012	335727,55	12814,92	155,95	A?	0,3	1,5	Feinsand, schluffig	24	15.11.2017
190	26894013	335734,8	12842,55	155,47	A?	0,4	1,7	Feinsand, gering schluffig, sehr kiesig	24	15.11.2017
191	26894014	335734,8	12842,55	155,47	Bw	0	0,3	Asphalt	24	15.11.2017
192	26894014	335734,8	12842,55	155,47	A	0,3	0,5	Schotter	24	15.11.2017
193	26894014	335734,8	12842,55	155,47	A	0,5	2,2	Feinsand, gering schluffig, ab 1,0m Blöcke, ab 1,5m Zie	24	15.11.2017

Figure 5: Example for well core data used in this study

The elevation in “GOK” is not, as it might be expected by its name (“GOK” = “*Geländeroberkante*”), always showing the ground level. In most cases, this elevation stands for the starting point of drilling. Yet, in well logs of older drillings, this information indicates the estimated ground level. Some of the drillings were done in cellars or construction pits, so in these cases the elevation mentioned in the logs deviates sharply from the actual ground surface.[13] For detecting the correct drilling location (in a cellar, construction pit or the actual ground level), the original PDFs of the well logs would have needed to be consulted, which was not possible in the frame of this study. Therefore, the "GOK" of the well cores have not been used, besides for calculating the actual height of the lower boundary of the anthropogenic sediments (in *m.ü.A.*).

By selecting the well cores in the study area, (using the SelectByLocation-Tool in ArcGIS, method: Within), the following data were obtained for the study:

Table 2: Well core data used in the study

Well cores in the study area	9,878	
Well cores without AMG	863	(8.7 % of total)
Well cores with AMG	9,015	(91.3 % of total)
Layers in the well cores with AMG (A, A?, Bw)	19,984	

According to the numbers, less than 10 percent of the well cores in the study area, i.e. 863 cores, do not contain anthropogenic sediments. With 9,015 well cores and 19,984 layers of AMG, a solid basis for the investigation of the anthropogenic modified ground of the study area exists.

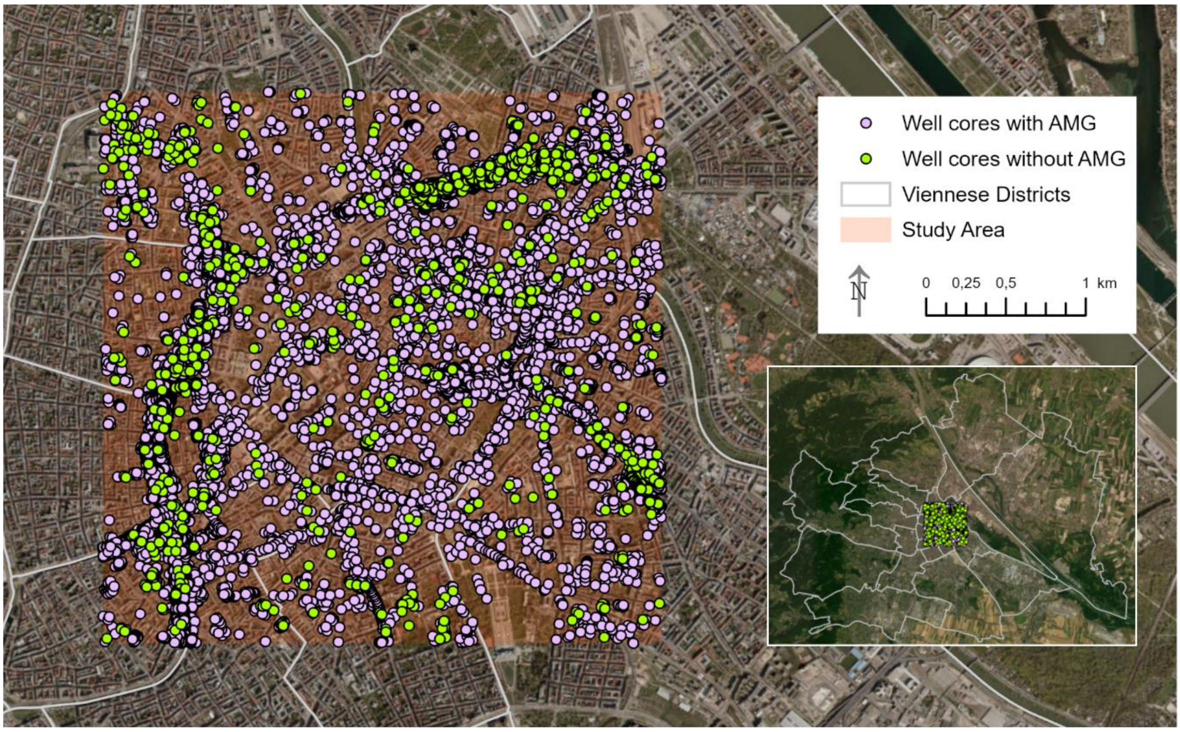

Figure 6: Distribution of well cores with and without anthropogenic sediments in the study area

[13] Personal comment by Christine Jawecki, MA 29, on 31st of January 2020.

Looking at the spatial distribution of the well cores (fig. 6), the well cores without AMG are clustered along the underground railway track of U2 and U3 and in the area of the AKH, the largest hospital of Austria. Interestingly, well cores without anthropogenic sediments seem always to be in direct neighbourhood of well cores with documented AMG. Thus, no obvious areas without anthropogenic sediments can be detected.

5.3.1.2 Accuracy

In praxis, well core data cannot be described as very accurate.[14] The well core is placed in the core boxes by the drilling foreman, parts might be cut ("*Überschnitt*") and there is bore detritus. Additionally, the accuracy of the data depends on the kind of drilling. Whereas core drillings can be counted as comparatively precise, this does not apply for grab excavations, where the material is taken by a grab sampler and afterwards put into the core boxes. The accuracy in general depends on a variety of factors, e.g. the scope of work, the type of drilling, the drilling foreman, the date of the drilling, the site supervision, the time pressure and the weather conditions, so that the precision of well core data can differ considerably.

Regarding the drilling location, the coordinates using floats are the result of a geodetic survey and therefore highly accurate. Well cores of older date have coordinates as integers and are thus less precise.[15] Moreover, the type of drilling might also affect the accuracy of the drilling localisation. So-called house shafts ("*Hausschächte*"), which are well represented in the well cores of the study area, are usually drilled near to house walls to determine the bottom edge of the building foundation. Until the 90s, the coordinates of those well cores were extracted from the site plan and therefore differ in their accuracy. Yet, generally they should be located in the correct building.

To sum up, the accuracy of the well core data can deviate sharply due to a variety of factors and hence should be treated with caution.

5.3.2 Archaeological data

In Vienna, more than 1,200 excavations and archaeological measures have been carried out by the Department of Urban Archaeology (Stadtarchäologie Wien, Museen der Stadt Wien). Since 1895 archaeological investigations have taken place. In the course of an archaeological

[14] This chapter summarises personal comments by Christine Jawecki, MA 29, on 22nd of August 2019 and 12th of December 2019.
[15] This applies to approximately half of well cores in the study area.

excavation, the different archaeological layers excavated are documented by a written report and a drawing showing the extent of the layer and its elevation. Since 2005, the layers are digitally measured using a tachymeter that is connected to a laptop and is drawing the measured points in the computer-aided design and drafting software application AutoCAD directly at the excavation site.[16] The older, manually drawn excavation maps have been subsequently digitised, so that now every archaeological site map is digitally available. Since 2003, the archaeological data is mapped in the ViennaGIS and several data sets are available via data.wien.gv.at.[17]

The archaeological data were directly received from the Department of Urban Archaeology (Stadtarchäologie Wien, Wien Museum) in the DWG (CAD files) and SHP format. For the ViennaGIS, the layers are assigned to major historical epochs, which are Prehistoric times, Roman times, Medieval times, Modern times and "Geology", which refers to the first layers without hints of human interference, i.e. the Boundary A (fig. 7). The elevation information of every layer is documented in the DWG file, using mainly "Wiener Null".

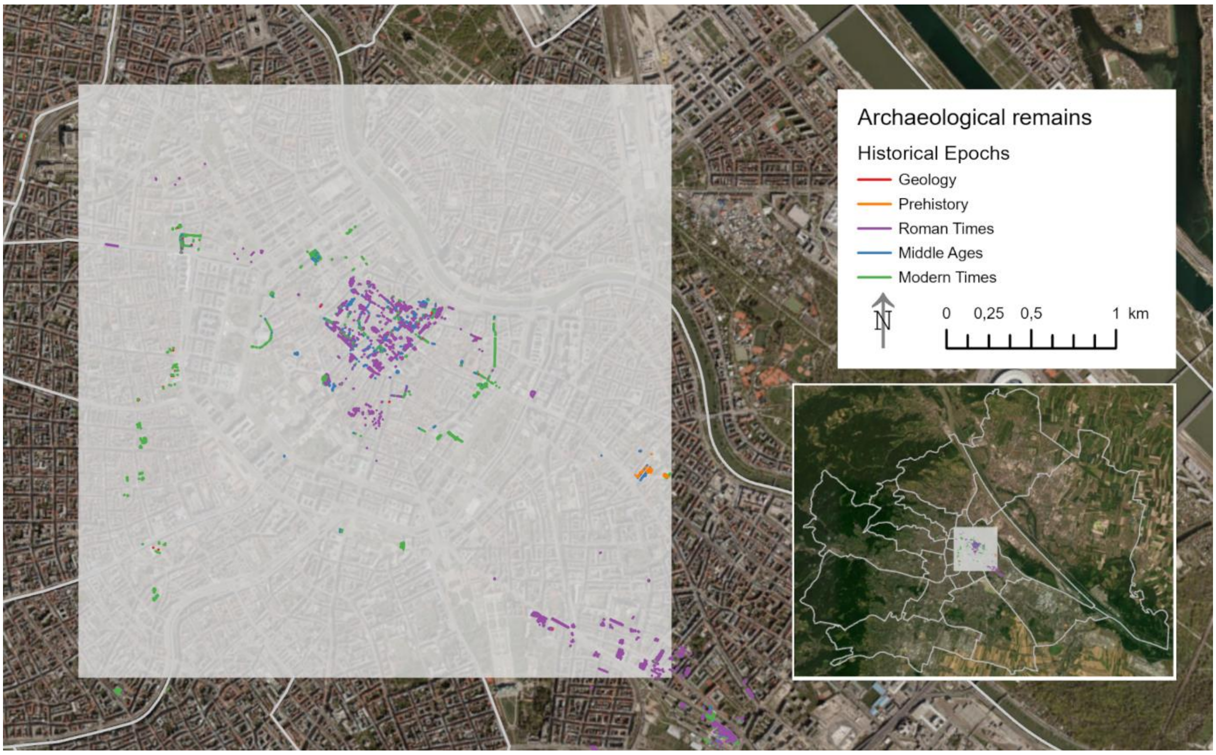

Figure 7: Archaeological remains in the study area

[16] The software connecting the tachymeter to the AutoCAD software is called TachyCAD.
[17] https://www.wien.gv.at/kulturportal/public/grafik.aspx; https://www.data.gv.at/auftritte/?organisation=stadt-wien&searchterm=arch%C3%A4ologie (accessed February 28, 2020).

As the archaeological measures are digitally surveyed since 2005, the excavations maps of earlier excavations have been digitised and implemented in the ViennaGIS, yet they do not include elevation information. The corresponding heights of Boundary A would need an extensive research of all published excavation reports of all sites excavated before 2005, which was not possible in the context of this study. Therefore, only archaeological sites investigated since 2005 have been included in this study.

5.3.2.1 Archaeological data in the study area

70 archaeological sites that have been investigated since 2005 are situated in the study area. For every archaeological measure, an individual DWG file was delivered, including a map of the surroundings and the archaeological layers and findings (fig. 8). The archaeological measures range from excavations (from short-term to several months) to construction monitoring, as trenches for infrastructure measures as sewage, electricity or gas. Depending on the construction work, the depth of construction and archaeological excavation was sometimes constrained and the Boundary A was not reached in all cases.

For this study, all information on Boundary A in archaeological contexts shall be implemented. So, the documented layers in the archaeological data sets were searched for the presence of layers representing the lower boundary of the anthropogenic sediments at one position. These layers are labelled in different ways, as "geology" ("*Geologie*"), "humous vegetation layer" ("*humose Vegetationsschicht*"), "loess" ("*Löss*", being the predominant sediment underlying the anthropogenic ground in the study area) or simply "forest floor" ("*Waldboden*"). These layers are used for this study. By using the 3D-orbit view of AutoCAD, for each of these excavation sites it is checked, if there are other, younger layers reaching deeper in the underground. If this is the case, those layers are implemented as well. Figure 8 displays the archaeological layers at the excavation site "Am Hof 10", trench 10 and 11. The anthropogenic sediments cover more than 4,200 different layers and thereby this site is one of the most extensive excavations in the study area. The elevation of the natural geological ground, here labelled as "forest floor", is depicted as reddish brown line, best visible on the right-hand side of the figure. As can clearly be seen, at this site the younger layers of the Middle Ages and Roman times are at different locations reaching significantly deeper, below the "geological ground". Here, the lowest layers are implemented in the study.

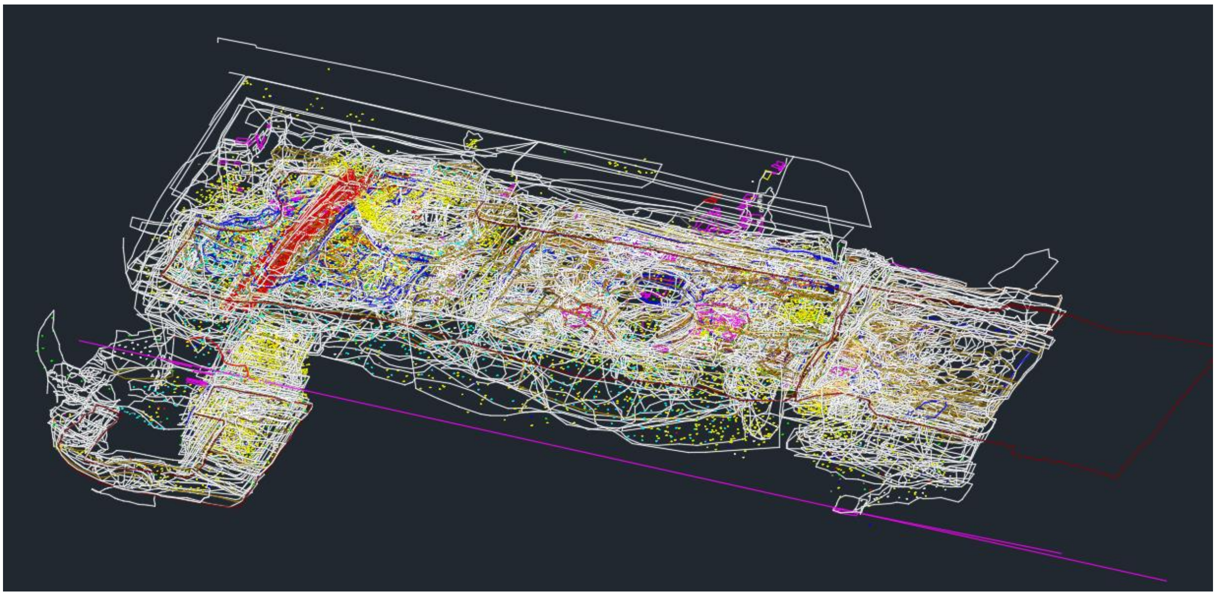

Figure 8: Map showing the archaeological layers at the excavation site Am Hof 10, trench 10-11

Of the 70 excavation sites in the study area, only those were used where the actual upper boundary of the natural ground was reached. Following this criterion, 31 excavation sites could be included in this study. 30 of those were using "*Wiener Null*" for elevation heights, one excavation had the elevation in "meters above the Adriatic" (m.ü.A.). Depending on the type of archaeological measure, the site maps include between only 25 and more than 4,000 layers.

For the interpolation, the 3D-polylines in AutoCAD have to be converted to point data. Layers representing the Boundary A have been copied to a new file in AutoCAD and the polylines have been discretised in points at a distance of one metre using the tool "measure". In case that the polyline is shorter than 1 m, the line is divided in the centre by "divide". The geometry of those points, visible in Figure 9, are exported by the command "dataextraction" into a file of CSV format. The extracted data points are transformed to elevations in "m.ü.A." by a Python script and afterwards visualised in ArcGIS Pro, showing a concentration of excavations in the inner city, the first district of Vienna (fig. 10). Generally, the excavations are located in direct neighbourhood of well cores, which can be explained by the fact that excavations are entirely done beforehand site redevelopment and therein share a common ground with the well cores. However, in few locations excavations add information where well core data are completely missing (especially areas without underground railway tracks). As one excavation site is only partially situated in the study area (located at Rennweg 64), the extracted data points outside the study area were discarded.

In total, 2,259 points are obtained by the archaeological data set.

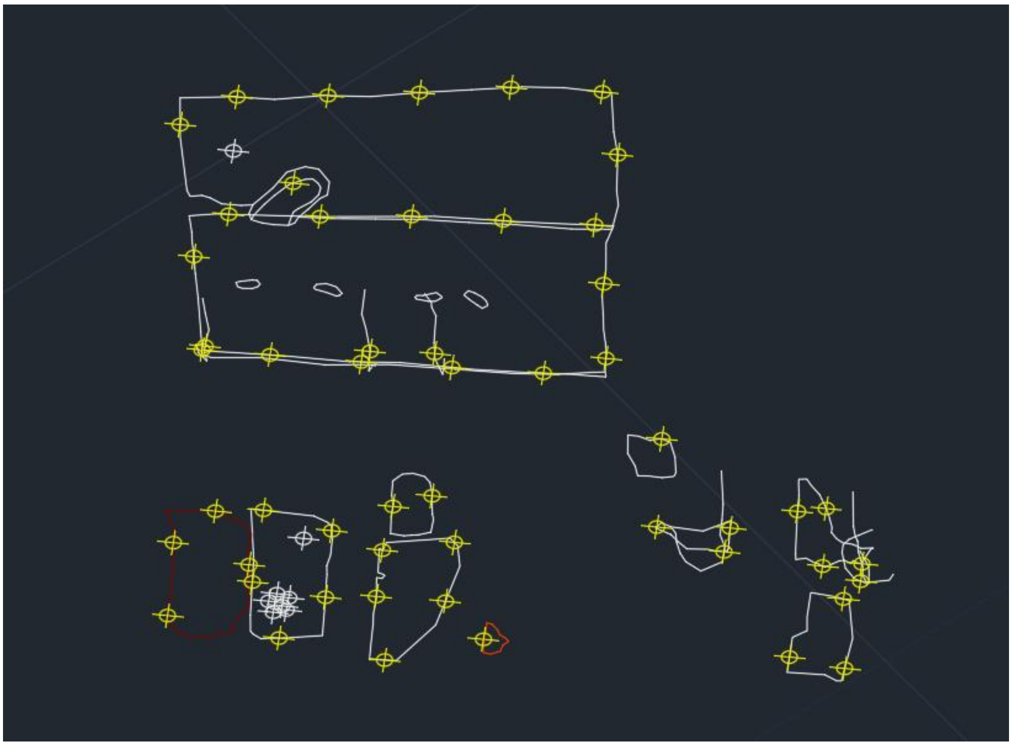

Figure 9: Data points extracted from the archaeological maps by "measure" and "divide"

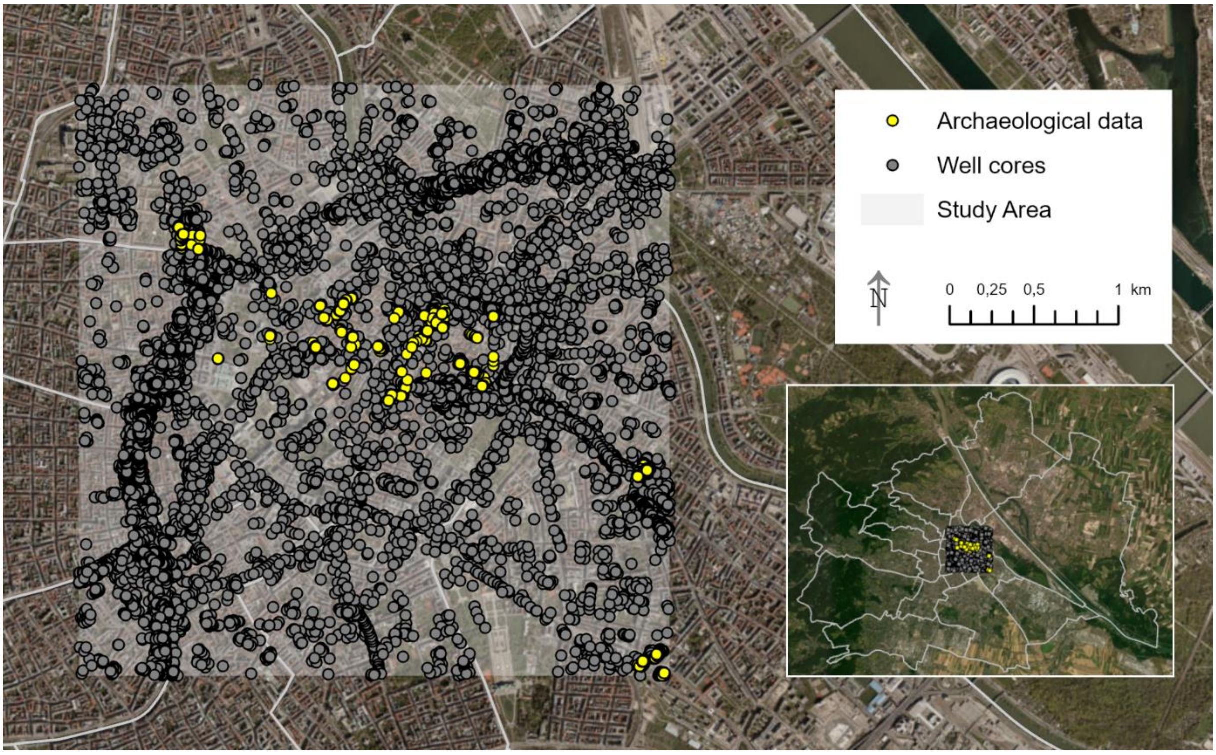

Figure 10: Distribution of extracted archaeological data points and the well cores of the study area

5.3.2.2 Accuracy

In contrast with the well core data, the excavation data is highly accurate, with deviations only in centimetre range.[18] For the stationing of the total station, survey points of the Municipal Department for Surveying and Mapping (MA 41 Stadtvermessung Wien, Stadt Wien) are used.

5.3.3 Administrative boundaries

The district boundaries of Vienna used in the maps of this study are downloaded from data.gv.at and are provided by the Municipal Department for Surveying and Mapping (MA 41 Stadtvermessung Wien, Stadt Wien) – Data source: Stadt Wien - data.wien.gv.at).[19]

5.3.4 Digital terrain model

Digital terrain models (DTM)[20] of the city area of Vienna are provided by the Municipal Department for Surveying and Mapping (MA 41 Stadtvermessung Wien, Stadt Wien). Those DTMs can be downloaded via the geodata viewer (*Geodatenviewer der Stadtvermessung Wien*) in tiles of 2,500 x 2,500 m as vector data (SHP and DXF format) or raster data (TIFF and ASCII format).[21] The data is using EPSG 31256 and the elevation information is in "*Wiener Null*".[22] The DTMs are mainly based on the multi-purpose map of the City of Vienna, calculating the DTM from more than 13 million points and lines relevant for the terrain (e.g. embankments, shorelines).[23] By iterative interpolations outliers are removed automatically. Afterwards, the model is interactively checked and breaklines are included for modelling retaining walls and staircases. For woodland areas, LiDAR data is implemented.

[18] Deviations of 1-2 cm are possible (personal comment by Martin Mosser, Department of Urban Archaeology, on 12th of February 2020).
[19] https://www.data.gv.at/katalog/dataset/2ee6b8bf-6292-413c-bb8b-bd22dbb2ad4b (accessed February 28, 2020).
[20] In this study, the term "DTM" is used for a bare-earth raster grid.
[21] https://www.wien.gv.at/ma41datenviewer/public/ (accessed February 28, 2020).
[22] https://www.wien.gv.at/stadtentwicklung/stadtvermessung/geodaten/viewer/geodatendownload.html (accessed February 28, 2020).
[23] https://www.wien.gv.at/stadtentwicklung/stadtvermessung/geodaten/dgm/produkt.html (accessed February 28, 2020). – PDF on the production of the DTM by the Municipal Department for Surveying and Mapping: https://www.wien.gv.at/stadtentwicklung/stadtvermessung/pdf/dgm-herstellung-mzk.pdf (accessed February 28, 2020).

Regarding the data quality, the elevation accuracy of the DTM in those areas that are based on the multipurpose map amounts to +/- 10 cm in the road space and +/- 25 cm inside a city block.[24]

The DTM is updated on a regular basis, region after region (fig. 11).

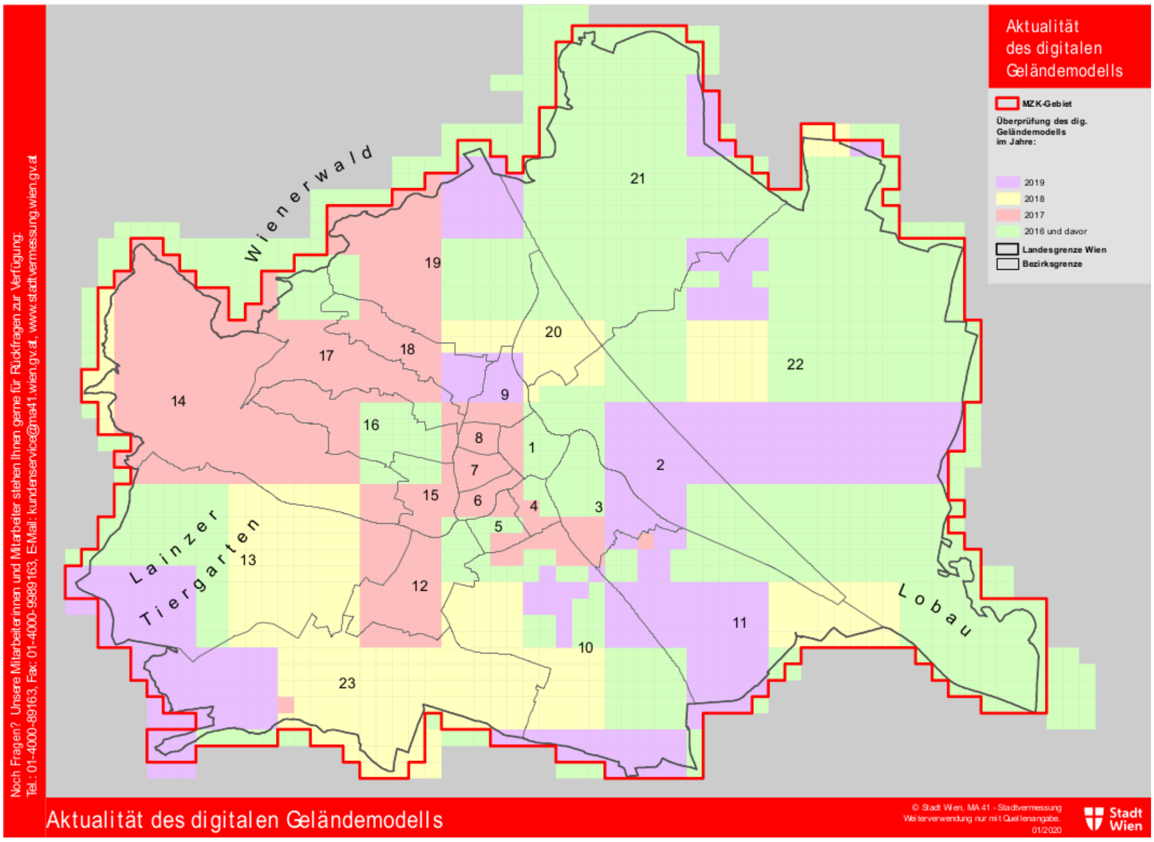

Figure 11: Revision year of the DTM by the Municipal Department for Surveying and Mapping (MA 41)

5.3.4.1 Digital terrain model of the study area

For this study, the TIFF raster data with a spatial resolution of 1 meter were used.[25] The six tiles covering the study area were downloaded[26], merged using the “Mosaic to New Raster”-tool in ArcGIS Pro and clipped to the extent of the study area (tool: “Clip Raster”). By the tool “Raster Calculator”, the raster values were recalculated from elevation heights in “*Wiener Null*” to metres above the Adriatic ("DTM study area" + 156.68). The elevation of the ground level in the study area ranges from 154.78 to 204.11 m.ü.A. (fig. 12).

[24] https://www.wien.gv.at/stadtentwicklung/stadtvermessung/geodaten/dgm/produkt.html (accessed February 28, 2020).

[25] https://www.data.gv.at/katalog/dataset/stadt-wien_gelndemodellrasterwien (accessed February 28, 2020).

[26] That are the tiles 35/1, 35/2, 35/3, 35/4, 45/1 and 45/2.

Concerning the currentness of the data, the DTMs of the study area have been updated in the last four years (fig. 13).

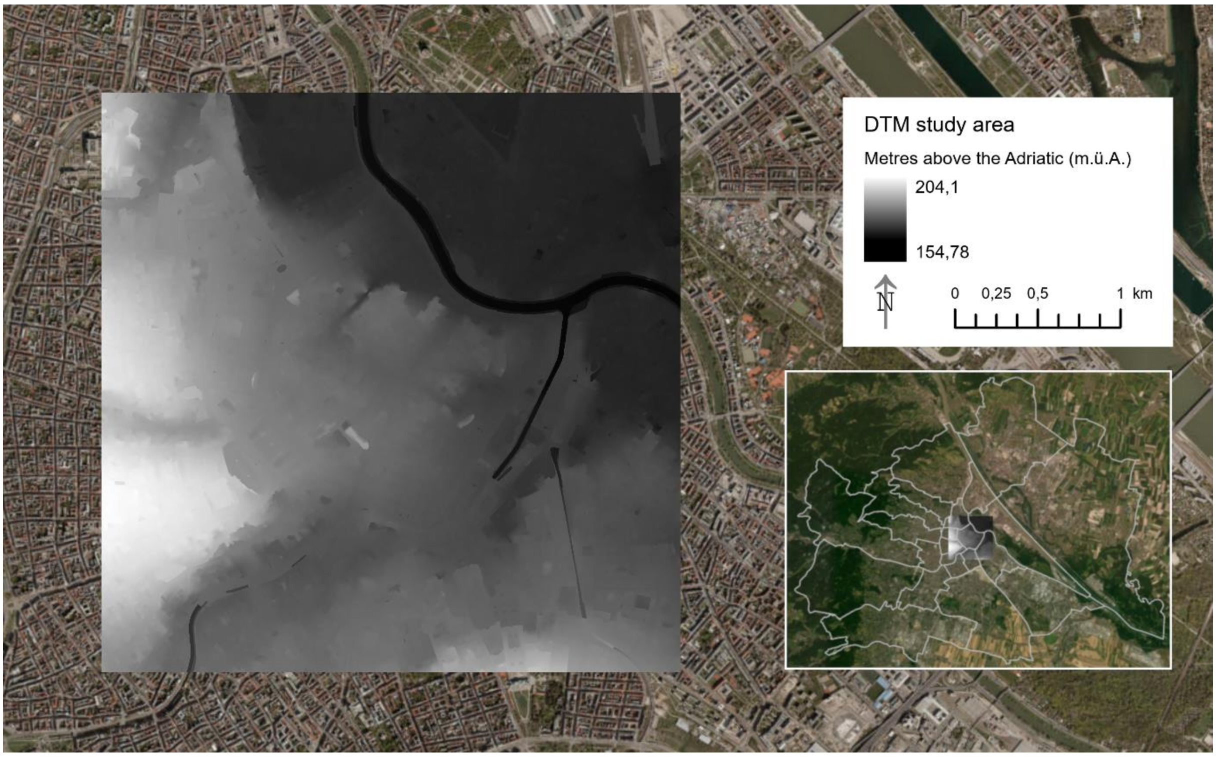

Figure 12: DTM by the MA 41, clipped to the study area and recalculated to m.ü.A.

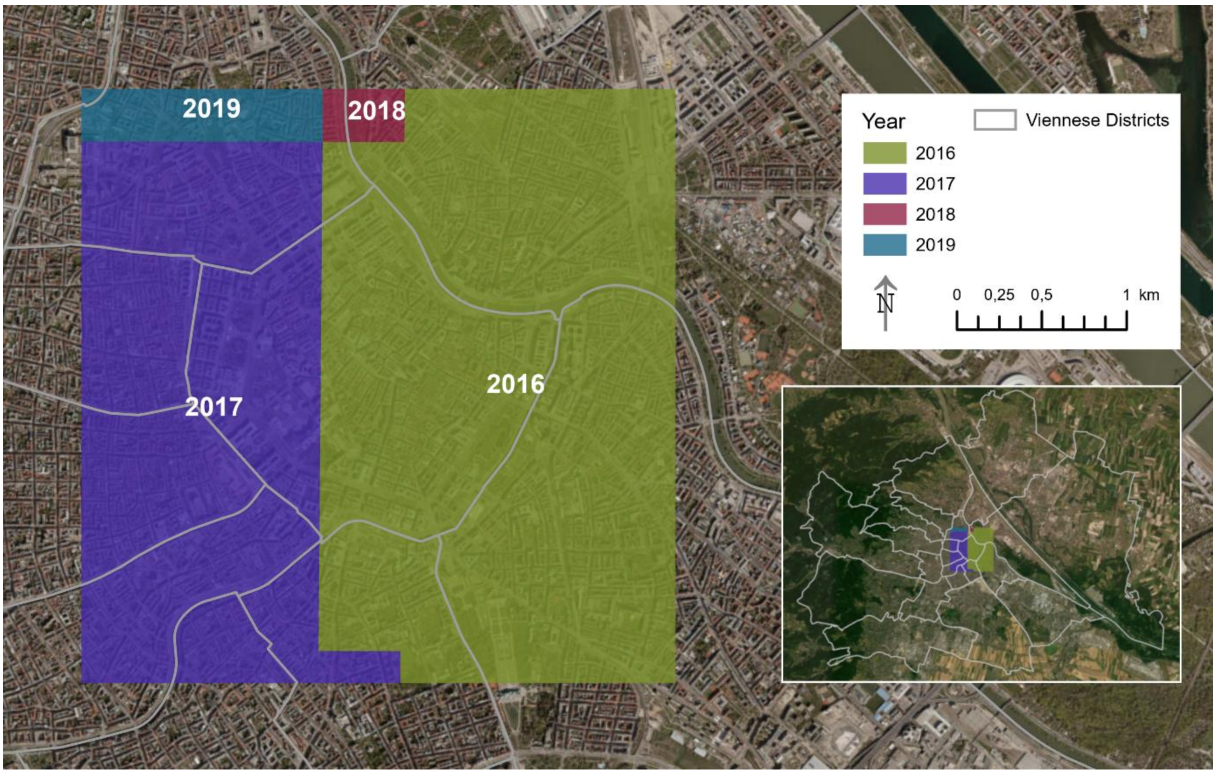

Figure 13: Revision year of the DTM in the study area

6. Results

6.1 Data preparation

Data preparation was mainly done using Python 3. The raw data included different CSV files: individual files for the categories “Bw”, “A” and “A?” as well as a file of well cores without anthropogenic sediments and further files on the total depth of the well cores (two columns: “EDVNR” and “ENDTEUFE” i.e. TD) and related building projects (two columns: “EDVNR” and “PROJEKTTITEL” i.e. project title). The tables covering anthropogenic sediments and structures (“Bw”, “A” and “A?”) contain one entry per layer, so that one well core can extend over several rows.

First, the different CSV files for the three classes “Bw”, “A” and “A?” were concatenated, resulting in one table containing all well cores with anthropogenic sediments and structures. As mentioned above, a total of 19,984 anthropogenic layers is documented in the study area.

Second, the total depths of the well cores were appended to the layer file by merging the two files. Next, a new field was added, with values representing the difference from subtracting the lower boundary (“TEUFE_BIS”) from the total depth (“ENDTEUFE”). If the difference equals zero, well core drillings that have not reached the lower boundary of the anthropogenic sediments can be detected. Since no other layers underneath an AMG layer are documented, it cannot be guaranteed that “Boundary A” at this position equals the lower boundary of the lowest anthropogenic layer of this well core. Thus, it can only be stated with certainty that at this position the anthropogenic sediments are reaching **at least** to this depth, yet anthropogenic layers underneath cannot be excluded. For these well cores, a new category is introduced, called “A_min” (i.e. minimum depth of AMG at this location). Well cores classified as “A_min” were extracted from the total list by the following script:

```
# Import module
import pandas as pd
# Open a new file
result = open("A_min.csv", "w")
# Read the original CSV
AMG = pd.read_csv("wellcores.csv", sep=';', decimal = ',',
encoding='ISO-8859-1')
# Create a dataframe from the two columns ID and the calculated
difference between total depth and lower boundary of AMG
df = pd.DataFrame(AMG, columns = ['EDVNR','A_min'])
# Set a boolean for difference = 0
df['A_min_bool'] = AMG['A_min'].apply(lambda x : 'True' if x == 0 else
'False')
# List of IDs of well cores where boolean = 0
listAmin = list(df.loc[df['A_min_bool'] == 'True', 'EDVNR'])
```

```
# Filter original CSV by IDs from new list
Amin = AMG.query('EDVNR == @listAmin')
# Set well core ID as Index
Amin.set_index('EDVNR', inplace=True)
# Save as CSV
Amin.to_csv(result, sep=';', decimal = ',')
# Close the file
result.close()
```

In total, 2,715 layers of 1,086 well cores are assigned to A_min. The IDs of these well cores were removed from the total list, which now counts 7,929 well cores with 17,269 anthropogenic layers.

Looking at the spatial distribution of those two groups, the well cores without a certain lower Boundary A, i.e. classified as "A_min", are for one part concentrated along the underground railway tracks of the U2 (fig. 14). However, numerous well cores belonging to A_min are also distributed in the first district. There, these well cores are not mainly limited to the railway tracks of the underground as the other well cores, but also spread out in the blank areas in between.

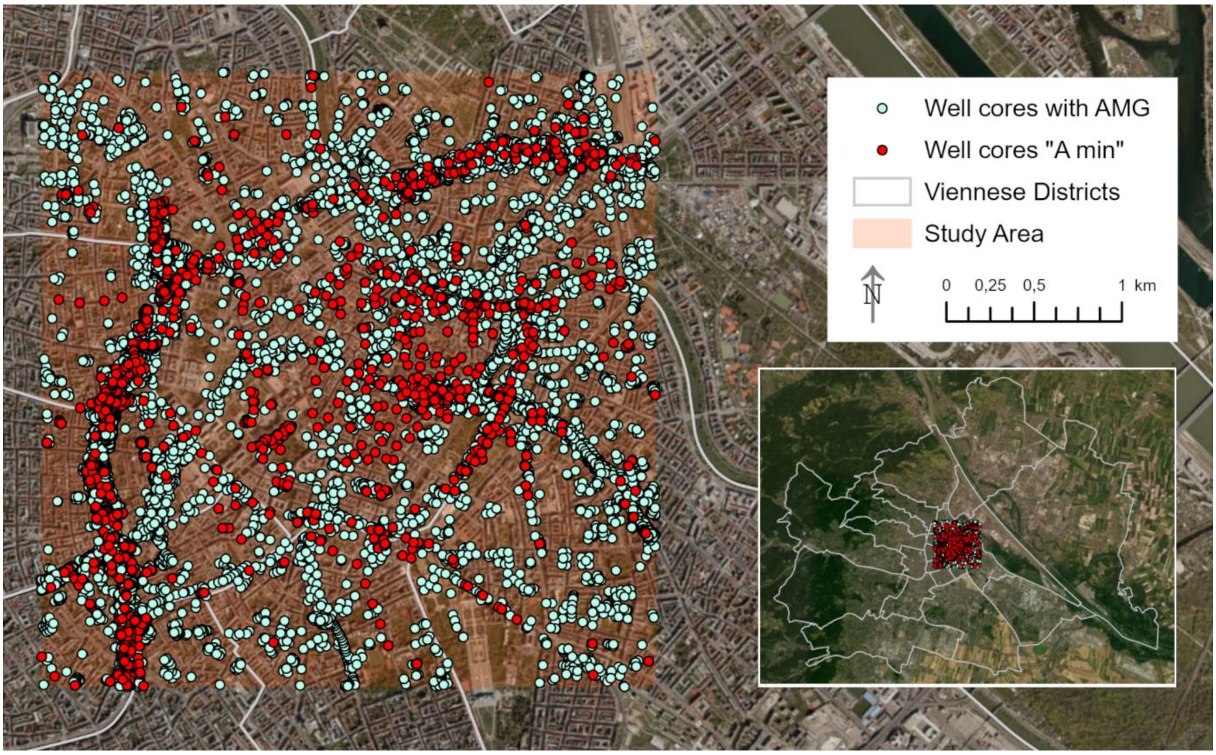

Figure 14: Distribution of well cores with AMG and well cores "A min"

For calculating the thickness of the anthropogenic sediments, the CSV files of the separate layers were summarised to one row per well core. This was achieved by dropping the duplicate values of the well core IDs and saving the first as well as the last entry in a new data frame. The lower boundary (“TEUFE_BIS”) of the first entry was replaced by the lower boundary of the last entry of each well core. Finally, the thickness of AMG was calculated by subtracting the lower boundary (“TEUFE_BIS”) from the upper boundary (“TEUFE_VON”). The code used is the following:

```
# Import module
import pandas as pd
# Open a new file
result = open("wellcores_thickness.csv", "w", newline='')
# Read the original CSV
orig = pd.read_csv("wellcores_layers.csv", sep=';', decimal = ',',
encoding='ISO-8859-1')
# Sort by well core ID and drilled depth
orig_sort = orig.sort_values(by = ['EDVNR', 'TEUFE_VON'])
# Drop duplicates and keep the first row
first = orig_sort.drop_duplicates(subset='EDVNR', keep='first')
# Drop duplicates and keep the last row
last = orig_sort.drop_duplicates(subset='EDVNR', keep='last')
# Set well core ID as Index
first = first.set_index('EDVNR')
last = last.set_index('EDVNR')
# Update the drilled depth
first.TEUFE_BIS.update(last.TEUFE_BIS)
first.reset_index(inplace=True)
# Drop unused columns
first = first.drop(['HAUPTANTEIL_SCHICHT_1', 'ERGAENZUNG_SCHICHT',
'A_min'], axis=1)
# Calculate thickness of AMG
first['AnschSt'] = first.TEUFE_BIS - first.TEUFE_VON
# Set well core ID as Index
first.set_index('EDVNR', inplace=True)
# Save as CSV
first.to_csv(result, sep=';', decimal = ',')
# Close the file
result.close()
```

The same procedure was completed with the well cores classified as “A_min”.

The class “A?” is providing another possible lower boundary that shall be analysed in this study. Therefore, two other CSV files were calculated excluding bottom layers declared as “A?”. Yet, as mentioned above, layers classified as “A?” do not only appear as the lowest layers of the AMG, but sometimes “A?” layers are documented as the uppermost layers or in the middle between two or more layers of anthropogenic sediments and structures. For this study, only the classification of the lowest layers as “A?” are used, since these make a difference for the depth and thickness of anthropogenic ground at this position. Thus, the script has to be changed to remove layers with the classification “A?” by adding two lines:

```
# Import module
import pandas as pd
# Open a new file
result = open("wellcores_thickness_excl.csv", "w", newline='')
# Read the original CSV
orig = pd.read_csv("wellcores_layers.csv", sep=';', decimal = ',',
encoding='ISO-8859-1')
# Sort by well core ID and drilled depth
orig_sort = orig.sort_values(by = ['EDVNR', 'TEUFE_VON'])
# Drop duplicates and keep the first row
first = orig_sort.drop_duplicates(subset='EDVNR', keep='first')
# Remove layers with classification "A?"
last = orig_sort.query('HAUPTANTEIL_SCHICHT_1 != "A?"')
# Drop duplicates and keep the last row
last = last.drop_duplicates(subset='EDVNR', keep='last')
# Set well core ID as Index
first = first.set_index('EDVNR')
last = last.set_index('EDVNR')
# Update the drilled depth
first.TEUFE_BIS.update(last.TEUFE_BIS)
first.reset_index(inplace=True)
# Remove layers with classification "A?"
# by this, well cores with only layers classified as "A?" are removed
too
first = first.query('HAUPTANTEIL_SCHICHT_1 != "A?"')
# Drop unused columns
first = first.drop(['HAUPTANTEIL_SCHICHT_1', 'ERGAENZUNG_SCHICHT',
'A_min'], axis=1)
# Calculate thickness of AMG
first['AnschSt'] = first.TEUFE_BIS - first.TEUFE_VON
# Set well core ID as Index
first.set_index('EDVNR', inplace=True)
# Save as CSV
first.to_csv(result, sep=';', decimal = ',')
# Close the file
result.close()
```

Again, the same script was used for creating a table of well cores belonging to “A_min” excluding “A?” as lowest layer. To well cores without anthropogenic materials, a thickness of AMG of “0” was assigned by script.

Processing the well core data resulted in the following numbers of individual well cores and layers of the different classes:

Table 3: Numbers of different classes of well cores in the study area

Well cores (total)	9,878
Well cores with AMG	9,015
Well cores without AMG	863
Well cores with AMG excl. A_min	7,929
Well cores A_min	1,086
Layers of AMG (total)	19,984
Layers of AMG (excl. A_min)	17,269
Layers of AMG A_min	2,715

6.2 Defining categories

During the process of data preparation, four categories became apparent that are going to represent the basis of the following analyses:

(1) Well cores including A_min excluding A?
(2) Well cores including A_min including A?
(3) Well cores excluding A_min excluding A?
(4) Well cores excluding A_min including A?

These four categories were created by merging the CSV files prepared according to the category description. In all four categories, the well cores without AMG are included.

The CSV files are extended by two fields, showing the year of the drilling (derived from the date (column "ERSTELLT_VON")) and displaying the elevation of Boundary A (lower boundary of AMG) in *m.ü.A.* of each well core (calculated by subtracting the total depth from the drill starting point).

Table 4: Number of well cores in the four categories established for the well core data

(1) Incl. Amin excl. A?	9,831
(2) Incl. Amin incl. A?	9,878
(3) Excl. Amin excl. A?	8,760
(4) Excl. Amin incl. A?	8,792

6.3 Explorative Spatial Data Analysis (ESDA)

As starting point for the analysis of the data, the Explorative Spatial Data Analysis (ESDA)[27] for the four categories was performed in ArcGIS and R.

6.3.1 Dates of well cores

The dates of drillings in the study area reach from the first drilling known in the database from 1844 to the 15th of May 2019, covering a time span of 176 years (fig. 15 and 16). The drillings stem from 126 different years, only in 50 years no drillings were conducted in the study area.[28]

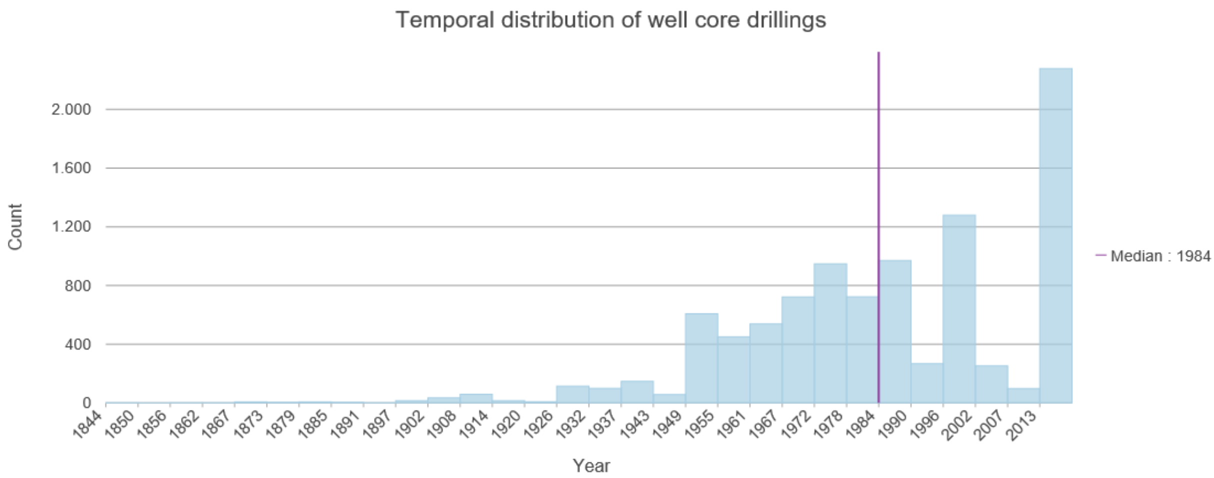

Figure 15: Histogram on the distribution of drillings over time, excl. drillings without known date ("1500")

179 well cores show the date "01.01.1500", which is used for drillings without known date. By far the most drillings in the study area were conducted in the year of 2016 (1,915 well cores), followed by the years 2001 (993 well cores) and 1976 (345 well cores). With the exception of five drillings, all the well cores of 2016 stem from foundation examinations for the planned new underground railway tracks U2 and U5 (in total: 1,910 well cores). Also in 2001, most of the well cores were drilled for the extension of the underground line U2 (973 of 993 well cores) as well as in 1976 for the extensions of the underground lines U1, U3 and U4 (239 of 345 well cores). The periods of extensive drilling are therefore mainly connected to the extension of the

[27] On ESDA see Kitanidis 1997.
[28] These years are mainly in the 19th century and during and after WWI. Since 1924, drillings have been done every year in the study area. – Years without drillings: 1845-1859, 1861, 1863-1868, 1872-1874, 1876-1880, 1882, 1884-1885, 1889-1891, 1893-1896, 1904-1906 and 1917-1923.

underground system in Vienna, also clearly visible in the histogram showing the distribution (fig. 15).

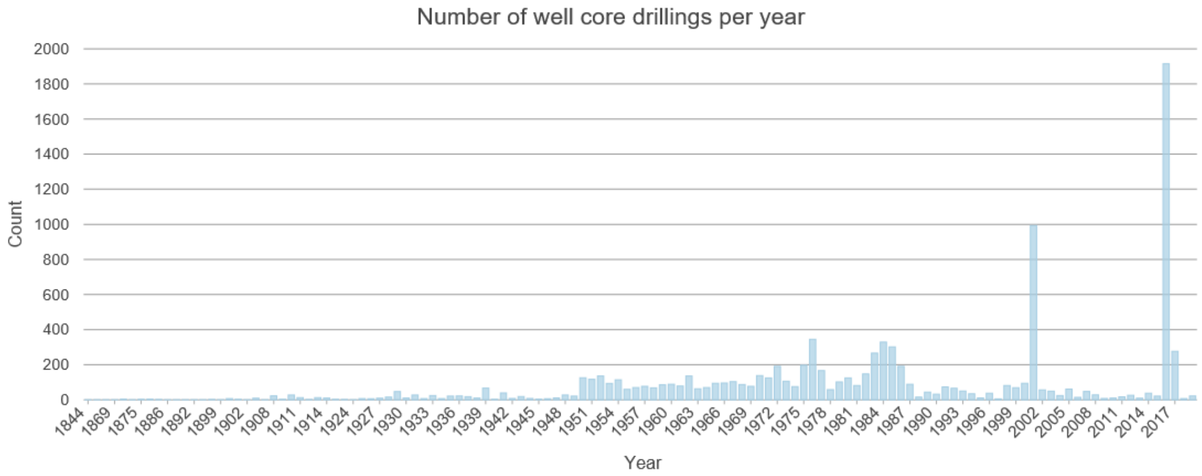

Figure 16: Number of well core drillings per year, excl. drillings without known date (“1500”)

6.3.2 Thickness of artificially modified ground (AMG)

In the study area, the thickness of anthropogenic sediments in the well logs reach from 0.02 to 19 m (fig. 22). One outlier of 93.76 m belongs to the year 1898[29] and can be detected by its description as well shaft. Since other well shafts are not included in the data set, this well core was removed, by which the number of well cores in the four categories are reduced by one each.

For a better understanding of the data, histograms were produced for each category in ArcGIS Pro and further Statistics were calculated using R (fig. 17–20 and tab. 5–8).

[29] EDVNR 11289001.

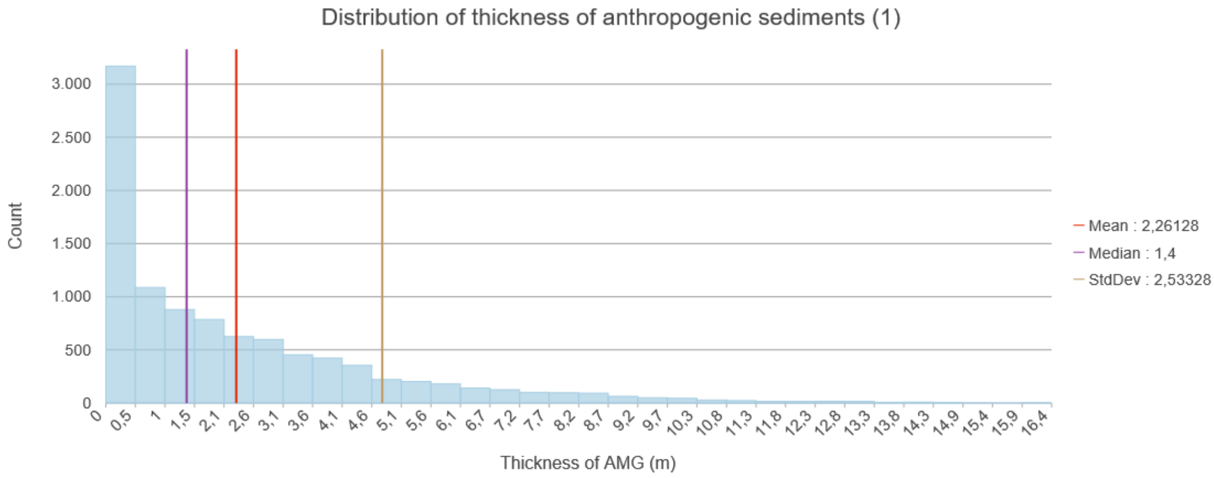

Figure 17: Histogram of the thickness of AMG in cat. (1) Incl. Amin excl. A?

Table 5: Statistics of the thickness of AMG in cat. (1) Incl. Amin excl. A?

Count	Min	1st Qu.	Median	Mean	3rd Qu.	Max	Skewness	Kurtosis
9830	0	0.3	1.4	2.26	3.3	16.4	1.69	6.22

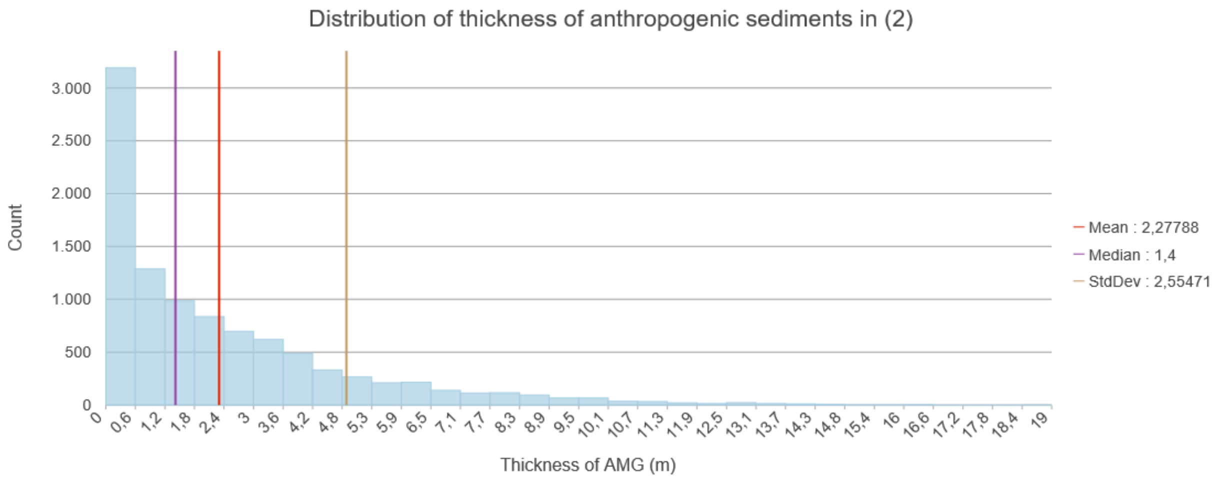

Figure 18: Histogram of the thickness of AMG in cat. (2) Incl. Amin incl. A?

Table 6: Statistics of the thickness of AMG in cat. (2) Incl. Amin incl. A?

Count	Min	1st Qu.	Median	Mean	3rd Qu.	Max	Skewness	Kurtosis
9877	0	0.3	1.4	2.28	3.3	19	1.71	6.30

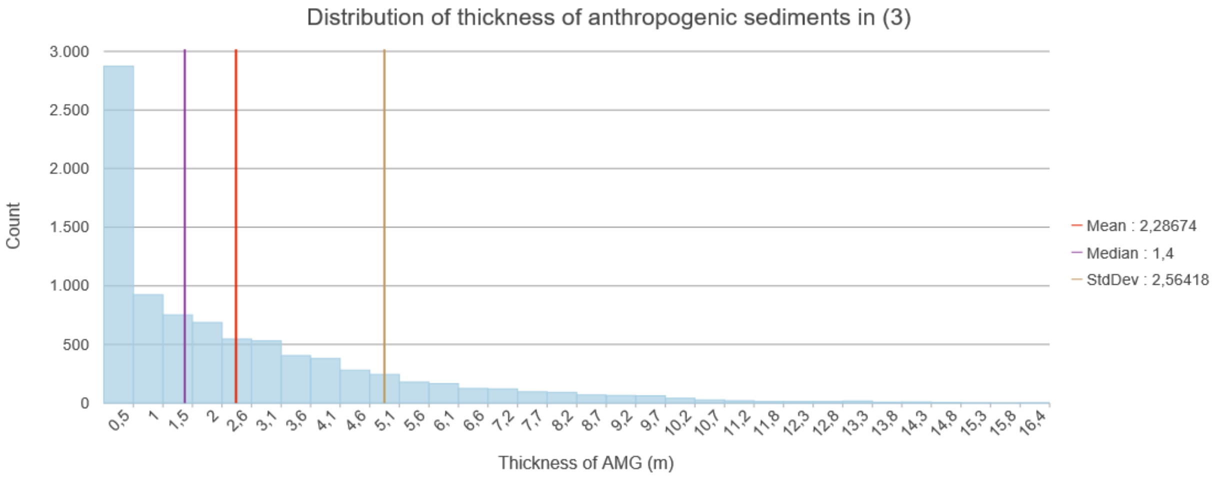

Figure 19: Histogram of the thickness of AMG in cat. (3) Excl. Amin excl. A?

Table 7: Statistics of the thickness of AMG in cat. (3) Excl. Amin excl. A?

Count	Min	1st Qu.	Median	Mean	3rd Qu.	Max	Skewness	Kurtosis
8759	0	0.3	1.4	2.29	3.4	16.35	1.65	5.96

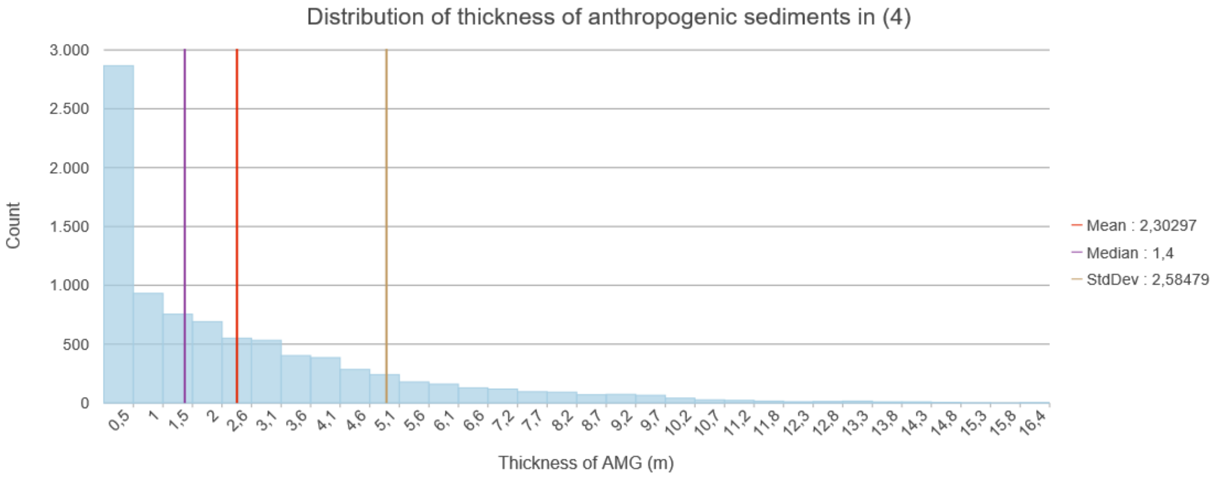

Figure 20: Histogram of the thickness of AMG in cat. (4) Excl. Amin incl. A?

Table 8: Statistics of the thickness of AMG in cat. (4) Excl. Amin incl. A?

Count	Min	1st Qu.	Median	Mean	3rd Qu.	Max	Skewness	Kurtosis
8791	0	0.3	1.4	2.3	3.4	16.35	1.66	5.96

All four categories show a clear positively skewed distribution (skewness 1.65 to 1.71) with a high kurtosis of 5.96 to 6.3 (leptokurtic distribution). Well cores with massive anthropogenic sediments are comparatively seldom, which is also shown by a high standard deviation in relation to the mean value. The median of all four categories is 1.4, which confirms the statement by Edgeworth et al. (2015) that especially anthropogenic sediments of less than 1 m in thickness are important for the lateral continuity of the archaeosphere and its Boundary A. Ford et al. (2014, 67) emphasised that such shallow deposits “may be ubiquitous across much of the Greater London Area” and, as Edgeworth et al. (2015) added, “by extrapolation, the same applies to most cities, towns and suburban areas throughout the world”. This can be confirmed by the Viennese data, as half of the well cores in the study area show less than 1.4 m of anthropogenic sediments.

Interestingly, the thickest anthropogenic sediment is documented in one well core classified as A_min (19 m incl. A?, 16.4 m excl. A?), showing the importance of this data set.

A correlation between the thickness of anthropogenic sediments and the time of drilling (e.g. an increasing thickness over time) cannot be proven by the data at all (fig. 21) (using the dataset from category (2)).

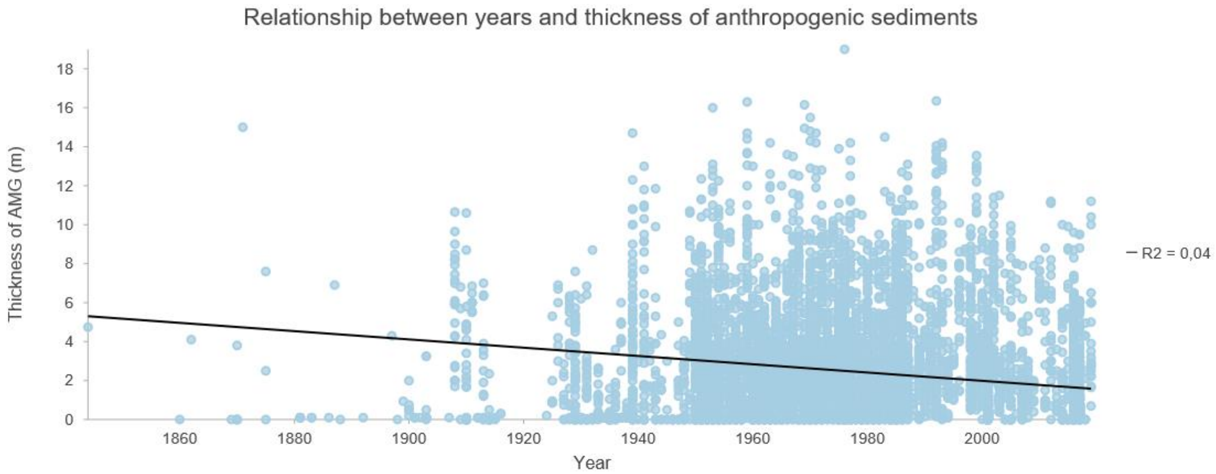

Figure 21: Relationship between the years of drilling and thickness of anthropogenic sediments documented in the well cores, excl. drillings without known date (“1500”)

The map (fig. 22) shows a clear concentration of the most massive anthropogenic sediments and structures in the eastern part of the first district, along the border to the second district.

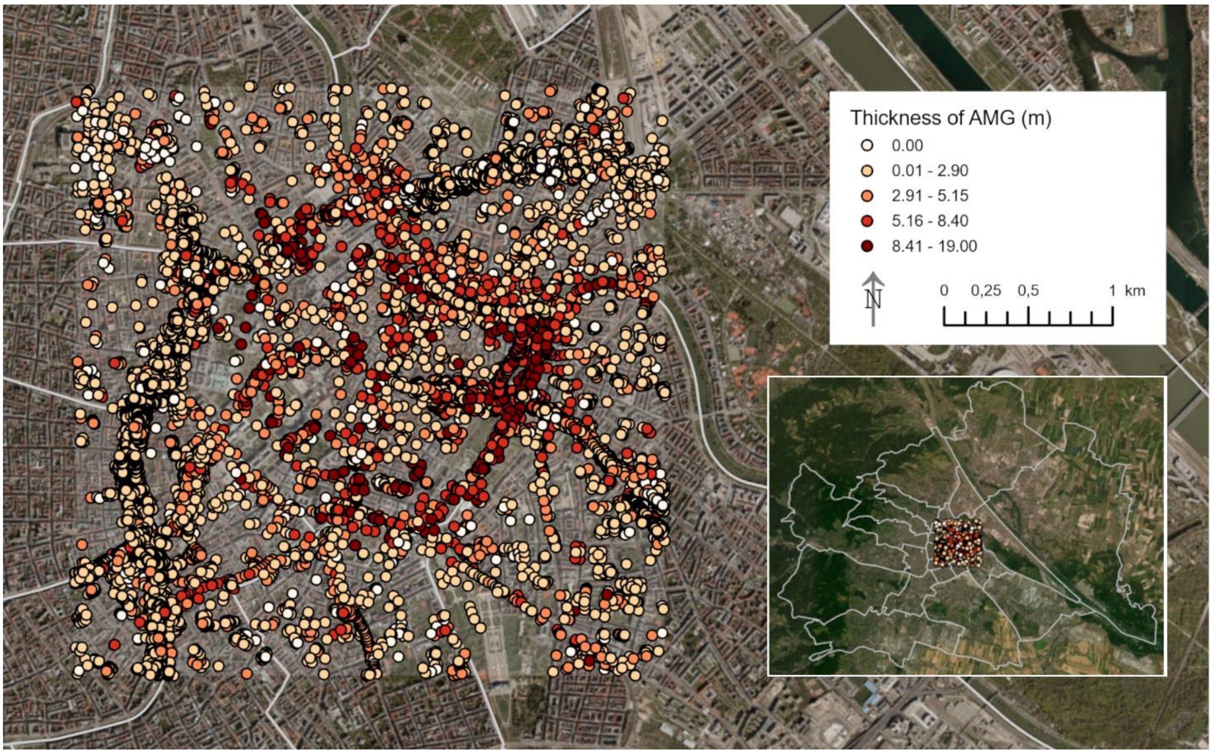

Figure 22: Thickness of anthropogenic sediments of dataset cat. (2)

6.3.3 Thickness regarding modern DTM

In the London study, Terrington et al. (2018) have called attention to changes in the thickness of AMG by using the start height of the well core only or by adding the modern DTM, including the AMG deposited during site redevelopment. Considering the modern ground level results in distinctly higher numbers: The mean thickness of 3.37 m in the City of London is increasing by almost 40 cm up to 3.74 m, and the maximum thickness in Tower Hamlets rises up to 13.52 m, which amounted 7.61 m by considering the thickness in the borehole records only.

Therefore, the modern DTM shall be included to compare the differences in the thickness calculations. For this, the elevation values of the modern DTM are extracted for every location of the well cores using the tool “Extract Values to Point” in ArcGIS Pro. The values are exported as CSV file and joined via Python script to the well core datasets. The elevation values of the drill starting points of the well cores are subtracted from the elevation value of the respective location and the difference is added to the previously calculated thickness of AMG documented in the well logs.

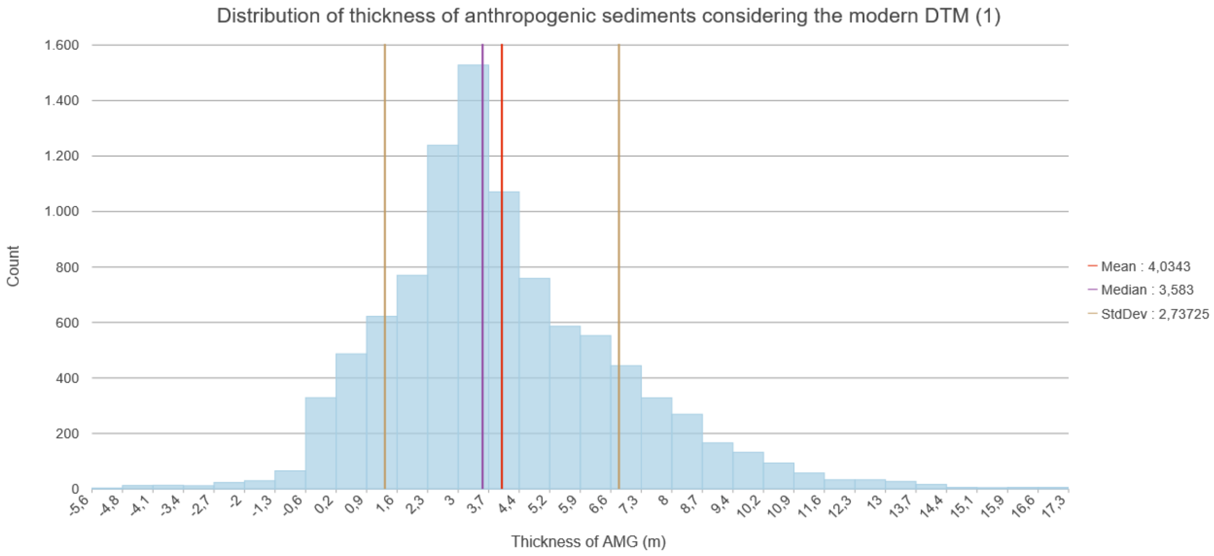

Figure 23: Histogram of the thickness of AMG considering the modern DTM in cat. (1) Incl. Amin excl. A?

Table 9: Statistics of the thickness of AMG considering the modern DTM in cat. (1) Incl. Amin excl. A?

Count	Min	1st Qu.	Median	Mean	3rd Qu.	Max	Skewness	Kurtosis
9830	-5.56	2.35	3.58	4.03	5.52	17.29	0.74	4.27

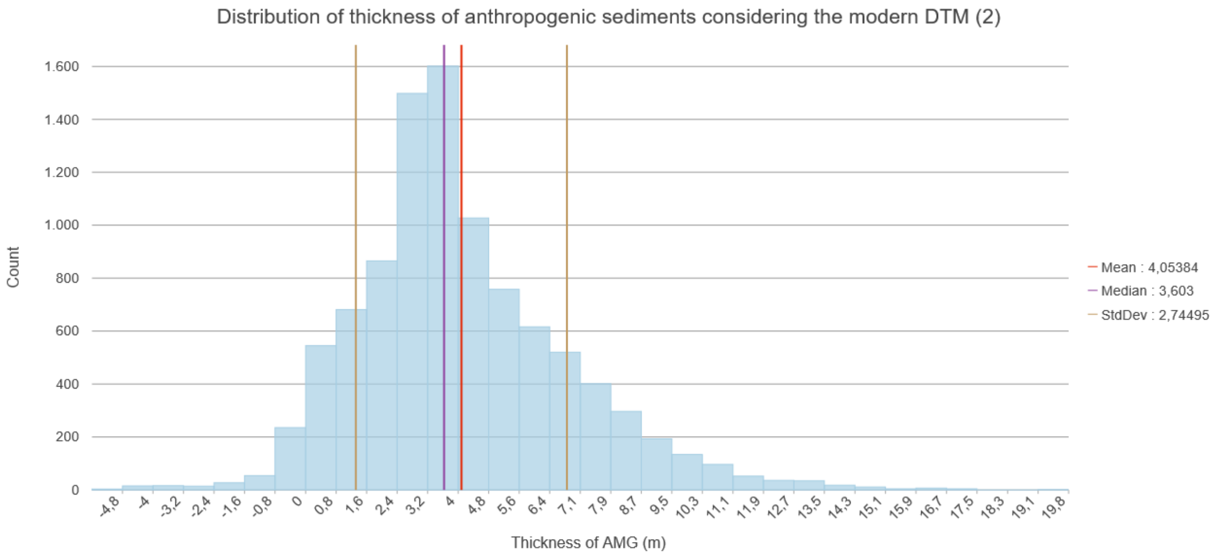

Figure 24: Histogram of the thickness of AMG considering the modern DTM in cat. (2) Incl. Amin incl. A?

Table 10: Statistics of the thickness of AMG considering the modern DTM in cat. (2) Incl. Amin incl. A?

Count	Min	1st Qu.	Median	Mean	3rd Qu.	Max	Skewness	Kurtosis
9877	-5.56	2.38	3.6	4.05	5.54	19.85	0.75	4.34

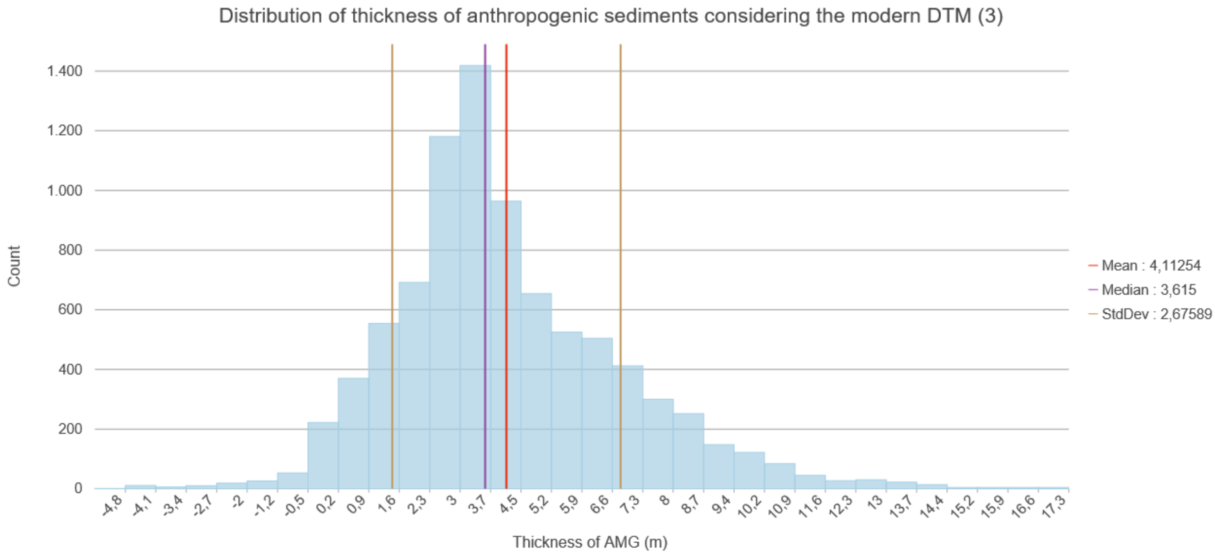

Figure 25: Histogram of the thickness of AMG considering the modern DTM in cat. (3) Excl. Amin excl. A?

Table 11: Statistics of the thickness of AMG considering the modern DTM in cat. (3) Excl. Amin excl. A?

Count	Min	1st Qu.	Median	Mean	3rd Qu.	Max	Skewness	Kurtosis
8759	-5.53	2.47	3.62	4.11	5.6	17.29	0.78	4.31

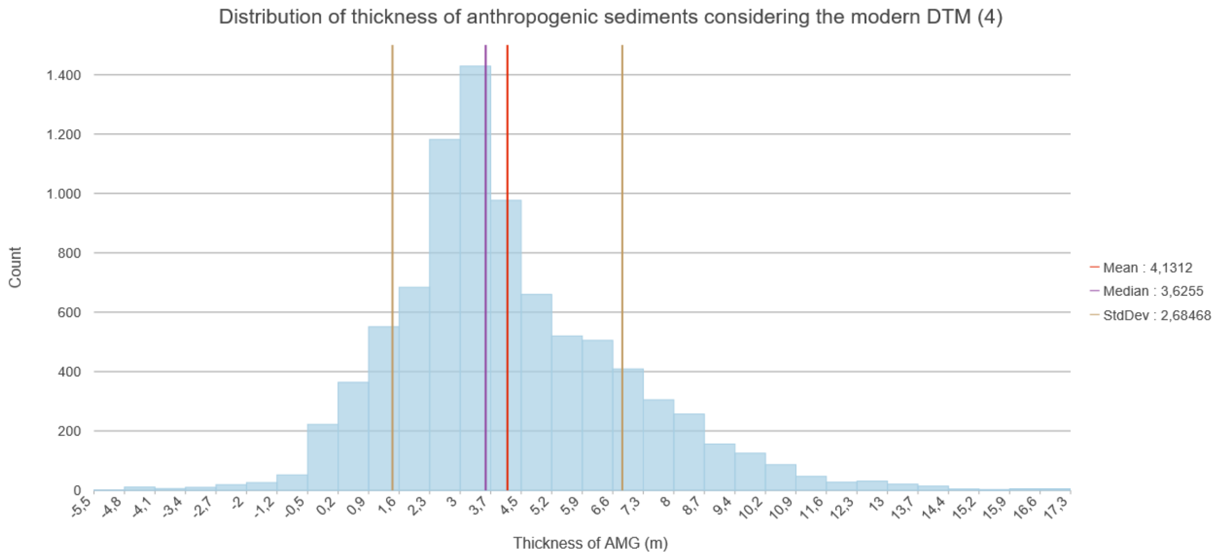

Figure 26: Histogram of the thickness of AMG considering the modern DTM in cat. (4) Excl. Amin incl. A?

Table 12: Statistics of the thickness of AMG considering the modern DTM in cat. (4) Excl. Amin incl. A?

Count	Min	1st Qu.	Median	Mean	3rd Qu.	Max	Skewness	Kurtosis
8791	-5.53	2.48	3.63	4.13	5.61	17.29	0.78	4.32

Recalculating the statistics considering the modern DTM results in completely different distributions than before (fig. 23–26 and tab. 9–12). In some areas, the current ground level is lower than at the time of the drilling, therefore negative values of thickness are included as well. The values cover a significantly larger range than before, reaching from -5.5 to 17.3 and 19.9 m. The distribution of the values approaches a normal distribution, still positively skewed and with a high kurtosis, yet lower than without considering the modern DTM. Although also negative values are included, the new distributions show a considerable rising of the Mean from about 2.3 to ca. 4.1 m, which means an increase of 1.8 m compared to data sets of the well cores only. Thus, the removal of anthropogenic sediments and the lowering of the terrain is obviously rare. Yet, from these results it cannot be directly derived that massive amounts of anthropogenic sediments have been deposited in the last 170 years. As mentioned above, the drilling starting points of the Viennese well cores often do not reflect the actual terrain level of that time. Therefore, the drastic increase of median and mean may simply reflect this elevation difference.

Finally, also the statistics regarding the distribution of AMG thickness in the archaeological data points have been calculated. Using Python, the Z-value of the data points are subtracted from the values of the DTM at the corresponding position. The data set is considerably smaller counting only 2,259 points, nevertheless it reflects almost the same range as the well cores, reaching from -0.2 to 16.7 m of deposits of anthropogenic origin (fig. 27 and tab. 13). The kurtosis of 12.7 displays a high dispersion of the distribution, which is caused by a single outlier with 16.7 m thickness of AMG, followed by the second highest value with only 10 m.

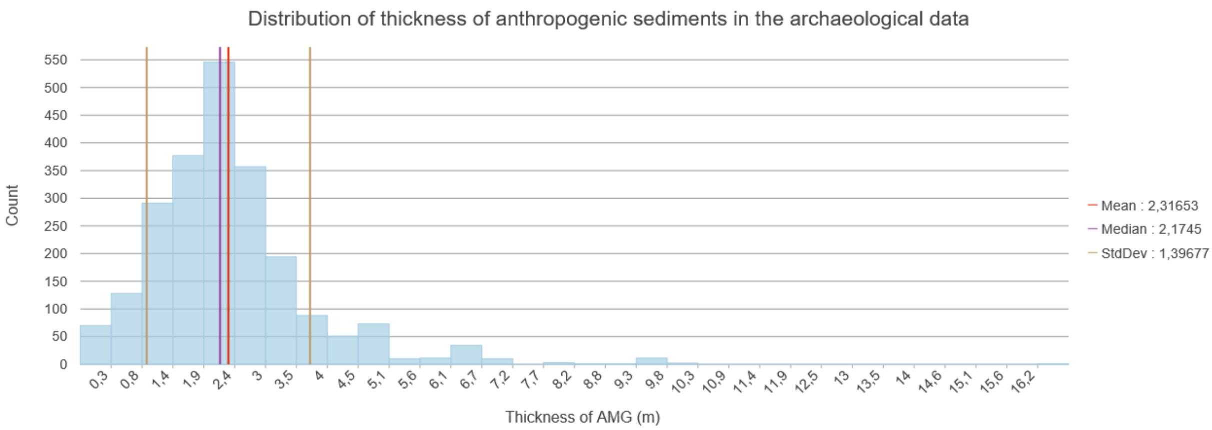

Figure 27: Histogram of the thickness of AMG in the archaeological data, considering the modern DTM

Table 13: Statistics of the thickness of AMG in the archaeological data, considering the modern DTM

Count	Min	1st Qu.	Median	Mean	3rd Qu.	Max	Skewness	Kurtosis
2259	-0.22	1.45	2.17	2.32	2.69	16.69	2.07	12.68

6.4 Comparison of categories

To determine how the inclusion of the well cores classified as A_min affects the results of the gridding, the volumes of the four categories are compared. For the calculation of the volume of the anthropogenic soils, the volume calculator of Surfer is used. The modern DTM of the study area represents the top layer for this task, by which the actual volume is calculated. As bottom layer, the gridded surfaces are used. For calculating the volume, both grids, the upper and lower surface, must have the same grid file geometry, so must be equal in their X/Y-extense and their grid resolution (number of grid nodes). Moreover, X, Y and Z units have to match, which is fulfilled by the data (all of them are in metres).

Four grids are calculated as lower surface, using the lower boundary values in m.ü.A. They were using the datasets of the four categories defined in Chapter 6.2 (Defining categories) and display (1) well cores including A_min excluding A?, (2) well cores including A_min including A?, (3) well cores excluding A_min excluding A? and (4) well cores excluding A_min including A?. The calculation of the volume of anthropogenic sediments for each of these four grids shall show the extent of difference between the four categories. For this, each of the four data sets is gridded using the "Triangulation with Linear Interpolation" method and the tool "Grid Data" in the Surfer software. This is an exact interpolation method, not extrapolating grid values beyond the data's Z range. For the output grid geometry, the bounding box extents are used as well as a spacing (grid cell size) of 10 m.

The DTM, which has a resolution of 1 m, needs to be resampled to match the grid of the lower surface. By the tool "Grid Mosaic", the DTM of the study area is gridded to the extent of the study area with a spacing (grid cell size) of 10 m and 351 nodes.

Already the visual analysis of the four grids (as contours) reveals strong varieties between the data sets with and without well cores classified as A_min. Calculating the volume using the tool "Grid Volume" produces the following results (tab. 14, the complete Grid Volume Reports are included in Appendix A).

Table 14: Calculated grid volumes by using the modern DTM and the grids of the four categories (gridded by Triangulation with Linear Interpolation)

	Category (1)	**Category (2)**	**Category (3)**	**Category (4)**
Cut & Fill Volumes				
Positive Volume [Cut]	41,838,144.61	42,032,512.76	45,834,166.74	46,109,656.13
Negative Volume [Fill]	1,126,236.31	1,123,126.20	941,994.86	937,204.66
Net Volume [Cut-Fill]	40,711,908.31	40,909,386.56	44,892,171.88	45,172,451.47
Planar Areas				
Positive Planar Area [Cut]	11,545,516.89	11,546,282.72	11,597,250.01	11,603,177.72
Negative Planar Area [Fill]	501,133.11	500,367.28	442,299.99	436,372.28
NoData Planar Area	203,350	203,350	210,450	210,450
Total Planar Area	12,250,000	12,250,000	12,250,000	12,250,000
Surface Areas				
Positive Surface Area [Cut]	11,645,768.16	11,647,195.08	11,685,548.74	11,691,829.42
Negative Surface Area [Fill]	526,901.55	526,113.88	466,633.96	460,652.53

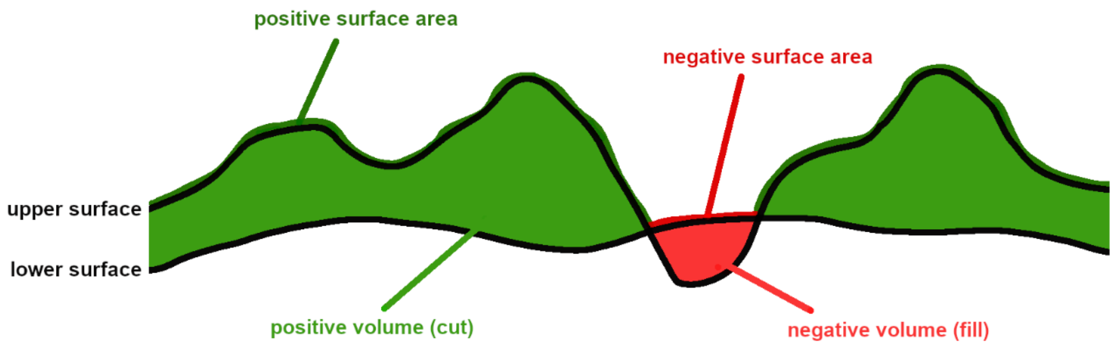

Figure 28: Principles of volume calculation in Surfer

The volumes calculated display the positive volume, the negative volume and the net volume. The positive volume or "cut" represents those parts, where the upper surface (in this study that is the modern DTM) is higher than the elevation of the Boundary A documented in the well cores (highlighted in green in fig. 28). The opposite is the case with the negative volume or "fill", where the upper surface, i.e. today's ground level, is lower than Boundary A at this location at the time of drilling, which means that the land has been lowered since the well core was drilled (highlighted in red in fig. 28). The net volume constitutes the difference cut and fill.

Comparing the results of the different volume calculations reveal major differences between the data sets including or excluding A_min well cores. Data sets (1) and (2), including A_min, display a significantly smaller positive volume (of about 4 million m³) than data sets (3) and (4) without A_min. Correspondingly, the negative volume of category (1) and (2) is about 180.000 m³ larger than the one of category (3) and (4). By these results it becomes obvious that including well cores classified as A_min leads to higher elevation values of the boundary A at different locations, which are apparently nowadays higher than the current ground level of the DTM. This conclusion is reflected in the values of the areas as well. So is the negative planar area about 60.000 m² larger using the well cores from the categories (1) and (2) than those from (3) and (4).

Regarding the differences between the data sets including or excluding A? (so (1) vs. (2) and (3) vs. (4)), those including A? have a higher positive volume of about 194,000 m³ (between (1) and (2)) and 275,000 m³ (between (3) and (4)), respectively. The negative volume is slightly lower with about 3,000 – 4,700 m³ by including A?. As the layers of A? included in these data sets always represent the bottom layers of the well cores, Boundary A is located lower in these cases, which leads to a higher positive volume.

To sum up, including A_min in the data sets leads to a clear raising of Boundary A in the interpolation. Since the bottom surface of A_min well cores do not necessarily equal Boundary A at this location, their inclusion delivers a distorted image of Boundary A. To overcome this issue, the well cores classified as A_min should only be included, if the interpolated Boundary A is higher than the values in the specific well cores at this position.

6.5 Removal of duplicates

The Gridding Report in Surfer has revealed duplicates that has automatically been removed. These well cores have shared the exact same coordinates, leading to different Boundary A elevation values at one position. In the data set with the most well cores, category (2), these duplicates counted 204 well cores. As a correction of these has to be done by the data provider, i.e. the Municipal Department for Bridge Construction and Foundation Engineering (MA 29 Brückenbau und Grundbau, Stadt Wien), a workaround had to be found for this study.

Using Python, the duplicates in the data sets of the four categories had been removed by keeping the one with the lowest Boundary A at this location. By this, well cores of later date are taken into account and the maximum extent of the artificially modified ground is considered in the data.[30] The script used is the following:

```
# Import module
import pandas as pd
# Open a new file
result = open("cat_1_without_dupl.csv", "w", newline='')
# Read the original CSV
orig = pd.read_csv("cat_1.csv", sep=';', decimal = ',', encoding='ISO-8859-1')
# Sort by elevation of Boundary A
orig = orig.sort_values(by = ['UK_Ansch'])
# Drop duplicates of every location, keep the one with lowest Boundary A
noDup =
orig.drop_duplicates(subset=['X','Y'],keep='first').set_index('EDVNR')
# Set well core ID as Index
noDup.set_index('EDVNR', inplace=True)
# Save as CSV
noDup.to_csv(result, sep=';', decimal = ',')
# Close the file
result.close()
```

The statistics of the data sets changed slightly due to this adaptation (tab. 15).

Table 15: Updated statistics due to the removal of duplicates

	Count	**Min**	**1st Qu.**	**Median**	**Mean**	**3rd Qu.**	**Max**	**Skewness**	**Kurtosis**
Cat. (1)	9717	0	0.3	1.4	2.28	3.35	16.4	1.69	6.18
Cat. (2)	9763	0	0.3	1.4	2.3	3.4	19	1.7	6.25
Cat. (3)	8683	0	0.3	1.45	2.31	3.4	16.35	1.64	5.93
Cat. (4)	8714	0	0.3	1.5	2.32	3.4	16.35	1.65	5.93

6.6 Trend and outlier analysis

Spatial trends can affect the interpolation results, therefore, the data sets are analysed visually by building Voronoi polygons using ArcGIS Pro (tool: “Create Thiessen Polygons”). The polygons are symbolised using the elevation heights of Boundary A of every well core (in *m.ü.A.*) (fig. 29 is showing the polygons for the well cores of category (2)). A clear spatial trend

[30] This workflow has been approved afterwards by the corrections sent by the MA 29: the majority of duplicate well cores with no AMG were driving tests and should not have been included in the data set. Other duplicates were started as shaft and then continued by drilling (personal comment by Christine Jawecki, MA 29, on the 13th of February 2020). Regarding this information, taking the lowest boundary of anthropogenic sediments at every position is correct.

is visible, with high elevation levels in the western and southern part of the study area, which are descending in a north-easterly direction. This reflects the natural topography of the study area, which shows a slope towards the Danube Canal and is visible in the modern DTM as well (cf. fig. 12). This trend will be removed in the later interpolation processes.

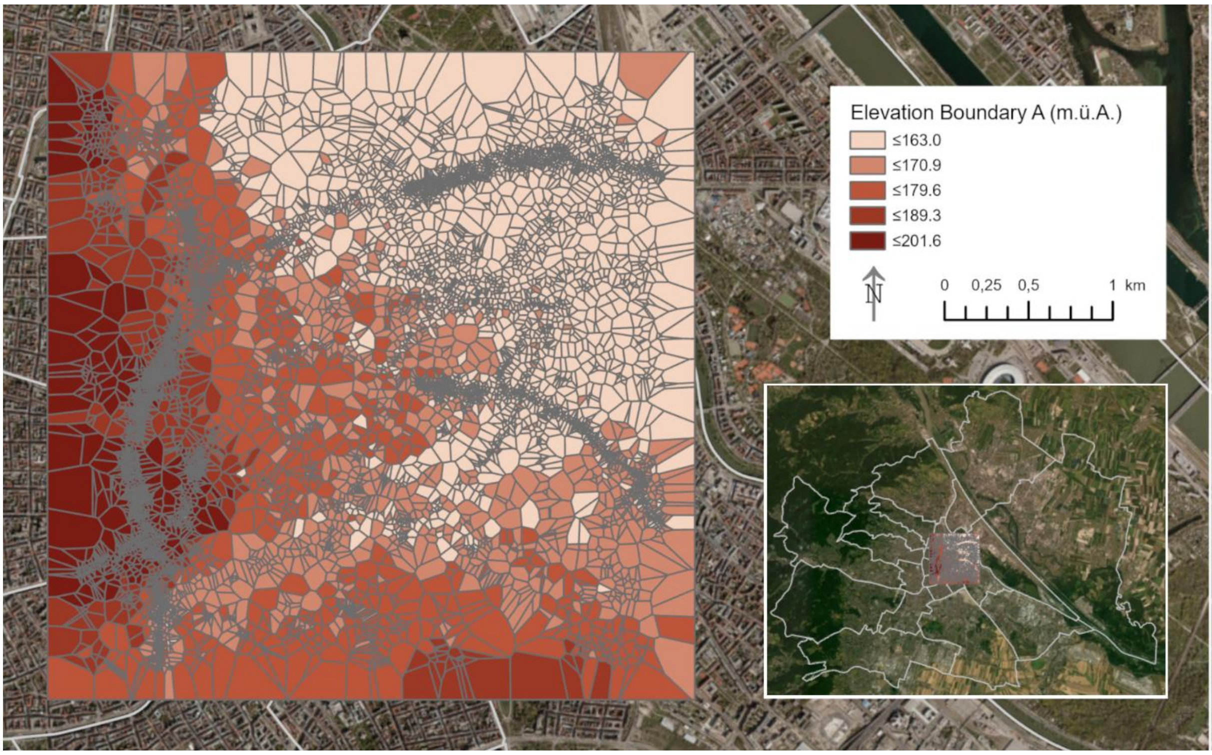

Figure 29: Voronoi polygons reflecting the elevation of Boundary A of the data set cat. (2)

Additionally, the quality of the interpolation process depends on the detection of global and local outliers.[31] Global outliers have been detected and corrected or removed from the data sets already during the ESDA phase using histograms and statistics. By checking the neighbourhood of every well core comparing the Voronoi polygons, only one well core stands out by varying widely from all neighbouring drillings (fig. 30, position visible in fig. 29: the single light polygon in the south-western third).[32] This well core is situated in front of the museums area "Museumsquartier", with a Boundary A elevation of 162,88 m, yet being encircled by well cores documenting the Boundary A at an elevation of about 180 m.ü.A. In addition, this well core is the one with the thickest AMG of the whole study area, for A (16.4 m) as well as for A? (19 m). Furthermore, it belongs to the class "A_min". Apparently, a wall was hit at this depth and therefore all overlying layers were assigned as A or A? (which does not necessarily have

[31] On the treatment of outliers cf. Kitanidis 1997.
[32] EDVNR 17104002.

to be the case).[33] As anthropogenic sediments and structures do not follow strict logical rules, a local outlier can be a true reflection of the Boundary A at this location. Nevertheless, since the well core belongs to the class "A_min", it will be inserted only in a later step into the interpolation.

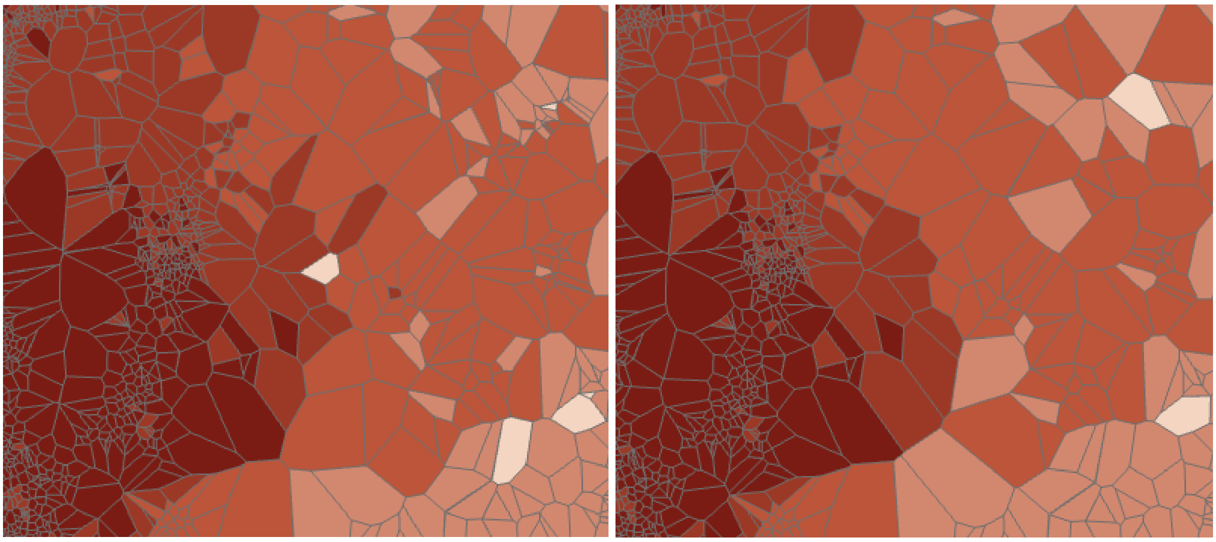

Figure 30: Comparison of the Voronoi polygons of cat. (2) (left), including the well core no. 17104002, and cat. (3) (right), excluding all well cores defined as "A_min". Location: South-western part of the study area, classification following fig. 29

6.7 Interpolation

The terms "interpolation" or "gridding" denote the estimation of values of a regionalised variable at locations where it has not been measured (Chilès and Delfiner 2012). Aim of this study is to deliver an approximation of Boundary A, i.e. the boundary between artificially modified ground and natural geological ground. Therefore, for the gridding process, the Boundary A values of the data sets are used. For testing the interpolation, the data set of category (3) is applied – excluding A_min to not deliver wrong values (cf. Chapter 6.4) and excluding A?, to show only the certain Boundary A. The values of category (3) range from 148.53 to 201.6 m.ü.A (fig. 31 and tab. 16). As could have been expected from the ESDA regarding the AMG thickness, the elevation values show a positively skewed distribution (skewness 0.64), yet with a low kurtosis of 2.11. As determined in Chapter 6.6, these differences can be explained by the global trend in the study area.

[33] Personal comment by Christine Jawecki, MA 29, on 12th of Febrary 2020, who kindly delivered the original PDF of the well log.

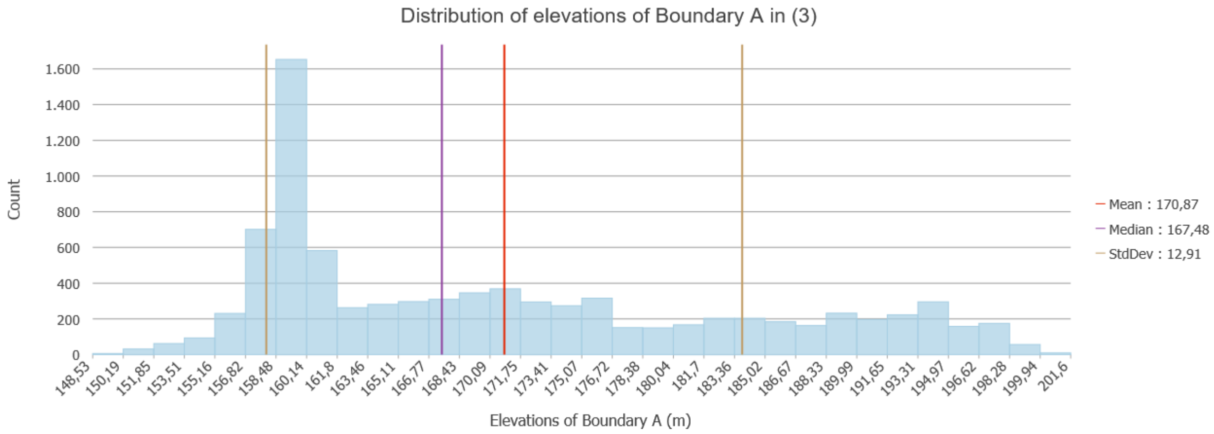

Figure 31: Histogram of the elevation of Boundary A in cat. (3) Excl. Amin excl. A?

Table 16: Statistics of the elevation of Boundary A in cat. (3) Excl. Amin excl. A?

Count	Min	1st Qu.	Median	Mean	3rd Qu.	Max	Skewness	Kurtosis
8683	148.53	159.47	167.48	170.87	181.08	201.6	0.64	2.11

6.7.1 Variogram

A variogram displays the spatial continuity or roughness of a data set and thereby reveals correlations between measured values. (Kitanidis 1997; Chilès and Delfiner 2012; Barnes 2003; Golden Software 2019).[34] The knowledge about existing autocorrelation in the data set is a prerequisite for the interpolation process. For the variogram analysis, the "empirical" or "experimental variogram" is calculated from the values of the data set and a fitting "variogram model" is chosen by matching the shape of the curve of the empirical variogram (Barnes 2003). The mathematical definition of the theoretical variogram is

$$\gamma(\vec{h}) = \frac{1}{2}\mathrm{E}\left[[Z(\vec{x}+\vec{h}) - Z(\vec{x})]^2\right] = \frac{1}{2}\mathrm{Var}\left[Z(\vec{x}+\vec{h}) - Z(\vec{x})\right] \tag{1}$$

where $Z(\vec{x})$ and $Z(\vec{x}+\vec{h})$ are regionalized random variables (in this case the elevation values of Boundary A) and $\vec{x}$ and $\vec{x}+\vec{h}$ represent the spatial positions separated by a vector $\vec{h}$ (Bachmaier and Backes 2008).

[34] On the terms "variogram" and "semivariogram" see Bachmaier and Backes 2008.

The empirical variogram is calculated by the following formula

$$\hat{\gamma}(\vec{h}) = \frac{1}{2} \cdot \frac{1}{N(\vec{h})} \sum_{i=1}^{N(\vec{h})} \left[z(\vec{x}_i + \vec{h}) - z(\vec{x}_i) \right]^2 \qquad (2)$$

where $z(\vec{x_i} + \vec{h})$ and $z(\vec{x_i})$ are the measured values of Z at $N(\vec{h})$ pairs of comparisons, $\vec{x}_i + \vec{h}$ and $\vec{x}_i$, separated by the vector $\vec{h}$. So, the variogram function shows the average dissimilarity between points separated by the specified vector $\vec{h}$.

Linear detrending is used to remove the trend detected before (cf. Chapter 6.6 Trend and outlier analysis). As can be seen in Figure 31, a drift or trend distorts the empirical variogram, so by using a trend removal, a polynomial least squares regression is carried out, computing the variogram for the remaining residuals only (Kitanidis 1997; Chilès and Delfiner 2012; Golden Software 2019). Figure 32 shows the omni-directional variogram model of the data set of cat. (3) without trend removal. By applying linear detrending, the linear drift in the study area is considered and as a result, the elevation levels of Boundary A are approximately normally distributed, as can be seen in Figure 33 (value points are almost equally visible on the top and the bottom view). Therefore, the linear detrending was assessed as sufficient for the further interpolation process (cf. fig. 34 showing the variogram models using linear trend removal).

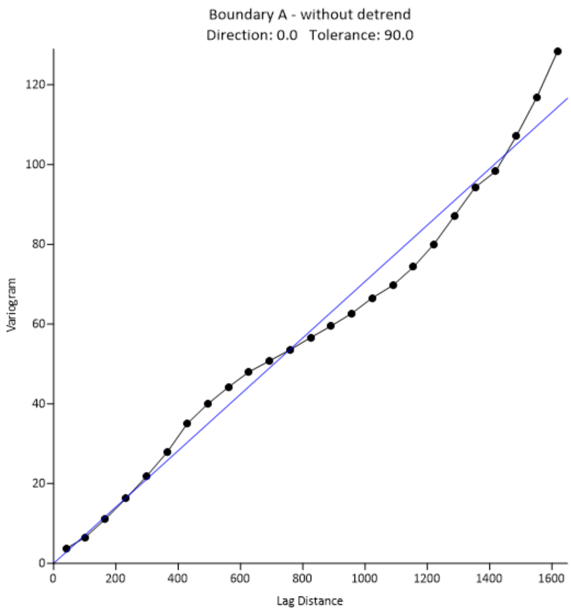

Figure 32: Variogram model showing the empirical model of data set cat. (3) without trend removal

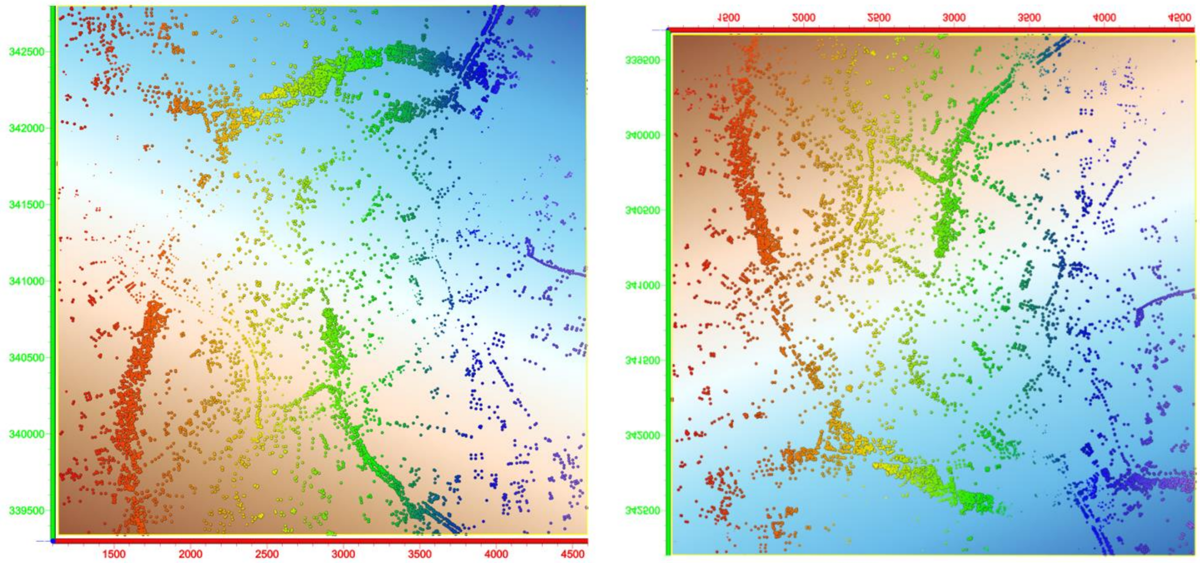

Figure 33: Distribution of elevation values of Boundary A of data set cat. (3) on a grid simulating the linear drift of the study area. Visualisation in Voxler (Golden Software). On the left: view on top, on the right: view on bottom

Besides the detection of autocorrelation, the variogram displays the existence of “geometric anisotropy”, which is present if the empirical variogram shows different length ranges in different directions (Barnes 2003). The variogram surface shows a strong correlation in southwest–northeast direction for short distances and in southeast-northwest direction for very short and long distances. This can also be seen in the variogram itself: the omni-directional empirical model is consistently to the right of the ascending part of the model variogram between 0° and 70° as well as between 160° and 180°. In contrast, between 70° and 160° degrees, the omni-directional model is consistently to the left of the ascending part of the model variogram. This can be evaluated as a clear indication of geometric anisotropy (Barnes 2003, cf. Chilès and Delfiner 2012). By defining an anisotropy ratio and angle, points in specific directions are given more weight in determining the value of the estimated point (Golden Software 2019).

Using the variogram tool in Surfer, two variogram models have been created that shall be tested in the interpolation. The first one is a Gaussian model combined with a nugget effect, the second a so-called nested model, combining a nugget effect, a Gaussian at the lower range and a spherical model at the higher range (fig. 34). Both show an anisotropy ratio of 3 (in the nested model divided between Gaussian and spherical part) and an anisotropy angle of 30°.

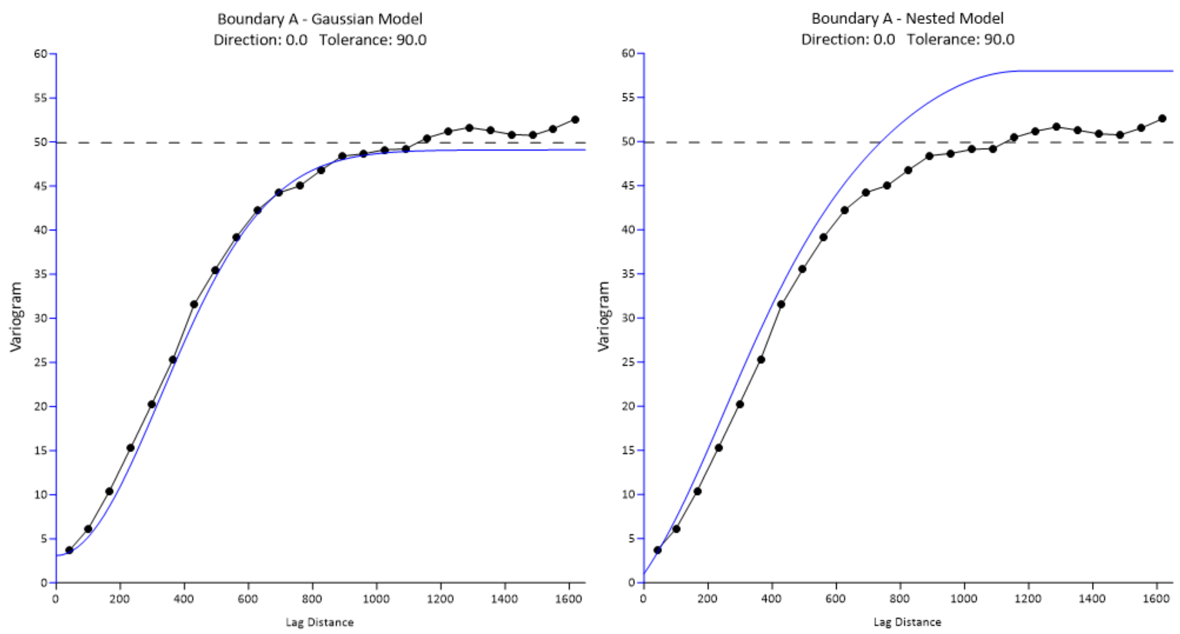

Figure 34: Omni-directional variogram models created for the data set of cat. (3). On the left side the Gaussian Model with nugget effect, on the right side the nested model (nugget effect, Gaussian and spherical model). The variance of the observed data is depicted as dashed line

6.7.2 Kriging

For this study, the interpolation method "kriging" is used, a method named in 1963 by G. Matheron in honor of the mining engineer Danie Krige (Cressie 1990). Kriging applies the methodology known as best linear unbiased estimation (BLUE) and is used in various fields as mining, geology or hydrology. Compared to other methods as IDW and Thiessen polygons, it is more flexible and is considering distances and spatial autocorrelation between the measured values. Being based on the variogram model, an interpolation function is produced that is able to estimate appropriate values.

In Kriging, the linear function that deals as estimator determines weights that are unbiased and minimise the estimation variance (Kitanidis 1997; Chilès and Delfiner 2012). "Unbiased" means that (on the average) the error of estimation is zero, whereas "minimise the estimation variance" means that (on the average) the square estimation error is as small as possible. To sum up, the main controls on kriging weights are the distance of data to the location being estimated, the redundancy between data and the variogram (Pyrcz 2018).

The formula is the following:

$$Z(s) = \mu(s) + \varepsilon(s) \tag{3}$$

where $Z(s)$ is the estimated variable at location s, $\mu(s)$ is a deterministic trend and $\varepsilon(s)$ is formed by random, autocorrelated errors (Johnston et al., 2004).

If the nugget effect equals zero, kriging is an exact interpolator, i.e. the contour surface of the estimate reproduces the measurements. If a nugget effect is defined, the contour map will have a discontinuity at each observation point and the interpolation will be smoothed (Kitanidis 1997; Golden Software 2019). Since both variograms are including nugget effects, the interpolation outputs will not reproduce the exact measurements at each data point.

Since a global trend has been detected in the study area (sloping terrain towards the north-east), “universal kriging” or “kriging with a drift” is the best kriging method to be used (Kitanidis 1997; Chilès and Delfiner 2012). In universal kriging, the function is “considered as the sum of a deterministic drift m(x) (usually a polynomial with unknown coefficients) and a zero-mean stationary or intrinsic random residual Y(x)” (Chilès and Delfiner 2012, 122).

In Surfer, the data set of cat. (3) was gridded by choosing the gridding method “kriging”. For comparison, the process was done with both variograms, the Gaussian and the nested model. After the respective model was imported, the drift type in the kriging parameters was set to “linear”, considering the global trend in the study area. By choosing “linear”, universal kriging is applied. Regarding the distribution of data points, just one sector is used in the “search neighbourhood” parameters. The maximum data to use from all sectors is set to 65, the minimum to 8. As search ellipse, a circle with 400 m radius is applied, as by this setting no cells are assigned as NoData.

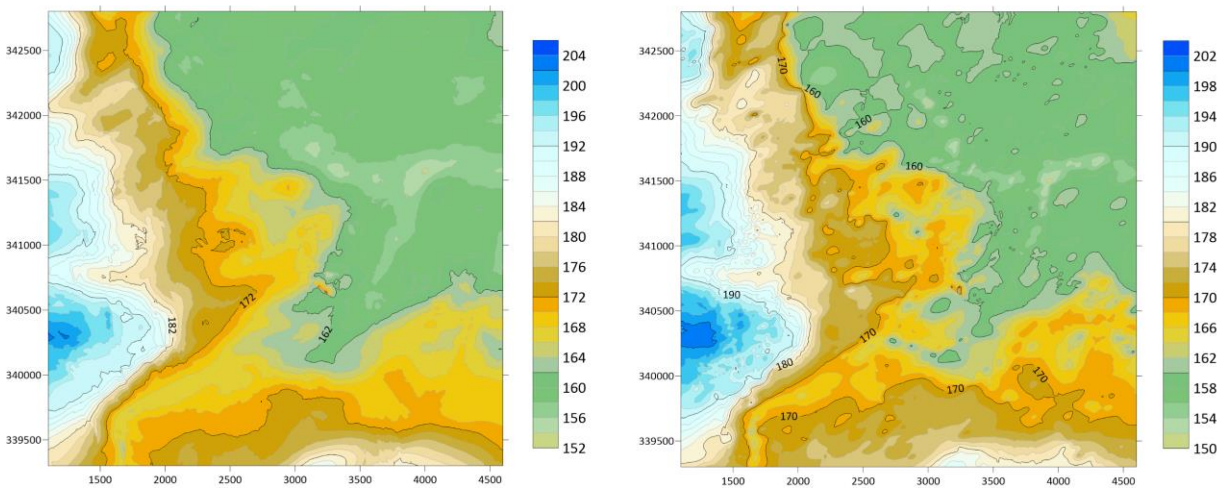

Figure 35: Gridding results of the Boundary A using Universal Kriging; on the left using the Gaussian variogram model, on the right using the nested variogram model

As can be seen in the results (fig. 35), the values in the interpolation using the Gaussian variogram model are slightly overestimated (compared to the actual range of data between 148.53 to 201.6 m) and the surface is considerably smoother, due to the higher nugget effect.

6.7.3 Cross validation

For assessing the quality of the kriging results, cross validation is used. During this process, each measurement point is successively removed from the interpolation model and replaced by its estimated value. By comparing the values of the measured point and the estimated point the difference, i.e. the residuals, are obtained (error = interpolated value – observed value). The sum of the squared residuals over all measurement points is then a measure for the quality of the model (Golden Software 2019).

As recommended by Surfer, three values of the cross validation report are used as quantitative measures to evaluate the variograms: the median absolute deviation of the cross validation residuals, the standard deviation of the cross validation residuals, and the rank correlation between the measurements and the estimates (tab. 17). Regarding the values of the cross validation as well as the gridding results, the nested variogram model seem to be a better fit for the actual data, providing a more reliable estimation model (the complete Cross Validation Reports are included in Appendix C).

Table 17: Cross validation reports for the Gaussian and the Nested variogram model using the data set cat. (3)

	Gaussian variogram model	**Nested variogram model**
Median Absolute Deviation	1.067	0.824
Standard Deviation	2.092	1.849
Rank Correlation	0.962	0.969

6.7.4 Adding the archaeological data set

To ameliorate the kriging result, the archaeological data points representing Boundary A, extracted from the digital excavation maps, shall be added to the data set of category (3). Regarding the statistics, inserting the 2,259 archaeological data points leads to a slightly higher median (fig. 36 and tab. 18). Minimum and maximum value stay the same, yet, the new data points are mainly adding elevations to the medium range of the spectrum. This can be easily explained by the location of the new data points: As the excavations are mostly situated in the first district, their elevation neither reflect the highest values of the topography to the west nor the lowest elevations to the north-east (cf. fig. 10 showing the spatial distribution of the archaeological data).

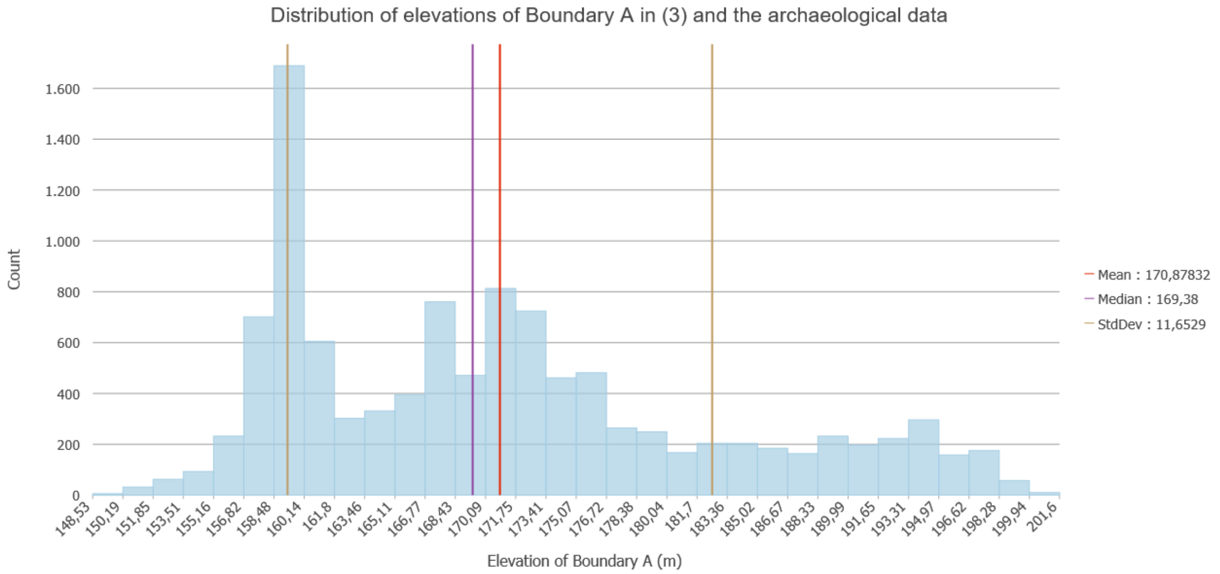

Figure 36: Histogram of the elevation of Boundary A in cat. (3) (excl. Amin excl. A?) and the archaeological data

Table 18: Statistics of the elevation of Boundary A in cat. (3) (excl. Amin excl. A?) and the archaeological data

Count	Min	1st Qu.	Median	Mean	3rd Qu.	Max	Skewness	Kurtosis
10942	148.53	160.0	169.38	170.88	177.2	201.6	0.69	2.54

The combined data set is gridded by universal kriging, using the nested variogram and the settings mentioned above in Chapter 6.7.2 (Kriging). The results are clearly enhancing the gridding in the centre of the study are, i.e. the first district, where most of the added excavation sites are situated (fig. 37). The more detailed information in the city centre leads to a more differentiated Boundary A that is often higher than in the grid based on the well cores only. The disperse areas with dense archaeological data show the potential for improvement if more archaeological data would be available for the whole study area.[35]

[35] Also, the above mentioned factors of the cross validation were improved by adding the archaeological data: the median absolute deviation of the cross validation residuals now accounts for 0.648 (compared to 0.824), the standard deviation of the cross validation residuals amounts to 1.700 (compared to 1.849). However, the rank correlation between the measurements and the estimates is slightly higher with 0.978 (compared to 0.969).

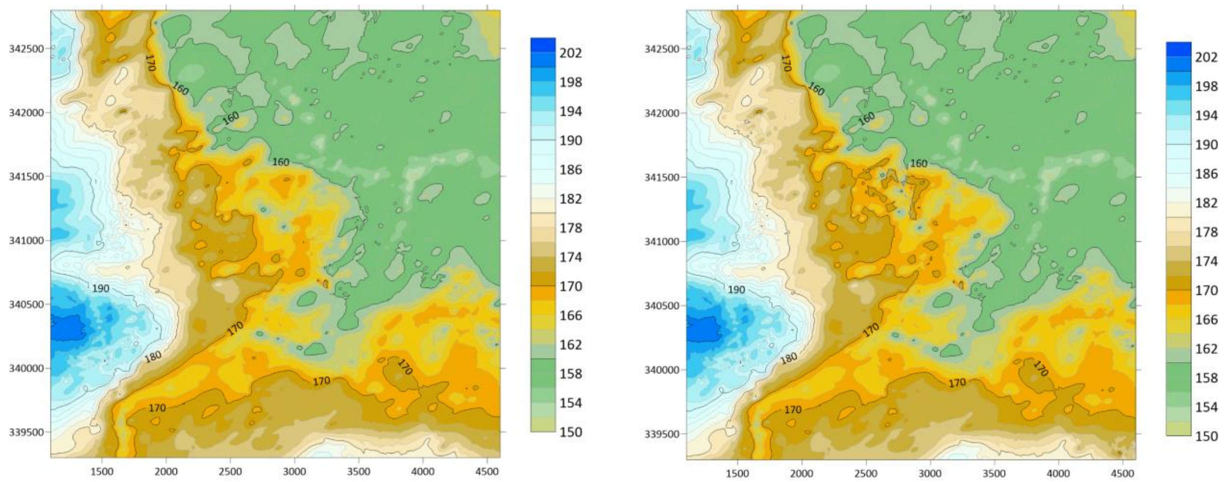

Figure 37: Comparison between the kriging results of the data set of cat. (3) without (on the left) and with the archaeological data added (on the right)

6.7.5 Adding the well cores of class "A min"

As mentioned above in Chapter 6.4 (Comparison of categories), the well cores classified as "A_min" only show the minimum extent of the anthropogenic sediments at this location and therefore should only be implemented, if the interpolation of Boundary A at this location is too high. Thus, the following workflow has been developed: From the grids, obtained by interpolating the data sets without "A_min" well cores, the elevation value is extracted at the locations of the drillings classified as "A_min" by the "Point Sample" tool in Surfer. In Python, a new field was calculated by subtracting the extracted elevation grid values from the lower boundary elevation of the A_min well cores. If the result is < 0, the interpolation of Boundary A is too high at this location and the well core is extracted (for a better understanding, see fig. 38). The extracted well cores of A_min are then added to the data set used for gridding and the interpolation is redone.[36] In case of the data set of cat. (3), the lower boundary of 387 of the 1034 well cores of A_min is not correctly represented by the interpolation and those well cores are added to the data set of cat. (3). The deviations of the lower boundaries of those 387 well cores range from 0.08 cm to 15.39 m in case of well core no. 17104002, which is the well core that stood out by its difference in elevation compared to its neighbours (cf. Chapter 6.6 Trend and outlier analysis). This well core is also visible in the gridding result (highlighted with a red square on fig. 39). Besides that, only minor changes are visible in the produced grids.

[36] This workflow has been stimulated by a comment by Justine Carstairs, Golden Software Technical Support, on the 10th of February 2020.

The same procedure was performed using the grid and data set including the archaeological data points (fig. 39, on the right). In this case, slightly more well cores of A_min have to be added for regridding (399 well cores), as the archaeological data has shifted Boundary A little higher compared to the data set including only well cores.

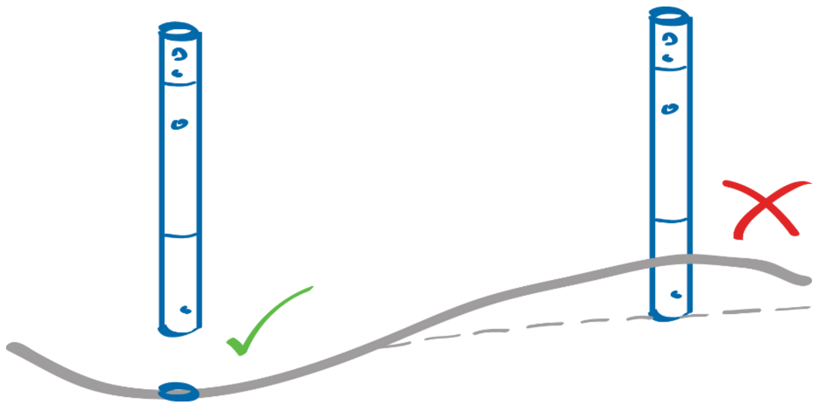

Figure 38: Visualisation of the workflow regarding the well cores “A_min”: On the left, the interpolation fits the data whereas on the right, Boundary A is interpolated too high. This well core has to be included into the data set

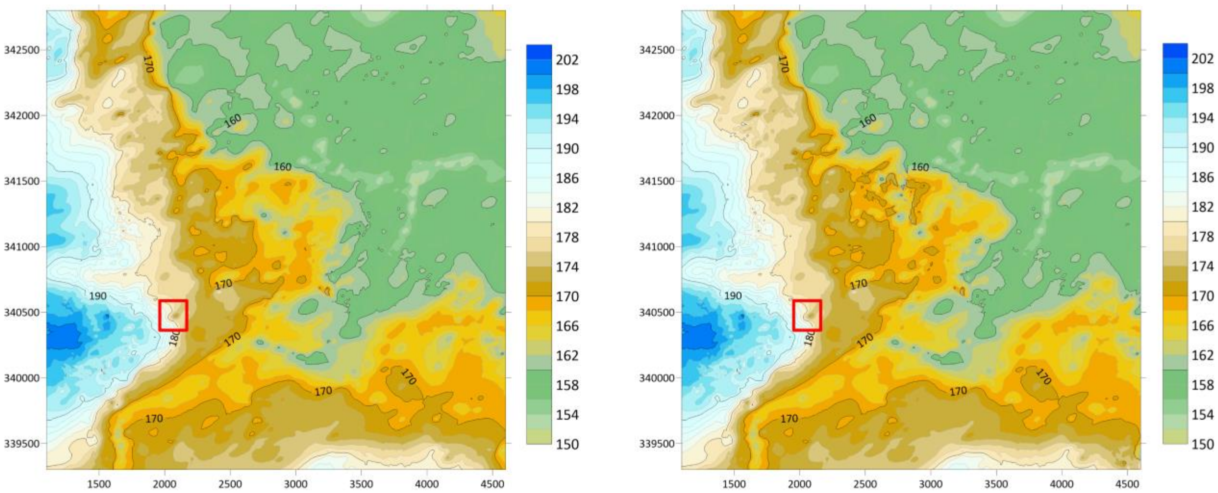

Figure 39: Comparison between the kriging results of the data set of cat. (3) without (on the left) and with the archaeological data implemented (on the right), both including the well cores classified as A_min. Well core no. 17104002 is marked in red

6.7.6 Comparing A to A?

Categories (2) and (4) include layers labelled as “A?”, i.e. sediments that cannot be classified as of anthropogenic origin with certainty, as lower boundaries. To compare these data sets to the previous results, they are processed using the same steps. Adding the archaeological data leads to similar statistics as the data set of cat. (3) (fig. 40 and tab. 19).

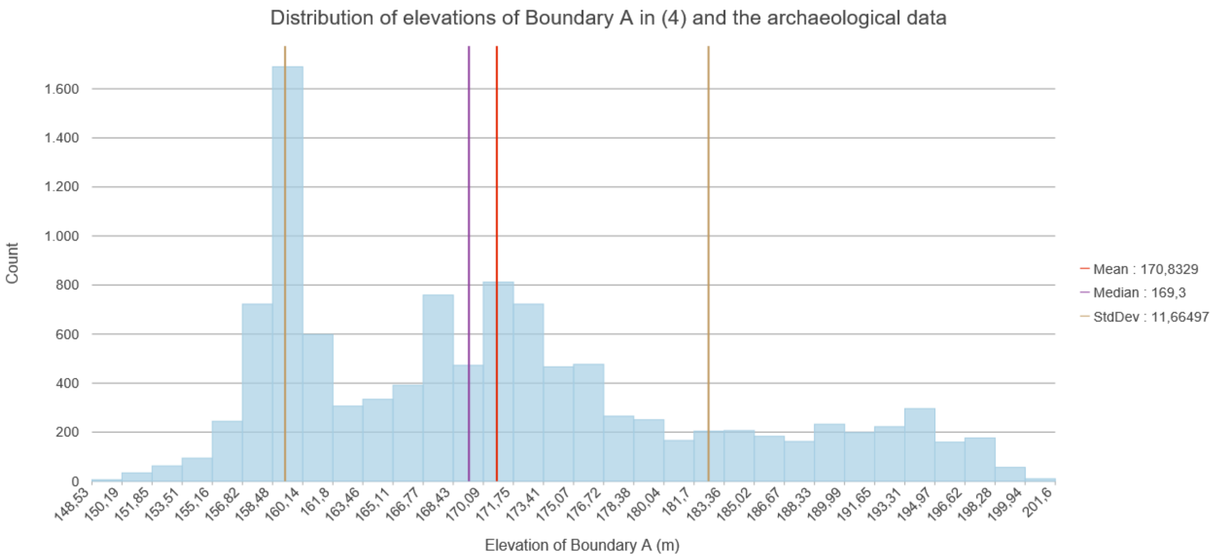

Figure 40: Histogram of the elevation of Boundary A in cat. (4) (excl. Amin excl. A?) and the archaeological data

Table 19: Statistics of the elevation of Boundary A in cat. (4) (excl. Amin excl. A?) and the archaeological data

Count	Min	1st Qu.	Median	Mean	3rd Qu.	Max	Skewness	Kurtosis
10973	148.53	160.0	169.3	170.83	177.2	201.6	0.69	2.54

Subsequently, the data sets with and without archaeological addition are gridded using the beforehand defined settings. Fig. 41 shows the gridding outcomes of the data set of cat. (4) with and without the archaeological data points added, for which the same observations can be stated as before: for the areas with archaeological excavation data available, a more differentiated and reliable interpolation can be seen.

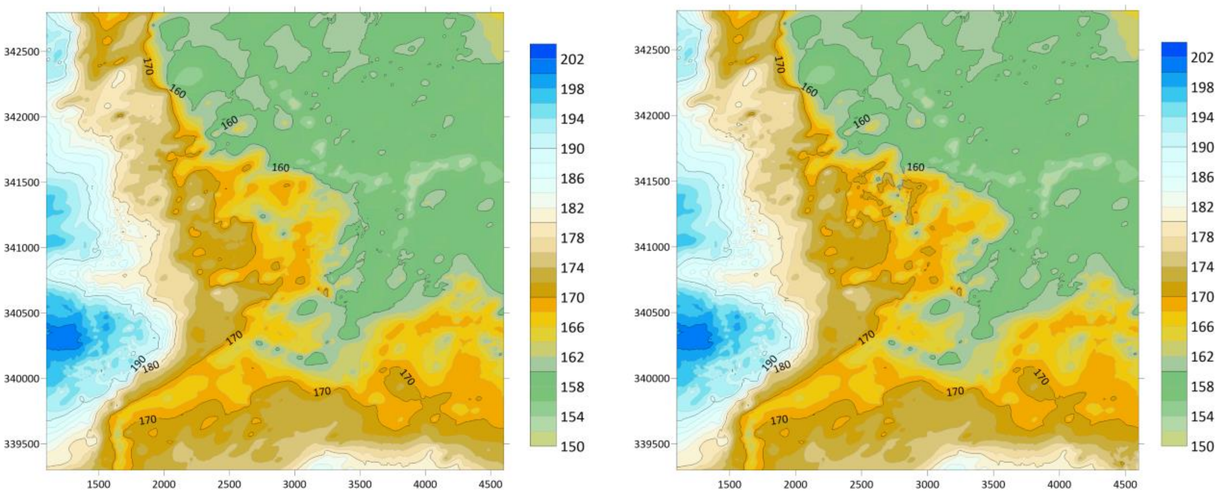

Figure 41: Comparison between the kriging results of the data set of cat. (4) without (on the left) and with the archaeological data implemented (on the right)

For the data set of cat. (4), the lower boundary of 401 of the 1049 well cores of A_min is gridded with too high values. The deviations of the lower boundaries range from 0.1 cm to 17.99 m, which reflects again the situation of well core no. 17104002 (cf. chapter implementing Amin). When the archaeological data points are added, 411 well cores have to be newly gridded.

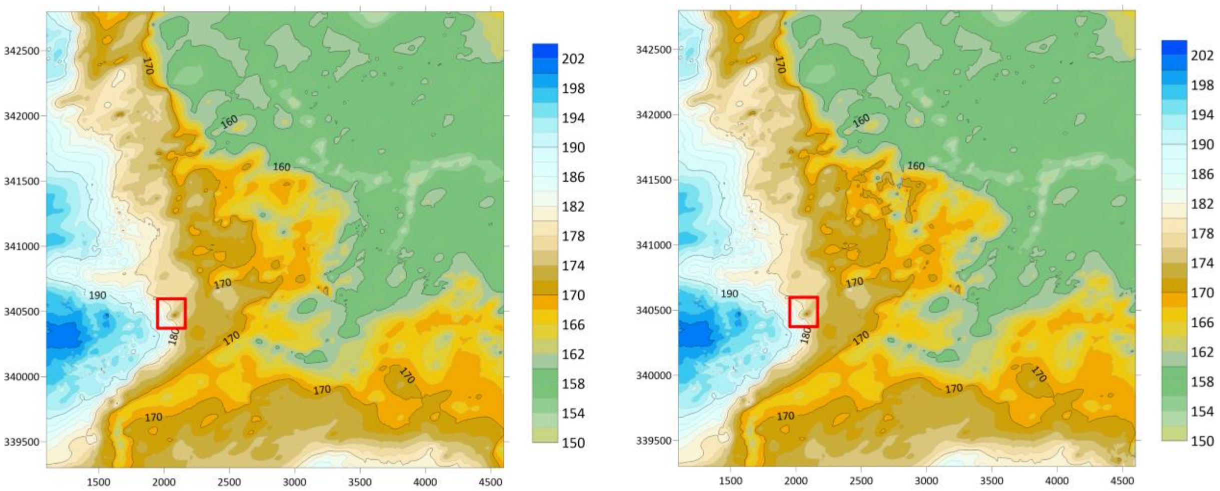

Figure 42: Comparison between the kriging results of the data set of cat. (4) without (on the left) and with the archaeological data implemented (on the right), both including the well cores classified as A_min. Well core no. 17104002 is marked in red

By comparing the outcomes only visually (fig. 42), no clear differences can be detected to the grids without implementing “A?”. For this, the actual volume of the anthropogenic sediments has to be calculated.

6.8 Vienna’s underground in numbers – Calculating the volume of AMG

The volume of the thickness of anthropogenic sediments is calculated using the “Grid Volume” tool in Surfer. As upper surface, the modern DTM, gridded to a grid cell size of 10 m, is used; the obtained grids of the preceding chapters are used as lower surface for the volume calculation. The results are summarised in Tables 20 and 21 (for an explanation of principles of cut and fill cf. Chapter 6.4 and fig. 28; the complete Grid Volume Reports are included in Appendix B).

As already observed in Chapter 6.7.4, including the archaeological data set results in lower positive volume values (and as a consequence higher values of negative volume), because in the areas of excavations sites the more detailed information gained from the archaeological data points leads to an interpolation of a higher Boundary A. Adding the well cores classified as “A_min” to the data sets (thus comparing (a) to (c) and (b) to (d)), the positive volume of anthropogenic sediments is increasing. That was to be expected, as only those A_min well cores were added, whose lower boundary were underneath the interpolated Boundary A at this position (cf. Chapter 6.7.5 and fig. 38). Nevertheless, appending all available data (i.e. archaeological data as well as well cores “A_min”) results in a slightly lower positive volume than by using the layers of A and A/A? only (about 6.500 and 16.600 m³, respectively). Hence, adding additional data helps to produce a more realistic interpolation of Boundary A.

Observations made regarding cat. (3) and (4) are the same, yet, including A? leads to higher values of positive volume in all four classes (a) to (d). Comparing the two data sets comprising the most data available (i.e. (d)), the difference is 302,344.12 m³ for the positive and 1,147.8 m³ for the negative volume. By including A?, the positive volume for the whole study area amounts to 46,817,751.38 m³; excluding A?, the volume totals 46,515,407.26 m³. This is almost the half of the volume of Lake Fuschl in Salzburg, Austria, or equals ca. 233 times the volume of one of the four historical gasometer buildings in Vienna.[37] Regarding the surface areas, 11,936,210.61 m² and 11,933,877.22 m², respectively, belong to the positive surface area, while 310,624.54 m² and 308,423.07 m², respectively, of Boundary A are higher than the present ground level. This area accounts to approximately 2.5 % of the study area that is currently lower than in the time the well cores were drilled.[38]

[37] See https://de.wikipedia.org/wiki/Liste_der_Seen_in_%C3%96sterreich and https://de.wikipedia.org/wiki/Gasometer_(Wien) (accessed February 28, 2020).

[38] Calculating the percentage of the negative planar area regarding the total planar area (12.25 km²) results in 2.51 % for cat. 3 (d) and 2.49 % for cat. 4 (d).

Table 20: Calculated grid volumes by using the modern DTM and the grids of the category (3): a) well cores incl. A, b) well cores incl. A and archaeological data, c) well cores incl. A and A_min, d) well cores incl. A, archaeological data and A_min

	Cat. 3 (a)	**Cat. 3 (b)**	**Cat. 3 (c)**	**Cat. 3 (d)**
Cut & Fill Volumes				
Positive Volume [Cut]	46,521,915.31	45,572,392.79	47,509,093.07	46,515,407.26
Negative Volume [Fill]	345,350.44	352,531.33	326,322.24	330,034.82
Net Volume [Cut-Fill]	46,176,564.87	45,219,861.46	47,182,770.84	46,185,372.44
Planar Areas				
Positive Planar Area [Cut]	11,856,004.95	11,851,148.58	11,876,464.17	11,873,167.69
Negative Planar Area [Fill]	324,095.05	328,951.42	303,635.83	306,932.31
NoData Planar Area	69,900	69,900	69,900	69,900
Total Planar Area	12,250,000	12,250,000	12,250,000	12,250,000
Surface Areas				
Positive Surface Area [Cut]	11,911,530.66	11,910,809.01	11,932,842.37	11,933,877.22
Negative Surface Area [Fill]	327,910.32	332,993.24	307,191.96	310,624.54

Table 21: Calculated grid volumes by using the modern DTM and the grids of the category (4): a) well cores incl. A and A?, b) well cores incl. A and A? and archaeological data, c) well cores incl. A and A? and A_min, d) well cores incl. A and A?, archaeological data and A_min

	Cat. 4 (a)	**Cat. 4 (b)**	**Cat. 4 (c)**	**Cat. 4 (d)**
Cut & Fill Volumes				
Positive Volume [Cut]	46,834,396.98	45,875,309.24	47,820,791.22	46,817,751.38
Negative Volume [Fill]	344,743.22	352,081.33	325,148.30	328,887.02
Net Volume [Cut-Fill]	46,489,653.77	45,523,227.91	47,495,642.92	46,488,864.36
Planar Areas				
Positive Planar Area [Cut]	11,859,028.16	11,854,167.19	11,878,563.18	11,875,336.97
Negative Planar Area [Fill]	321,071.84	325,932.81	301,536.82	304,763.03
NoData Planar Area	69,900	69,900	69,900	69,900
Total Planar Area	12,250,000	12,250,000	12,250,000	12,250,000
Surface Areas				
Positive Surface Area [Cut]	11,914,638.91	11,913,925.71	11,935,089.95	11,936,210.61
Negative Surface Area [Fill]	324,849.09	329,936.34	305,060.88	308,423.07

6.9 Mapping the thickness of AMG

The thickness of anthropogenic sediments cannot only be calculated to receive the volume, yet it can be mapped as well. To receive a grid of the anthropogenic sediments, the obtained grids of Boundary A are subtracted from the modern DTM grid by the tool "Grid Math" in Surfer. The results are visible in the Figures 43 and 44 and visually confirm the conclusions of the volume calculations. Areas of "negative AMG", i.e. areas that have been lowered since the time of drilling or excavation, are depicted in blue.

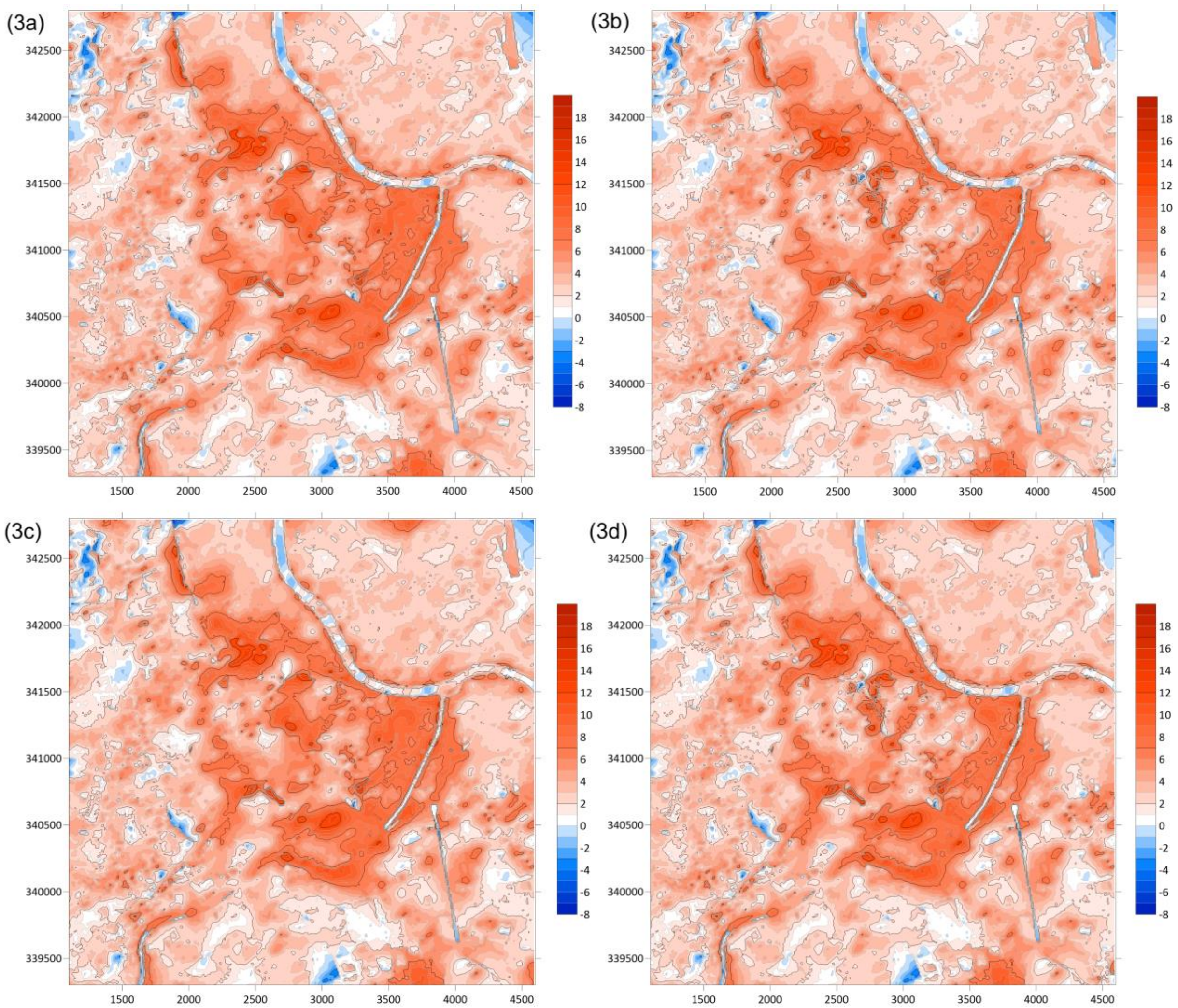

Figure 43: Thickness of AMG for the data set of cat. (3): a) well cores incl. A, b) well cores incl. A and archaeological data, c) well cores incl. A and A_min, d) well cores incl. A, archaeological data and A_min

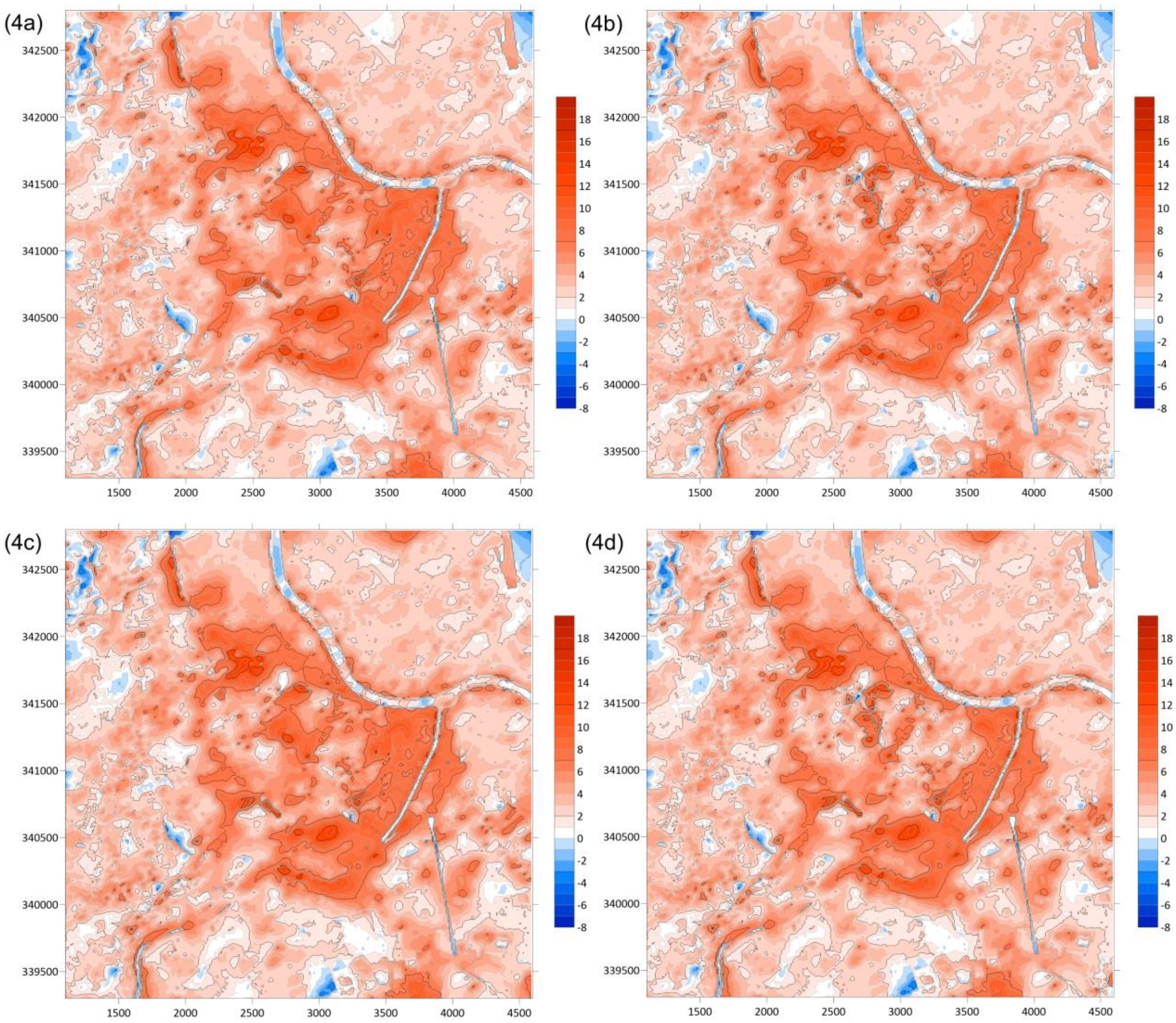

Figure 44: Thickness of AMG for the data set of category (4): a) well cores incl. A and A?, b) well cores incl. A and A? and archaeological data, c) well cores incl. A and A? and A_min, d) well cores incl. A and A?, archaeological data and A_min

For a better visual understanding, a so-called 3D view can be produced in Surfer. Figures 45 and 46 show two 3D views of data set (3d), so including every certain data regarding Boundary A in the study area – one of the interpolated Boundary A, one of the calculated thickness of anthropogenic sediments.

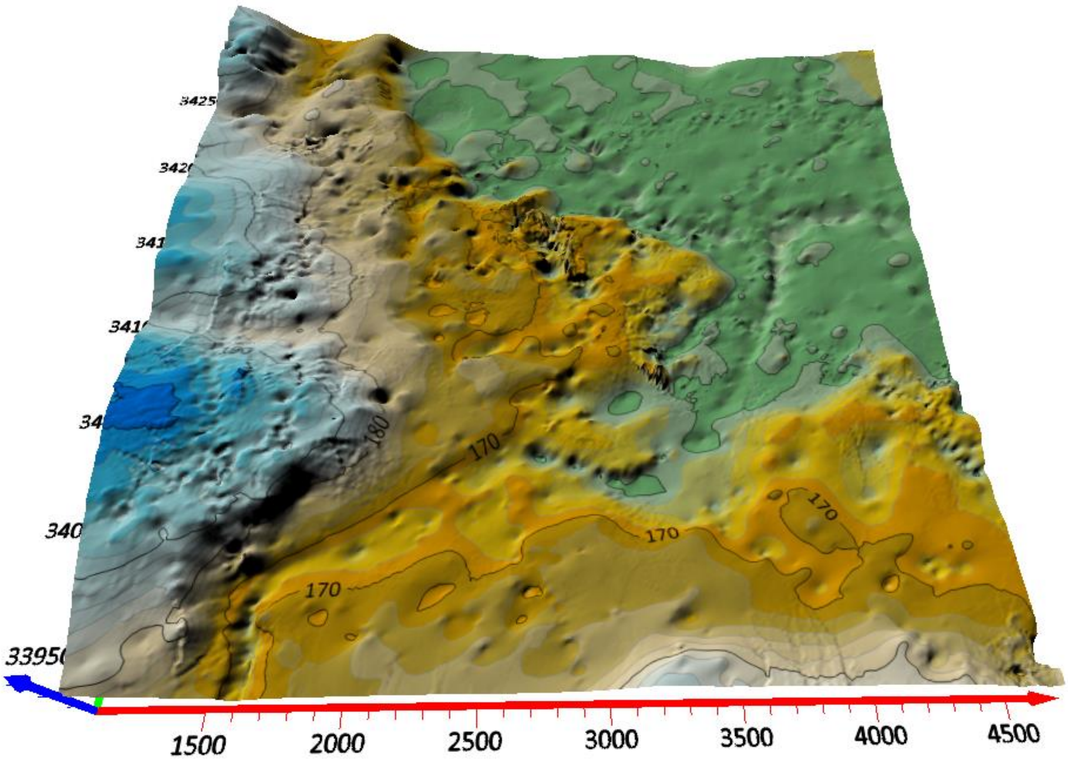

Figure 45: 3D view of Boundary A of the data set (3d), vertical exaggeration by 10

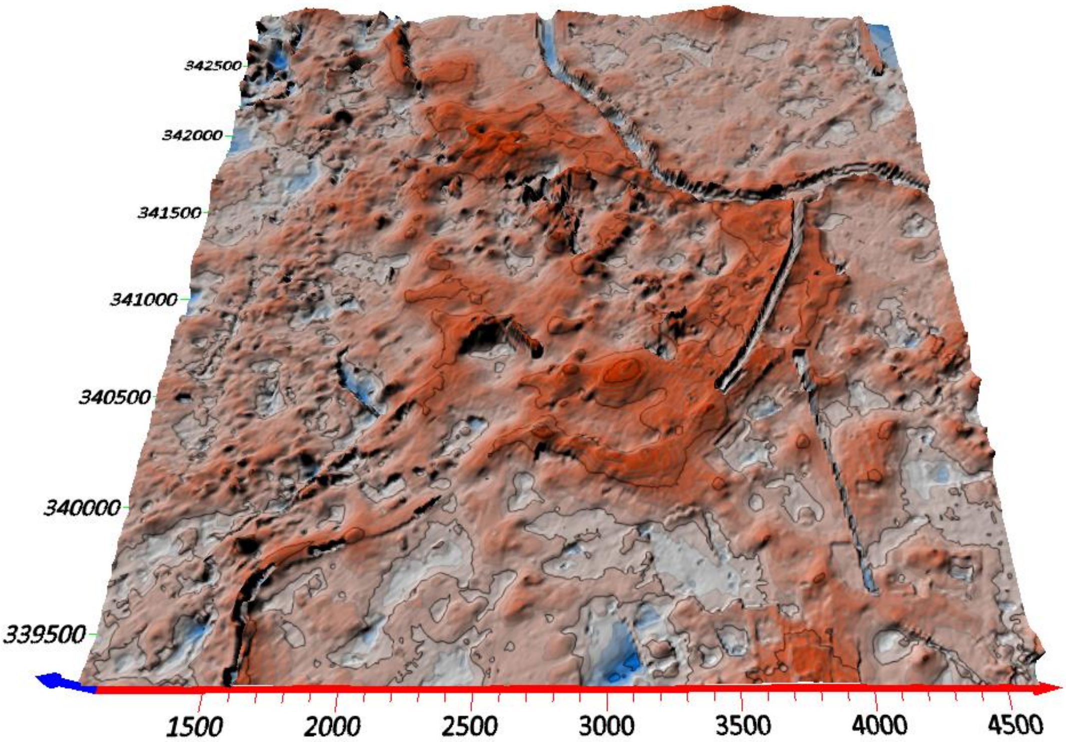

Figure 46: 3D view of the thickness of AMG of the data set (3d), vertical exaggeration by 10

6.10 Historical interpretation

The distribution and extent of anthropogenic sediments in the study area are closely intertwined with the history of the city. Interpreting the individual anomalies in these grids could easily be a Master's thesis on its own. Therefore, this study focuses only on the most conspicuous features.

As can be seen in the Figures 43, 44 and 46, the most massive anthropogenic sediments are situated in the centre of the study area, in the area of the first district of Vienna. Further accumulations of AMG are visible as a linear structure in the north-western part of the study area and following a curved line to the south and east of the city centre. Another straight linear feature is striking in the south-eastern part of the study area, yet, this time, it shows negative values and therefore is today lower than in the time when the well cores were drilled. Another area of negative AMG is in the north-western corner of the study area. By taking a look at the history of the city, most of these observations can be elucidated (fig. 47).

The most massive anthropogenic sediments follow the course of the "Ringstraße", the boulevard enclosing the first district. This boulevard has been erected in the 1860s, on the site of the former city walls. This fortification, stemming from the 16th century, was demolished by imperial edict at the end of the 1850s (Sakl-Oberthaler et al. 2016). The walls' deep foundations are visible in more than 12 m of anthropogenic sediments in the well cores. Superimposing the SHP file of the fortification show a close match with the areas of thickest AMG.[39]

Within the city walls, one area stands out with more accumulated sediments of anthropogenic origin than the remaining area inside the fortification. This area outlines the location of the Roman legionary camp, which is the first place of Roman settlement in Vienna. The fortification of the military camp is mapped in Figure 47.[40]

Other aggregations of AMG belong to natural phenomena. Along the banks of the Danube Canal and the Wien River, higher anthropogenic sediments can be observed, which can be explained with the river training and the reinforcement of the water bodies in the late 19th century. Within the framework of the river training, more than 2 km of the Wien River were vaulted and this part is also visible in the interpolation. The SHP file of water network of the city fits perfectly with the interpolation.[41] The straight structure of thicker anthropogenic

[39] The data set is available at: https://www.data.gv.at/katalog/dataset/4f5a37d7-6055-40b6-9cdd-de55a9ab5248 (accessed February 28, 2020).

[40] The SHP file of the Roman legionary camp is available at: https://www.data.gv.at/katalog/dataset/9886476f-9c2f-46c8-bf37-06870d1e7338 (accessed February 28, 2020).

[41] Available at: https://www.data.gv.at/katalog/dataset/ac4c2ac5-6be4-4471-bbf4-f09228f5db04 (accessed February 28, 2020).

deposits in the north-western part of the study area is caused by a terrace in the topography of the city that was formed by one branch of the Danube. The terrain level slopes down to the east, and to overcome the difference in terrain several staircases were built in the 9th district of Vienna[42], which can be seen in this accumulation of anthropogenic sediments.

Areas with nowadays lower terrain than at the time of drilling are connected with large construction projects of the city (fig. 48). The straight linear feature in the south-eastern part of the study area represents the tracks of the rapid transit railway erected in the beginning of the 1960s.[43] The area in the north-western part of the study area belongs to the largest hospital complex in Austria, the *Allgemeine Krankenhaus der Stadt Wien* (AKH). The construction of the building complex took from 1964 to 1994 and led to levelling measures of the terrain.

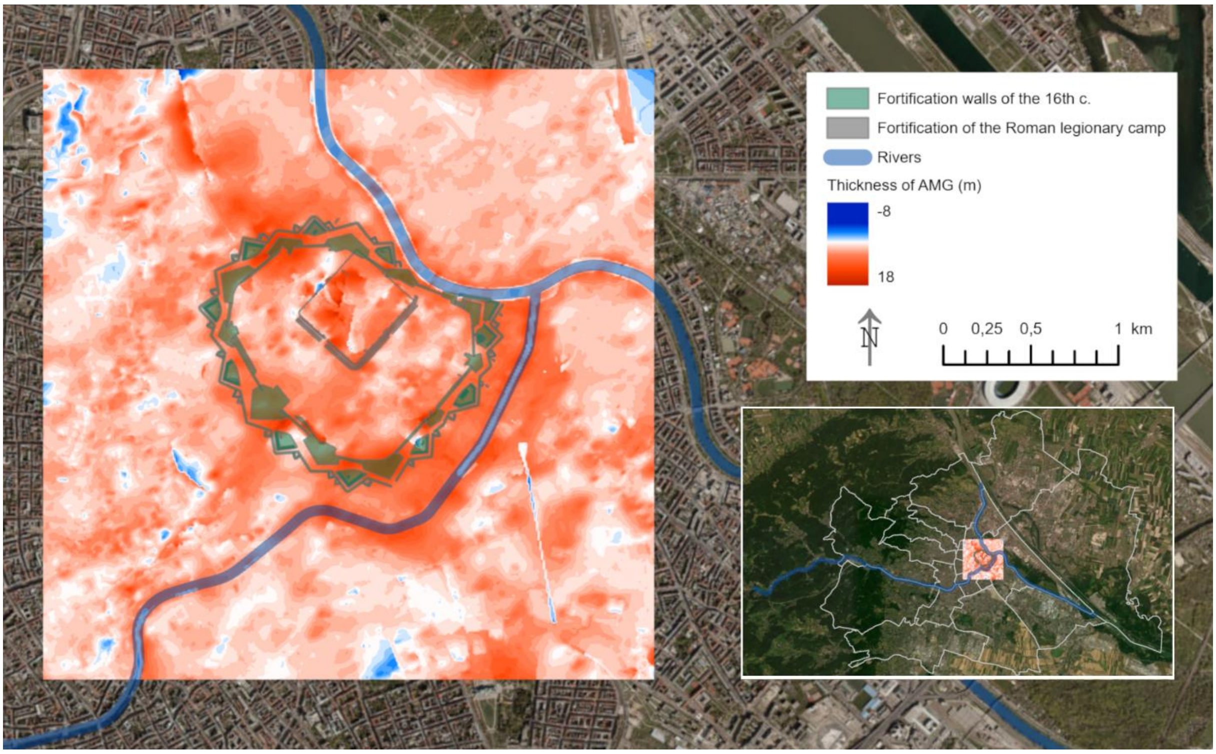

Figure 47: Interpolated thickness of AMG using cat. (3d) with superimposed historical and natural features

[42] E.g. the Strudelhofstiege, Vereinsstiege, Himmelpfortstiege etc.

[43] This track section connects the stations “Rennweg” and “Wien Mitte”. To the history of the rapid transit railway in Vienna cf. Haas 2007.

Figure 48: Areas with lowered terrain. Rapid transit track on the left, area of the hospital "AKH" on the right

6.11 Comparison between Vienna and London

The results of this study are interesting to compare with the results of the London study and thereby with the outcome for the borough "City of London", which covers approximately a quarter of the study area. Both areas, the present study area of Vienna and the City of London, are areas with a history of two millennia of development, starting with first major transformations as city foundations by the Romans and later on with fortifications with city walls in the Middle Ages. Yet, the study area of Vienna is not restricted to a modern district boundary, taking into account the historic development of the city by using a larger area than the first district (and by this the historic city walls of Vienna). However, the city walls of London were also mainly within the boundaries of today's City of London.

Methodologically the biggest difference between the two studies is that for London, the interpolation values were connected to the European Urban Atlas polygons. By this, no continuous interpolation grid was obtained. Yet, in case of large building complexes with several well core drillings, the mean of the AMG thickness documented in the well cores is used for the whole building area, which makes local variations unrecognisable. Therefore, in this study Boundary A is gridded as continuous surface.

The maximum thickness of AMG recorded in the well cores of the district City of London was 8.44 m when considering the borehole record only and 10.91 m when including the modern DTM (Terrington et al. 2018). In the study area in Vienna, much higher values are documented, by 19 m (including A?) and 16.4 m with the information of the well logs only and 19.9 and 17.3

m, respectively, when considering the modern DTM. In the archaeological data, a maximum thickness of 16.7 m is shown.

In London, the mean thickness accounts 3.37 m (borehole thickness only) and 3.74 m (with elevation change), whereas in Vienna 2.3 m (borehole thickness only) and 4.1 m (considering the modern DTM) are observed. As mentioned before, this increase of AMG thickness cannot be interpreted as total rise of the ground level, but must be read in the context of the documented elevation values in the well logs (see Chapter 5.3.1.1 Well core data in the study area). The mean thickness of the archaeological data is 2.3 m and, by this, correlates with the mean value recorded in the well logs. Nevertheless, it is interesting that regarding the values considering the DTMs the mean thickness of Vienna is exceeding that of London so much.

Ford et al. (2014) have proposed for Greater London the average value of 1.6 m of AMG, which Terrington et al. (2018) have stated as to be far too low. For Vienna, no clear response can be given to this proposal, as the area researched in this study cannot be considered representative for the whole city area (cf. Chapter 7.1).

In the London study, the volume of AMG deposits is simply calculated by multiplying the area against the mean thickness of AMG deposits (Terrington et al. 2018). By this, a subsurface volume of 10,615,500 m³ and 11,781,000 m³ for the City of London had been computed (depending on if the modern ground level is excluded or included). In Vienna, the actual volumes are calculated by using the interpolated Boundary A map and the modern DTM as upper surface. Using data sets (3d) and (4d), so using all available data, AMG deposits have a positive volume of 46,515,407 and 46,817,751 m³, if layers classified as A? are considered. This results in 3.80 and 3.82 m³ per m², respectively, which is slightly more than the 3.74 m³ per m² for the City of London. Yet, caution is required when comparing these values, as the approach of the authors of the London study is only a rough estimation. If the same method is applied to the Viennese data set by simply multiplying the area (12,250,000 m²) against the mean thickness of 2.3 or 4.1 m, this results in volumes of 28,175,000 or 50,225,000 m³, both of which are far from the correct result.

Both studies throw light on a subject that is often neglected – the subsurface of modern cities. By interpolating Boundary A and calculating the thickness of AMG, numbers are given to an abstract issue, making a comparison between similar areas possible. It is to be hoped that similar studies will be carried out for other cities in the future.

7. Discussion and outlook

7.1 Extending the interpolation on the whole city area

As this study is a pre-study for a larger research project, the methods tested in this thesis will be applied to investigate the subsurface of Vienna's whole city area. Problems to be expected are the following: Regarding the whole city area, the well cores are not as densely distributed as in the small study area, but more scattered and with large areas without any data. Only few excavation sites are located outside the study area, therefore the correction by archaeological data can only be used at a very reduced scale. Large forest areas (e.g. the Vienna Woods) and green areas (as the National Reserve Lobau) do not contain any well drillings and therefore lack any data. So, the irregular distribution might be the greatest challenge.

7.2 Inconsistencies and errors of the data sets

When calculating the current thickness of the anthropogenic sediments by subtracting the Boundary A values of the well cores from the modern DTM, some surprisingly high values were obtained. To check the correctness of the data, all well cores with difference of the elevation of the drill starting point and the modern DTM of more than 10 m (in both directions, so < -10 m and > +10 m) were checked by controlling the original PDFs (a total of about 40 well cores). By this, several mistakes in the data set could be corrected, especially these cases, where the modern ground level was shown as more than 10 m below the drill starting point.[44] Those cases, where the modern ground level is above the drill starting point, could often be clarified by the fact that these well cores had been drilled in the second or third basement level. When extending this study to the whole city area of Vienna, "manual" corrections are far too laborious and time-consuming to be done for the number of more than 60,000 well cores. In this case, well cores showing high deviations will simply have to be removed from the data set.

Other insecurities regarding the well core data set were unclear definitions (e.g. A?) and the inconsistent use of the "GOK" (the elevation reference of the drill starting point or the ground level). Due to that, an analysis of the historic rise of the ground level, as had been done in the London study, was not possible for Vienna.

At this point I would like to thank once again Christine Jawecki from the Municipal Department for Bridge Construction and Foundation Engineering for her extremely quick and

[44] This included simple mistakes in the coordinates (wrong location) as well as drillings on a bridge, which were excluded from the study.

helpful responses and corrections regarding the data from the well core database of the City of Vienna.

7.3 Corrections of the map of AMG thickness

Controlling the gridded maps of AMG thickness, areas of high extremes are visible especially along the borders of the study area. One location with very massive anthropogenic deposits at the southern border of the study area is particularly striking: it is the largest area without well drillings in the study area, nonetheless it shows values of high accumulations of anthropogenic sediments, although the surrounding well cores do not reflect this (cf. fig. 22 and 43). This area is covered by the museum Belvedere, which is located in two Baroque palaces, with an extensive Baroque garden in-between (fig. 49, on the left). Adjacent to the east is the botanical garden of the University of Vienna. Massive accumulations of anthropogenic deposits are highly unlikely in this context. To the west, a small area with high negative values of AMG thickness is interpolated. This area represents the sports ground of the school Theresianum. Drillings at the sports field show no anthropogenic sediments at all (AMG thickness = 0 m), however, the adjacent site to the east with no well cores has received negative values in the interpolation process.

Figure 49: Areas with extreme values of AMG thickness at the southern border of the study area. On the right, the distribution of the supporting data points, highlighted in green.

These extreme values are caused by the absence of data points in those areas. These errors in the interpolation process can be corrected by setting additional supporting data points. The values of probable thickness of AMG of these new points are derived from neighbouring measured data points. To test this method, a new feature class is created, and two points are added to the sports ground in the west and six points to the garden of the Belvedere and the botanical garden (fig. 49, on the right). The elevation information of these points are extracted from the modern DTM of the study area. To receive the most probable elevation of Boundary A at these locations, the other well cores in those areas are consulted. For the sports field, no anthropogenic sediments are assumed (i.e. elevation of modern DTM = elevation of Boundary A). Regarding the garden areas to the east, anthropogenic deposits of 0.4 to 2 m are recorded in the surrounding green areas. Therefore, with 1 m a value approximately in the middle is chosen. The table of the eight new data points is appended to the data set of (3d), so including all certain data available.

The same gridding process is applied as described in Chapter 6.7.2 (Kriging), resulting in the new interpolation of Boundary A and the calculated grid displaying the thickness of AMG shown in Figure 50. Where the supporting data points have been set, the gridded values clearly have changed. Regarding the sports ground, the outcome has improved, representing values of zero or slightly negative thickness (fig. 51). In the area of the Belvedere museum, the extreme values of massive anthropogenic sediments have been replaced by values showing low AMG thickness. However, between the new data points, small areas of high negative thickness have been interpolated, resulting in three "blue islands" in this area. By this, it becomes obvious that in case of setting additional supporting data points, the exact location and the Z value have to be carefully chosen.

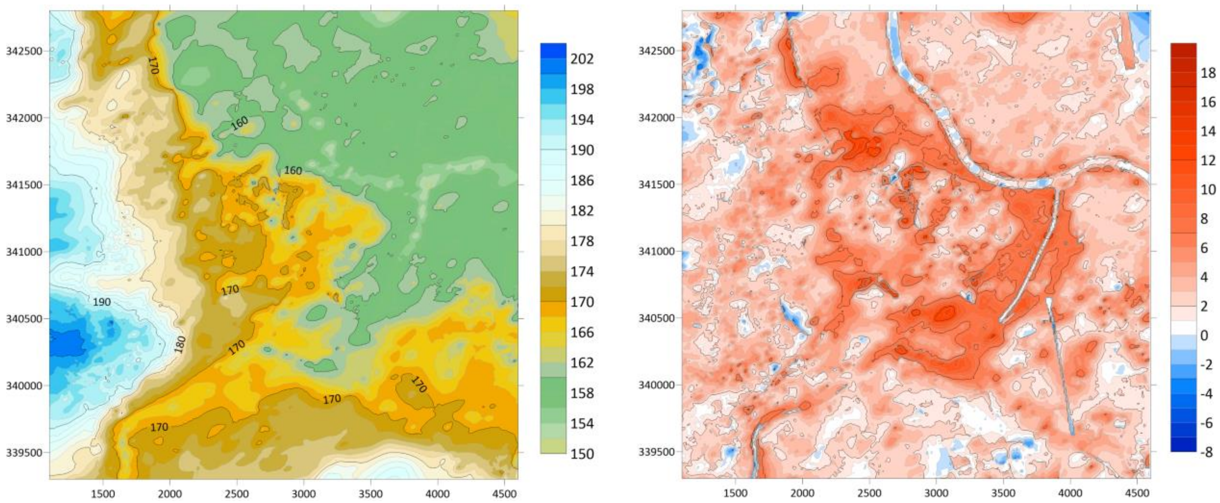

Figure 50: Gridding results using the updated data set of (3d) with the additional supporting data points: interpolation of Boundary A (on the left) and calculation of AMG thickness (on the right). The area concerned is in the eastern part of the southern border area (between 3000 and 4000 m on the X-axis)

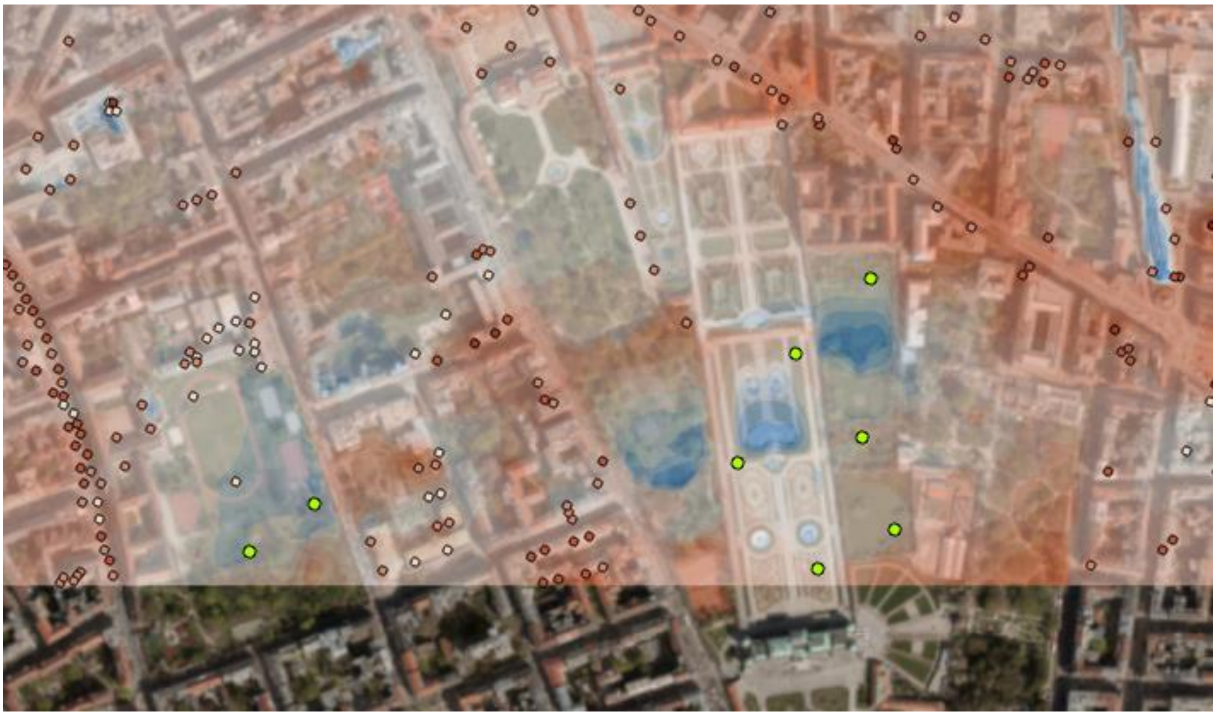

Figure 51: Result of the calculation of AMG thickness including the supporting data points

7.4 Buildings in the underground

The model of anthropogenic sediments in the study area as presented in this study is not complete. Large structures of anthropogenic origin are missing, and that are underground parking garages, the underground railway, cellars of residential buildings and underground storage vaults of museums and libraries. All these structures are part of the archaeosphere and should be included when calculating the volume of AMG. Unfortunately, these data are not publicly available and as most of these structures are privately owned, information are hard to receive. Nevertheless, the aim should be to include the underground structures in such a study, and this is planned for the future continuation of this research.

7.5 Calculating upward growth

In the London study, a comparison between the historical ground elevation and the modern ground elevation was possible, as for 71% and 78% respectively of the well cores of the two districts the start height was recorded (Terrington et al. 2018). By this, the amount of anthropogenic sediments removed or deposited since the time of the drilling can be estimated. In contrast, as mentioned before, in Vienna the “ground elevation” (“GOK”) in the well core data does not always represent the drill starting point and therefore cannot be clearly assigned to the historical ground elevation. However, an estimation of the "upward growth" is possible, following the methods applied by Luberti (2018) for the city of Rome. By using DTMs of different date, the change-in-elevation can be calculated and visualised. This approach might deliver interesting results for new urban development areas, as Seestadt Aspern and Hauptbahnhof, and will be tested in future research.

7.6 Dating and differentiating time horizons

In their study, Terrington et al. (2018) have used the descriptions of the materials recorded in the well cores as a proxy to allocate the different layers to historical epochs, which was, in case of the London study, pre- and post-World War II.

Dating layers by using well log descriptions is a difficult task. Just as the classification, the detail of the layer descriptions depended a long time on the person in charge. In the Viennese well logs, very detailed descriptions with information on color, consistency, even smell and all the materials in this layer in great accuracy exist next to very superficial, summarising short comments. This situation was overcome only in the early 2000s by introducing a new data acquisition program, which demands more detailed entries.[45] Since then, the level of detail in the layer descriptions is consistent.

The same observations have been done in the London study. Terrington et al. (2018) refer that a substantial number of well core records simply refer to "made ground" or "fill" whereas others contain information on the material present into each layer. In Terrington et al. 2018 Tab. 2, a lexicon of key anthropogenic materials and objects has been collected, showing the probable maximum age of a deposit. By this, the clearest lithological distinction has been possible between deposits that can be attributed to post-WWII activities.

If the same approach should be used for Vienna, then the materials in the layer descriptions must be drawn on for dating the layers. The material mentioned the most in the well logs of the whole city area are bricks, which is not surprising, since bricks have been used throughout the 2,000 years of history of the city. Material that can clearly be assigned to one epoch is seldom and a typological assignment to specific historical epochs is missing, since archaeologists or other experts on artefacts are not involved in the documentation process. Ceramic or glass fragments are documented as "ceramics" or "glass", without differentiating between "Roman ceramics" and "Medieval ceramics". By this, dating of the anthropogenic layers is only possible

[45] The name of this program is GEODE: https://www.wien.gv.at/verkehr/grundbau/geode.html (accessed February 28, 2020).

by referring to materials that are appearing for the first time in a certain epoch. This sets the *terminus post quem*, as it is referred to in archaeological sciences, determining that the layer with a medieval artefact has to date medieval or younger. Using this method, layers with modern material, as concrete, in it, could be assigned to the Modern times and therefore dated. Combined with archaeological excavation data, differentiations in the archaeosphere could be made, distinguishing between anthropogenic sediments of different epochs. This approach is beyond the scope of this paper, but will be the focus of future research.

8. Conclusio

Although we are in constant contact with it through underground railways, tunnels, underpasses and cellars, the underground of a city remains something abstract, elusive and difficult to grasp. While we are constantly aware of the human influence through the constructions and buildings erected on the Earth's surface, the human interventions in the ground remains hidden from our eyes, invisible. To throw a light on this impact, making the invisible visible, that was the aim of this study.

For this task, different data sets containing information on Vienna's subsurface have been combined: Almost 10,000 well cores and 70 excavation sites were available for the chosen study area in the heart of Vienna. Careful analysis of the well core data allowed to distinguish four different categories of data, depending on their certainty of representing the lower boundary of the archaeosphere, the so-called Boundary A.

The core of this study was the interpolation of Boundary A, which was achieved by using Universal Kriging. By testing two different variogram models to provide the best fit for the data, the nested variogram model proved to achieve better results by visual analysis as well as cross validation. The resulting grid was enhanced adding the archaeological data and well cores classified as "A_min".

Another main objective of this study was the estimation of volume of anthropogenic sediments and the analysis of the distribution of the thickness of artificially modified ground (AMG) in the study area. The volume of the deposits of anthropogenic origin was calculated by using the interpolated Boundary A as lower and the modern digital terrain model (DTM) as upper surface. Including only layers classified as certain anthropogenic sediments and structures, a volume of 46,515,407.26 m^3 is obtained, which equals ca. 233 times the volume of one of the four historical gasometer buildings in Vienna.

Maps of the thickness of AMG were created by subtracting the interpolation of Boundary A from the modern DTM. By a historical analysis, the areas with the highest amount of anthropogenic sediments could be linked to the historical (city fortification, Roman military camp) and natural (waterways, river terrace) reasons. Areas of negative thickness reflect modern construction measures.

Finally, comparing the results to a similar study conducted for the centre of London led to striking similarities in the results. Yet, in order to be able to make a definitive statement, similar studies would have to be carried out in other cities with a different history, ideally also on other continents. Nonetheless, the London study as well as the present thesis attempt to fulfil an important purpose: to raise awareness of a space in our environment that we perceive far too rarely – the underground beneath our cities.

9. References

Bachmaier, M., and M. Backes. 2008. 'Variogram or Semivariogram? Understanding the Variances in a Variogram'. *Precision Agriculture* 9 (3): 173–75. https://doi.org/10.1007/s11119-008-9056-2.

Balasubramani, D. P., and G. R. Dodagoudar. 2018. 'An integrated geotechnical database and GIS for 3D subsurface modelling: Application to Chennai City, India'. *Applied Geomatics* 10, 47–64. https://doi.org/10.1007/s12518-018-0202-x.

Barnes, R. 2003. Variogram tutorial. Golden, CO: GoldenSoftware. Accessed February 28, 2020. http://www.goldensoftware.com/variogramTutorial.pdf.

Chesnaux, R., M. Lambert, J. Walter, V. Dugrain, A. Rouleau, and R. Daigneault. 2017. 'A simplified geographical information systems (GIS)-based methodology for modeling the topography of bedrock: illustration using the Canadian Shield'. *Applied Geomatics* 9, 61–78. https://doi.org/10.1007/s12518-017-0183-1.

Chilès, J.-P., and P. Delfiner. 2012. *Geostatistics: Modeling Spatial Uncertainty*. 2nd ed. Wiley Series in Probability and Statistics. Hoboken, N.J: Wiley.

Cressie, N. 1990. 'The Origins of Kriging'. *Mathematical Geology* 22 (3): 239–52. https://doi.org/10.1007/BF00889887.

Edgeworth, M. 2014. 'The Relationship between Archaeological Stratigraphy and Artificial Ground and Its Significance in the Anthropocene'. *Geological Society, London, Special Publications* 395 (1): 91–108. https://doi.org/10.1144/SP395.3.

Edgeworth, M., D. deB Richter, C. Waters, P. Haff, C. Neal and S. J. Price. 2015. 'Diachronous beginnings of the Anthropocene: The lower bounding surface of anthropogenic deposits'. *The Anthropocene Review* 2 (1): 1–26. https://doi.org/10.1177/2053019614565394.

Ford, J. R., H. Kessler, A. H. Cooper, and C. N. Waters. 2010. *An Enhanced Classification for Artificial Ground.* British Geological Survey Open Report OR/10/036.

Ford, J. R., S. J. Price, A. H. Cooper, and C. N. Waters. 2014. 'An Assessment of Lithostratigraphy for Anthropogenic Deposits'. *Geological Society, London, Special Publications* 395 (1): 55–89. https://doi.org/10.1144/SP395.12.

Golden Software. 2019. *Surfer Full User's Guide. Contouring and 3D Surface Mapping for Scientists and Engineers.* November 2019. Accessed February 28, 2020. http://downloads.goldensoftware.com/guides/Surfer17UserGuide.pdf.

Haas, F., ed. 2007. *Die Wiener Schnellbahn: Stammstrecke Floridsdorf-Meidling*. Die Reihe auf Schienen unterwegs. Erfurt: Sutton.

Harris, E. C. 1989. *Principles of Archaeological Stratigraphy*. London: Academic Press.

Johnston, K., J. M. Ver Hoef, K. Krivoruchko, and N. Lucas. 2004. *ArcGIS 9: Using ArcGIS™ Geostatistical Analyst*. Redlands, CA: ESRI.

Kitanidis, P. K. 1997. *Introduction to Geostatistics: Applications in Hydrogeology*. 1st ed. Cambridge University Press. https://doi.org/10.1017/CBO9780511626166.

Luberti, G. M. 2018. 'Computation of Modern Anthropogenic-Deposit Thicknesses in Urban Areas: A Case Study in Rome, Italy'. *The Anthropocene Review* 5 (1): 2–27. https://doi.org/10.1177/2053019618757252.

McKinney, W., and the Pandas Development Team, 2020. pandas: *powerful Python data analysis toolkit.* Release 1.0.1. Accessed February 24, 2020. https://pandas.pydata.org/docs/pandas.pdf

Nirei, H., K. Furuno, K. Osamu, B. Marker, and J. Satkunas. 2012. 'Classification of Man Made Strata for Assessment of Geopollution'. *Episodes* 35 (2): 333–36. https://doi.org/10.18814/epiiugs/2012/v35i2/004.

Pyrcz, M. J. 2019. '12b Geostatistics Course: Kriging'. Uploaded November 8, 2018. Video, 36:09. Accessed February 28, 2020. https://www.youtube.com/watch?v=CVkmuwF8cJ8.

Rufo, M., A. Antolín, J.M. Paniagua, and A. Jiménez. 2018. 'Optimization and comparison of three spatial interpolation methods for electromagnetic levels in the AM band within an urban area'. *Environmental Research* 162: 219–225. https://doi.org/10.1016/j.envres.2018.01.014

Sakl-Oberthaler, S., M. Mosser, H. Krause, and G. Reichhalter. 2016. *Von der mittelalterlichen Stadtmauer zur neuzeitlichen Festung Wiens: historisch-archäologische Auswertung der Grabungen in Wien 1, Wipplingerstrasse 33-35*. Monografien der Stadtarchäologie Wien, Band 9. Wien: Phoibos Verlag.

Suess, E., 1862. *Der Boden der Stadt Wien nach seiner Bildungsweise, Beschaffenheit und seinen Beziehungen zum Bürgerlichen Leben. Eine geologische Studie.* Wien: Wilhelm Braumüller.

Suess, E., 1897. *Der Boden der Stadt Wien und sein Relief*. Separatabdruck aus Band I der "Geschichte der Stadt Wien" herausgegeben vom Alterthumsvereine zu Wien. Wien.

Terrington, R. L., É. C. N. Silva, C. N. Waters, H. Smith, and S. Thorpe. 2018. 'Quantifying Anthropogenic Modification of the Shallow Geosphere in Central London, UK'. *Geomorphology* 319 (October): 15–34. https://doi.org/10.1016/j.geomorph.2018.07.005.

10. Appendix A: Grid volume computations using triangulated grids

Grid Volume Computations – Cat. (1)

Mon Feb 10 11:39:13 2020

Upper Surface

Grid File Name: E:\Anthropocene Surge\Wien GIS\MA_UNIGIS\Surfer\dtm_grid_10m.grd
Grid Size: 351 rows x 351 columns

X Minimum: 1100
X Maximum: 4600
X Spacing: 10

Y Minimum: 339300
Y Maximum: 342800
Y Spacing: 10

Z Minimum: 155.50675582858
Z Maximum: 203.93125152586

Lower Surface

Grid File Name: E:\Anthropocene Surge\Wien GIS\MA_UNIGIS\Surfer\BK_Daten\BK_A_oA_Amin_exkl_oB_1.grd
Grid Size: 351 rows x 351 columns

X Minimum: 1100
X Maximum: 4600
X Spacing: 10

Y Minimum: 339300
Y Maximum: 342800
Y Spacing: 10

Z Minimum: 148.84349196907
Z Maximum: 274.57139269238

Volumes

Z Scale Factor: 1

Total Volumes by:

Trapezoidal Rule: 40711908.30667
Simpson's Rule: 40746023.640108
Simpson's 3/8 Rule: 40751592.278573

Cut & Fill Volumes

Positive Volume [Cut]: 41838144.613001
Negative Volume [Fill]: 1126236.3063311
Net Volume [Cut-Fill]: 40711908.30667

Areas

Planar Areas

Positive Planar Area [Cut]: 11545516.892766
Negative Planar Area [Fill]: 501133.10723371
NoData Planar Area: 203350
Total Planar Area: 12250000

Surface Areas

Positive Surface Area [Cut]: 11645768.162725
Negative Surface Area [Fill]: 526901.55414134

Grid Volume Computations – Cat. (2)

Mon Feb 10 11:41:02 2020

Upper Surface

Grid File Name:	E:\Anthropocene Surge\Wien GIS\MA_UNIGIS\Surfer\dtm_grid_10m.grd
Grid Size:	351 rows x 351 columns
X Minimum:	1100
X Maximum:	4600
X Spacing:	10
Y Minimum:	339300
Y Maximum:	342800
Y Spacing:	10
Z Minimum:	155.50675582858
Z Maximum:	203.93125152586

Lower Surface

Grid File Name:	E:\Anthropocene Surge\Wien GIS\MA_UNIGIS\Surfer\BK_Daten\BK_A_oA_Amin_inkl_oB_2.grd
Grid Size:	351 rows x 351 columns
X Minimum:	1100
X Maximum:	4600
X Spacing:	10
Y Minimum:	339300
Y Maximum:	342800
Y Spacing:	10
Z Minimum:	148.84349196907
Z Maximum:	274.57139269238

Volumes

Z Scale Factor:	1

Total Volumes by:

Trapezoidal Rule:	40909386.559065
Simpson's Rule:	40943214.835095
Simpson's 3/8 Rule:	40949316.536968

Cut & Fill Volumes

Positive Volume [Cut]:	42032512.759533
Negative Volume [Fill]:	1123126.2004685
Net Volume [Cut-Fill]:	40909386.559064

Areas

Planar Areas

Positive Planar Area [Cut]:	11546282.720964
Negative Planar Area [Fill]:	500367.27903573
NoData Planar Area:	203350
Total Planar Area:	12250000

Surface Areas

Positive Surface Area [Cut]:	11647195.075091
Negative Surface Area [Fill]:	526113.87593687

Grid Volume Computations – Cat. (3)

Mon Feb 10 11:41:52 2020

Upper Surface

Grid File Name:	E:\Anthropocene Surge\Wien GIS\MA_UNIGIS\Surfer\dtm_grid_10m.grd
Grid Size:	351 rows x 351 columns
X Minimum:	1100
X Maximum:	4600
X Spacing:	10
Y Minimum:	339300
Y Maximum:	342800
Y Spacing:	10
Z Minimum:	155.50675582858
Z Maximum:	203.93125152586

Lower Surface

Grid File Name:	E:\Anthropocene Surge\Wien GIS\MA_UNIGIS\Surfer\BK_Daten\BK_A_oA_exkl_oB_3.grd
Grid Size:	351 rows x 351 columns
X Minimum:	1100
X Maximum:	4600
X Spacing:	10
Y Minimum:	339300
Y Maximum:	342800
Y Spacing:	10
Z Minimum:	149.0860957365
Z Maximum:	273.86660041672

Volumes

Z Scale Factor:	1

Total Volumes by:

Trapezoidal Rule:	44892171.878695
Simpson's Rule:	44929979.151089
Simpson's 3/8 Rule:	44936117.980617

Cut & Fill Volumes

Positive Volume [Cut]:	45834166.737929
Negative Volume [Fill]:	941994.85923391
Net Volume [Cut-Fill]:	44892171.878695

Areas

Planar Areas

Positive Planar Area [Cut]:	11597250.00895
Negative Planar Area [Fill]:	442299.99105036
NoData Planar Area:	210450
Total Planar Area:	12250000

Surface Areas

Positive Surface Area [Cut]:	11685548.744003
Negative Surface Area [Fill]:	466633.95701772

Grid Volume Computations – Cat. (4)

Mon Feb 10 11:42:31 2020

Upper Surface

Grid File Name:	E:\Anthropocene Surge\Wien GIS\MA_UNIGIS\Surfer\dtm_grid_10m.grd
Grid Size:	351 rows x 351 columns
X Minimum:	1100
X Maximum:	4600
X Spacing:	10
Y Minimum:	339300
Y Maximum:	342800
Y Spacing:	10
Z Minimum:	155.50675582858
Z Maximum:	203.93125152586

Lower Surface

Grid File Name:	E:\Anthropocene Surge\Wien GIS\MA_UNIGIS\Surfer\BK_Daten\BK_A_oA_inkl_oB_4.grd
Grid Size:	351 rows x 351 columns
X Minimum:	1100
X Maximum:	4600
X Spacing:	10
Y Minimum:	339300
Y Maximum:	342800
Y Spacing:	10
Z Minimum:	149.0860957365
Z Maximum:	273.86660041672

Volumes

Z Scale Factor:	1

Total Volumes by:

Trapezoidal Rule:	45172451.46664
Simpson's Rule:	45210059.420929
Simpson's 3/8 Rule:	45216739.263105

Cut & Fill Volumes

Positive Volume [Cut]:	46109656.12905
Negative Volume [Fill]:	937204.6624103
Net Volume [Cut-Fill]:	45172451.466639

Areas

Planar Areas

Positive Planar Area [Cut]:	11603177.724297
Negative Planar Area [Fill]:	436372.27570254
NoData Planar Area:	210450
Total Planar Area:	12250000

Surface Areas

Positive Surface Area [Cut]:	11691829.423285
Negative Surface Area [Fill]:	460652.52703166

11. Appendix B: Grid volume computations using kriging grids

Grid Volume Computations – Cat. (3a)

Fri Feb 21 10:43:42 2020

Upper Surface

Grid File Name:	E:\Anthropocene Surge\Wien GIS\MA_UNIGIS\Surfer\dtm_grid_10m.grd
Grid Size:	351 rows x 351 columns
X Minimum:	1100
X Maximum:	4600
X Spacing:	10
Y Minimum:	339300
Y Maximum:	342800
Y Spacing:	10
Z Minimum:	155.50675582858
Z Maximum:	203.93125152586

Lower Surface

Grid File Name:	E:\Anthropocene Surge\Wien GIS\MA_UNIGIS\Surfer\tests_2020_02_18\nes2_400_65.grd
Grid Size:	351 rows x 351 columns
X Minimum:	1100
X Maximum:	4600
X Spacing:	10
Y Minimum:	339300
Y Maximum:	342800
Y Spacing:	10
Z Minimum:	151.33824932969
Z Maximum:	201.92960705127

Volumes

Z Scale Factor:	1

Total Volumes by:

Trapezoidal Rule:	46176600.54664
Simpson's Rule:	46200903.310639
Simpson's 3/8 Rule:	46207494.931694

Cut & Fill Volumes

Positive Volume [Cut]:	46521915.309894
Negative Volume [Fill]:	345350.43942655
Net Volume [Cut-Fill]:	46176564.870468

Areas

Planar Areas

Positive Planar Area [Cut]:	11856004.949372
Negative Planar Area [Fill]:	324095.05062778
NoData Planar Area:	69900
Total Planar Area:	12250000

Surface Areas

Positive Surface Area [Cut]:	11911530.658846
Negative Surface Area [Fill]:	327910.31763561

Grid Volume Computations – Cat. (3b)

Fri Feb 21 10:47:09 2020

Upper Surface

Grid File Name:	E:\Anthropocene Surge\Wien GIS\MA_UNIGIS\Surfer\dtm_grid_10m.grd
Grid Size:	351 rows x 351 columns
X Minimum:	1100
X Maximum:	4600
X Spacing:	10
Y Minimum:	339300
Y Maximum:	342800
Y Spacing:	10
Z Minimum:	155.50675582858
Z Maximum:	203.93125152586

Lower Surface

Grid File Name:	E:\Anthropocene Surge\Wien GIS\MA_UNIGIS\Surfer\2020_02_20\Bk3_u_Arch.grd
Grid Size:	351 rows x 351 columns
X Minimum:	1100
X Maximum:	4600
X Spacing:	10
Y Minimum:	339300
Y Maximum:	342800
Y Spacing:	10
Z Minimum:	151.33824932948
Z Maximum:	201.92960705127

Volumes

Z Scale Factor:	1

Total Volumes by:

Trapezoidal Rule:	45219897.134196
Simpson's Rule:	45241590.959432
Simpson's 3/8 Rule:	45251980.803237

Cut & Fill Volumes

Positive Volume [Cut]:	45572392.785318
Negative Volume [Fill]:	352531.32729564
Net Volume [Cut-Fill]:	45219861.458023

Areas

Planar Areas

Positive Planar Area [Cut]:	11851148.576254
Negative Planar Area [Fill]:	328951.42374624
NoData Planar Area:	69900
Total Planar Area:	12250000

Surface Areas

Positive Surface Area [Cut]:	11910809.014377
Negative Surface Area [Fill]:	332993.23571561

Grid Volume Computations – Cat. (3c)

Fri Feb 21 10:49:16 2020

Upper Surface

Grid File Name:	E:\Anthropocene Surge\Wien GIS\MA_UNIGIS\Surfer\dtm_grid_10m.grd
Grid Size:	351 rows x 351 columns
X Minimum:	1100
X Maximum:	4600
X Spacing:	10
Y Minimum:	339300
Y Maximum:	342800
Y Spacing:	10
Z Minimum:	155.50675582858
Z Maximum:	203.93125152586

Lower Surface

Grid File Name:	E:\Anthropocene Surge\Wien GIS\MA_UNIGIS\Surfer\2020_02_20\Bk3_u_Amin.grd
Grid Size:	351 rows x 351 columns
X Minimum:	1100
X Maximum:	4600
X Spacing:	10
Y Minimum:	339300
Y Maximum:	342800
Y Spacing:	10
Z Minimum:	151.2485779969
Z Maximum:	201.82640758829

Volumes

Z Scale Factor:	1

Total Volumes by:

Trapezoidal Rule:	47182806.510878
Simpson's Rule:	47214937.802382
Simpson's 3/8 Rule:	47221527.113512

Cut & Fill Volumes

Positive Volume [Cut]:	47509093.072781
Negative Volume [Fill]:	326322.23807726
Net Volume [Cut-Fill]:	47182770.834704

Areas

Planar Areas

Positive Planar Area [Cut]:	11876464.173049
Negative Planar Area [Fill]:	303635.82695092
NoData Planar Area:	69900
Total Planar Area:	12250000

Surface Areas

Positive Surface Area [Cut]:	11932842.367336
Negative Surface Area [Fill]:	307191.96400922

Grid Volume Computations – Cat. (3d)

Fri Feb 21 10:51:34 2020

Upper Surface

Grid File Name:	E:\Anthropocene Surge\Wien GIS\MA_UNIGIS\Surfer\dtm_grid_10m.grd
Grid Size:	351 rows x 351 columns
X Minimum:	1100
X Maximum:	4600
X Spacing:	10
Y Minimum:	339300
Y Maximum:	342800
Y Spacing:	10
Z Minimum:	155.50675582858
Z Maximum:	203.93125152586

Lower Surface

Grid File Name:	E:\Anthropocene Surge\Wien GIS\MA_UNIGIS\Surfer\2020_02_20\Bk3Arch_u_Amin.grd
Grid Size:	351 rows x 351 columns
X Minimum:	1100
X Maximum:	4600
X Spacing:	10
Y Minimum:	339300
Y Maximum:	342800
Y Spacing:	10
Z Minimum:	151.24857799709
Z Maximum:	201.82640758829

Volumes

Z Scale Factor:	1

Total Volumes by:

Trapezoidal Rule:	46185408.11639
Simpson's Rule:	46215215.44768
Simpson's 3/8 Rule:	46225642.649831

Cut & Fill Volumes

Positive Volume [Cut]:	46515407.261267
Negative Volume [Fill]:	330034.82105044
Net Volume [Cut-Fill]:	46185372.440217

Areas

Planar Areas

Positive Planar Area [Cut]:	11873167.691286
Negative Planar Area [Fill]:	306932.30871358
NoData Planar Area:	69900
Total Planar Area:	12250000

Surface Areas

Positive Surface Area [Cut]:	11933877.222201
Negative Surface Area [Fill]:	310624.53936787

Grid Volume Computations – Cat. (4a)

Fri Feb 21 10:54:13 2020

Upper Surface

Grid File Name:	E:\Anthropocene Surge\Wien GIS\MA_UNIGIS\Surfer\dtm_grid_10m.grd
Grid Size:	351 rows x 351 columns
X Minimum:	1100
X Maximum:	4600
X Spacing:	10
Y Minimum:	339300
Y Maximum:	342800
Y Spacing:	10
Z Minimum:	155.50675582858
Z Maximum:	203.93125152586

Lower Surface

Grid File Name:	E:\Anthropocene Surge\Wien GIS\MA_UNIGIS\Surfer\2020_02_20\Bk4.grd
Grid Size:	351 rows x 351 columns
X Minimum:	1100
X Maximum:	4600
X Spacing:	10
Y Minimum:	339300
Y Maximum:	342800
Y Spacing:	10
Z Minimum:	151.33824932964
Z Maximum:	201.92960705127

Volumes

Z Scale Factor:	1

Total Volumes by:

Trapezoidal Rule:	46489689.442725
Simpson's Rule:	46513606.999317
Simpson's 3/8 Rule:	46520509.935137

Cut & Fill Volumes

Positive Volume [Cut]:	46834396.984899
Negative Volume [Fill]:	344743.21834684
Net Volume [Cut-Fill]:	46489653.766552

Areas

Planar Areas

Positive Planar Area [Cut]:	11859028.156817
Negative Planar Area [Fill]:	321071.84318283
NoData Planar Area:	69900
Total Planar Area:	12250000

Surface Areas

Positive Surface Area [Cut]:	11914638.908706
Negative Surface Area [Fill]:	324849.08512579

Grid Volume Computations – Cat. (4b)

Fri Feb 21 10:56:47 2020

Upper Surface

Grid File Name:	E:\Anthropocene Surge\Wien GIS\MA_UNIGIS\Surfer\dtm_grid_10m.grd
Grid Size:	351 rows x 351 columns
X Minimum:	1100
X Maximum:	4600
X Spacing:	10
Y Minimum:	339300
Y Maximum:	342800
Y Spacing:	10
Z Minimum:	155.50675582858
Z Maximum:	203.93125152586

Lower Surface

Grid File Name:	E:\Anthropocene Surge\Wien GIS\MA_UNIGIS\Surfer\2020_02_20\Bk4_u_Arch.grd
Grid Size:	351 rows x 351 columns
X Minimum:	1100
X Maximum:	4600
X Spacing:	10
Y Minimum:	339300
Y Maximum:	342800
Y Spacing:	10
Z Minimum:	151.33824932947
Z Maximum:	201.92960705127

Volumes

Z Scale Factor:	1

Total Volumes by:

Trapezoidal Rule:	45523263.584132
Simpson's Rule:	45544954.917746
Simpson's 3/8 Rule:	45555282.130894

Cut & Fill Volumes

Positive Volume [Cut]:	45875309.234961
Negative Volume [Fill]:	352081.3270024
Net Volume [Cut-Fill]:	45523227.907959

Areas

Planar Areas

Positive Planar Area [Cut]:	11854167.193746
Negative Planar Area [Fill]:	325932.8062543
NoData Planar Area:	69900
Total Planar Area:	12250000

Surface Areas

Positive Surface Area [Cut]:	11913925.711606
Negative Surface Area [Fill]:	329936.33534931

Grid Volume Computations – Cat. (4c)

Fri Feb 21 10:59:26 2020

Upper Surface

Grid File Name:	E:\Anthropocene Surge\Wien GIS\MA_UNIGIS\Surfer\dtm_grid_10m.grd
Grid Size:	351 rows x 351 columns
X Minimum:	1100
X Maximum:	4600
X Spacing:	10
Y Minimum:	339300
Y Maximum:	342800
Y Spacing:	10
Z Minimum:	155.50675582858
Z Maximum:	203.93125152586

Lower Surface

Grid File Name:	E:\Anthropocene Surge\Wien GIS\MA_UNIGIS\Surfer\2020_02_20\Bk4_u_Amin.grd
Grid Size:	351 rows x 351 columns
X Minimum:	1100
X Maximum:	4600
X Spacing:	10
Y Minimum:	339300
Y Maximum:	342800
Y Spacing:	10
Z Minimum:	151.24807284736
Z Maximum:	201.82640758829

Volumes

Z Scale Factor:	1

Total Volumes by:

Trapezoidal Rule:	47495678.594762
Simpson's Rule:	47527355.821274
Simpson's 3/8 Rule:	47534354.969898

Cut & Fill Volumes

Positive Volume [Cut]:	47820791.220298
Negative Volume [Fill]:	325148.30170849
Net Volume [Cut-Fill]:	47495642.918589

Areas

Planar Areas

Positive Planar Area [Cut]:	11878563.180436
Negative Planar Area [Fill]:	301536.8195636
NoData Planar Area:	69900
Total Planar Area:	12250000

Surface Areas

Positive Surface Area [Cut]:	11935089.954863
Negative Surface Area [Fill]:	305060.88274997

Grid Volume Computations – Cat. (4d)

Fri Feb 21 11:01:19 2020

Upper Surface

Grid File Name:	E:\Anthropocene Surge\Wien GIS\MA_UNIGIS\Surfer\dtm_grid_10m.grd
Grid Size:	351 rows x 351 columns
X Minimum:	1100
X Maximum:	4600
X Spacing:	10
Y Minimum:	339300
Y Maximum:	342800
Y Spacing:	10
Z Minimum:	155.50675582858
Z Maximum:	203.93125152586

Lower Surface

Grid File Name:	E:\Anthropocene Surge\Wien GIS\MA_UNIGIS\Surfer\2020_02_20\Bk4Arch_u_Amin.grd
Grid Size:	351 rows x 351 columns
X Minimum:	1100
X Maximum:	4600
X Spacing:	10
Y Minimum:	339300
Y Maximum:	342800
Y Spacing:	10
Z Minimum:	151.24807284768
Z Maximum:	201.82640758829

Volumes

Z Scale Factor:	1

Total Volumes by:

Trapezoidal Rule:	46488900.035822
Simpson's Rule:	46518576.969047
Simpson's 3/8 Rule:	46529156.206135

Cut & Fill Volumes

Positive Volume [Cut]:	46817751.379269
Negative Volume [Fill]:	328887.01961997
Net Volume [Cut-Fill]:	46488864.359649

Areas

Planar Areas

Positive Planar Area [Cut]:	11875336.96952
Negative Planar Area [Fill]:	304763.03047951
NoData Planar Area:	69900
Total Planar Area:	12250000

Surface Areas

Positive Surface Area [Cut]:	11936210.610783
Negative Surface Area [Fill]:	308423.0683697

12. Appendix C: Cross validation reports

Cross Validation Report – Gaussian variogram

Wed Feb 19 15:32:43 2020

Data Source

Source Data File Name:	E:\Anthropocene Surge\Wien GIS\MA_UNIGIS\Deskriptive Statistik\Aufbereitung Daten\Ergebnis\doppelte Koordinaten\BK_A_oA_exkl_oB_oD_.csv
X Column:	C
Y Column:	B
Z Column:	G

Gridding Rules

Gridding Method:	Kriging
Kriging Type:	Point
Polynomial Drift Order:	1
Kriging std. deviation grid:	no

Semi-Variogram Model

Component Type:	Nugget Effect
Error Variance:	3.1
Micro Variance:	0
Component Type:	Gaussian
Anisotropy Angle:	30
Anisotropy Length:	800
Anisotropy Ratio:	3
Variogram Partial Sill:	46

Search Parameters

Search Ellipse Radius #1:	400
Search Ellipse Radius #2:	400
Search Ellipse Angle:	0
Number of Search Sectors:	1
Maximum Data Per Sector:	65
Maximum Empty Sectors:	1
Minimum Data:	8
Maximum Data:	65

Data Counts at Validation Points

Active Results:	8683
NoData Results:	0
Attempted Results:	8683
Requested Results:	8683

Univariate Statistics

	X	Y	Z
Count:	8683	8683	8683
1%-tile:	1160	339368.09	153.18
5%-tile:	1376.9	339606	156.86
10%-tile:	1455.49	339838	158.16
25%-tile:	1649.63	340339.2	159.47
50%-tile:	2794	341002	167.48
75%-tile:	3669.53	341862	181.08
90%-tile:	4207.31	342308.47	191.99
95%-tile:	4408	342417	194.81
99%-tile:	4557	342693	197.99

Minimum:	1100	339300.07	148.53
Maximum:	4600	342800	201.6
Mean:	2729.27625936	341066.474987	170.865904641
Median:	2794	341002	167.48
Geometric Mean:	2511.04595258	341065.253949	170.391770714
Harmonic Mean:	2300.01071575	341064.032901	169.93192037
Root Mean Square:	2929.4384946	341067.696008	171.353038249
Trim Mean (10%):	2713.40795751	341072.256676	170.307764269
Interquartile Mean:	2669.81028558	341049.81298	167.781292031
Midrange:	2850	341050.035	175.065
Winsorized Mean:	2722.40755269	341076.683654	170.735776805
TriMean:	2726.79	341051.3	168.8775
Variance:	1132791.4546	832996.486017	166.725549801
Standard Deviation:	1064.3267612	912.686411653	12.9122248199
Interquartile Range:	2019.9	1522.8	21.61
Range:	3500	3499.93	53.07
Mean Difference:	1215.64962246	1051.5341511	14.3787973821
Median Abs. Deviation:	1047.97	746	8.48
Average Abs. Deviation:	962.926149948	773.677462858	10.807830243
Quartile Dispersion:	0.37974041014	0.00223218604717	0.0634561738364
Relative Mean Diff.:	0.445410983331	0.00308307684342	0.0841525254102
Standard Error:	11.4219454472	9.79459953873	0.138569030557
Coef. of Variation:	0.389966665173	0.00267597808225	0.0755693468925
Skewness:	0.121473410033	-0.00337582762417	0.641865550132
Kurtosis:	1.55911110465	1.90480826157	2.11311883398
Sum:	23698305.76	2961480202.31	1483628.65
Sum Absolute:	23698305.76	2961480202.31	1483628.65
Sum Squares:	74514118706.6	1.01006884542e+15	254949062.657
Mean Square:	8581609.89366	116327173260	29361.8637173

Univariate Cross-Validation Statistics

	Estimated Z	Residual Z	Data Used
Count:	8683	8683	8683
1%-tile:	155.844698197	-5.04335765596	64
5%-tile:	157.478787959	-3.07553272617	64
10%-tile:	158.46193842	-2.33922148531	64
25%-tile:	159.377376718	-1.12552522039	64
50%-tile:	167.231846654	-0.0724656053356	64
75%-tile:	181.390778515	1.00439065654	64
90%-tile:	192.28864657	2.50921989354	64
95%-tile:	194.393621208	3.60428181754	64
99%-tile:	197.209875178	6.02125730875	64
Minimum:	149.016894265	-17.6631057345	22
Maximum:	202.099912905	14.4047710698	64
Mean:	170.8806392	0.0147345584883	63.9224922262
Median:	167.231846654	-0.0724656053356	64
Geometric Mean:	170.421035661	N/A	63.9034259598
Harmonic Mean:	169.975828531	N/A	63.8740049133
Root Mean Square:	171.353404457	2.0917521433	63.9356906903
Trim Mean (10%):	170.262057176	-0.0271785512521	64
Interquartile Mean:	167.649605728	-0.0718914802307	64
Midrange:	175.558403585	-1.62916733237	43
Winsorized Mean:	170.750442636	-0.0222712773856	64
TriMean:	168.807962135	-0.0665164436308	64
Variance:	161.815001368	4.37571386213	1.68772601569
Standard Deviation:	12.7206525528	2.09182070506	1.29912509624
Interquartile Range:	22.0134017971	2.12991587692	0
Range:	53.0830186394	32.0678768043	42
Mean Difference:	14.0966768328	2.22008671118	0.154530894052
Median Abs. Deviation:	8.21661526579	1.06681817323	0
Average Abs. Deviation:	10.6125584109	1.49166650469	0.0775077738109
Quartile Dispersion:	0.0645993513746	N/A	0
Relative Mean Diff.:	0.0824942889894	N/A	0.00241747292182

Standard Error:	0.136513150667	0.0224486152651	0.0139417108724
Coef. of Variation:	0.0744417425657	N/A	0.0203234425161
Skewness:	0.67006011402	0.353452457797	-19.9657846841
Kurtosis:	2.09048985464	6.76138559626	459.196211652
Sum:	1483756.59017	127.940171354	555039
Sum Absolute:	1483756.59017	12966.7500417	555039
Sum Squares:	254950152.387	37991.832893	35494129
Mean Square:	29361.9892188	4.37542702902	4087.77254405

Most under-estimated data:

X = 3177 Y = 340737 Z = 166.68

E = 149.01689426547 ID = 2331

Most over-estimated data:

X = 1117 Y = 342500 Z = 180.68

E = 195.08477106979 ID = 3167

Residual Regression at Validation Points: R = AX+BY+C

Fitted Parameters

	A	B	C
Parameter Value:	2.08986931002e-06	1.6739291507e-05	-5.70018042027
Standard Error:	2.19011893863e-05	2.55400120658e-05	8.69499151445

Inter-Parameter Correlations

	A	B	C
A:	1.000	-0.269	0.262
B:	-0.269	1.000	-1.000
C:	0.262	-1.000	1.000

ANOVA Table

Source	df	Sum of Squares	Mean Square	F
Regression:	2 0.254548601066	2.22804629229	1.11402314614	
Residual:	8680	37987.7197047	4.37646540377	
Total:	8682	37989.947751		

Coefficient of Multiple Determination (R^2): 5.86483115715e-05

Inter-Variable Correlation at Validation Points

	X	Y	Z	Estimated Z	Residual Z
X:	1.000	0.269	-0.799	-0.811	0.003
Y:	0.269	1.000	-0.454	-0.460	0.008
Z:	-0.799	-0.454	1.000	0.987	-0.172
E:	-0.811	-0.460	0.987	1.000	-0.010
R:	0.003	0.008	-0.172	-0.010	1.000

Rank Correlation at Validation Points

	X	Y	Z	Estimated Z	Residual Z
X:	1.000	0.273	-0.787	-0.807	0.003
Y:	0.273	1.000	-0.503	-0.517	0.014
Z:	-0.787	-0.503	1.000	0.962	-0.222
E:	-0.807	-0.517	0.962	1.000	-0.018
R:	0.003	0.014	-0.222	-0.018	1.000

Cross Validation Report – Nested variogram

Wed Feb 19 15:34:06 2020

Data Source

Source Data File Name: E:\Anthropocene Surge\Wien GIS\MA_UNIGIS\Deskriptive Statistik\Aufbereitung Daten\Ergebnis\doppelte Koordinaten\BK_A_oA_exkl_oB_oD_.csv
X Column: C
Y Column: B
Z Column: G

Gridding Rules

Gridding Method: Kriging
Kriging Type: Point

Polynomial Drift Order: 1
Kriging std. deviation grid: no

Semi-Variogram Model
Component Type: Nugget Effect
Error Variance: 1
Micro Variance: 0

Component Type: Gaussian
Anisotropy Angle: 30
Anisotropy Length: 440
Anisotropy Ratio: 1.5
Variogram Partial Sill: 15

Component Type: Spherical
Anisotropy Angle: 30
Anisotropy Length: 1350
Anisotropy Ratio: 1.5
Variogram Partial Sill: 42

Search Parameters
Search Ellipse Radius #1: 400
Search Ellipse Radius #2: 400
Search Ellipse Angle: 0

Number of Search Sectors: 1
Maximum Data Per Sector: 65
Maximum Empty Sectors: 1

Minimum Data: 8
Maximum Data: 65

Data Counts at Validation Points

Active Results: 8683
NoData Results: 0
Attempted Results: 8683
Requested Results: 8683

Univariate Statistics

	X	Y	Z
Count:	8683	8683	8683
1%-tile:	1160	339368.09	153.18
5%-tile:	1376.9	339606	156.86
10%-tile:	1455.49	339838	158.16
25%-tile:	1649.63	340339.2	159.47
50%-tile:	2794	341002	167.48
75%-tile:	3669.53	341862	181.08
90%-tile:	4207.31	342308.47	191.99
95%-tile:	4408	342417	194.81
99%-tile:	4557	342693	197.99

Minimum:	1100	339300.07	148.53
Maximum:	4600	342800	201.6
Mean:	2729.27625936	341066.474987	170.865904641
Median:	2794	341002	167.48
Geometric Mean:	2511.04595258	341065.253949	170.391770714
Harmonic Mean:	2300.01071575	341064.032901	169.93192037
Root Mean Square:	2929.4384946	341067.696008	171.353038249
Trim Mean (10%):	2713.40795751	341072.256676	170.307764269
Interquartile Mean:	2669.81028558	341049.81298	167.781292031
Midrange:	2850	341050.035	175.065
Winsorized Mean:	2722.40755269	341076.683654	170.735776805
TriMean:	2726.79	341051.3	168.8775
Variance:	1132791.4546	832996.486017	166.725549801
Standard Deviation:	1064.3267612	912.686411653	12.9122248199
Interquartile Range:	2019.9	1522.8	21.61
Range:	3500	3499.93	53.07
Mean Difference:	1215.64962246	1051.5341511	14.3787973821
Median Abs. Deviation:	1047.97	746	8.48
Average Abs. Deviation:	962.926149948	773.677462858	10.807830243
Quartile Dispersion:	0.37974041014	0.00223218604717	0.0634561738364
Relative Mean Diff.:	0.445410983331	0.00308307684342	0.0841525254102
Standard Error:	11.4219454472	9.79459953873	0.138569030557
Coef. of Variation:	0.389966665173	0.00267597808225	0.0755693468925
Skewness:	0.121473410033	-0.00337582762417	0.641865550132
Kurtosis:	1.55911110465	1.90480826157	2.11311883398
Sum:	23698305.76	2961480202.31	1483628.65
Sum Absolute:	23698305.76	2961480202.31	1483628.65
Sum Squares:	74514118706.6	1.01006884542e+15	254949062.657
Mean Square:	8581609.89366	116327173260	29361.8637173

Univariate Cross-Validation Statistics

	Estimated Z	Residual Z	Data Used
Count:	8683	8683	8683
1%-tile:	154.865732645	-4.94252795294	64
5%-tile:	157.179626822	-2.91181942679	64
10%-tile:	158.374691025	-2.01668341198	64
25%-tile:	159.420530764	-0.860790075779	64
50%-tile:	167.409356088	-0.0349328600747	64
75%-tile:	181.342348805	0.786843194578	64
90%-tile:	192.154026026	1.97941262873	64
95%-tile:	194.535706644	3.0412440975	64
99%-tile:	197.494822984	5.52407949419	64
Minimum:	151.859326266	-12.8467141232	22
Maximum:	200.907744568	15.739512163	64
Mean:	170.859299757	-0.00660488419339	63.9224922262
Median:	167.409356088	-0.0349328600747	64
Geometric Mean:	170.394189252	N/A	63.9034259598
Harmonic Mean:	169.943445579	N/A	63.8740049133
Root Mean Square:	171.337517016	1.84940341231	63.9356906903
Trim Mean (10%):	170.273801833	-0.0280430108657	64
Interquartile Mean:	167.673521205	-0.0315373714664	64
Midrange:	176.383535417	1.44639901987	43
Winsorized Mean:	170.741938935	-0.0306296713704	64
TriMean:	168.895397936	-0.0359531503378	64
Variance:	163.663272289	3.42064330414	1.68772601569
Standard Deviation:	12.7930947112	1.84949812223	1.29912509624
Interquartile Range:	21.9218180404	1.64763327036	0
Range:	49.0484183024	28.5862262862	42
Mean Difference:	14.2048296695	1.91258740385	0.154530894052
Median Abs. Deviation:	8.34317592625	0.824439706108	0
Average Abs. Deviation:	10.6947996908	1.26095831985	0.0775077738109
Quartile Dispersion:	0.0643315905421	N/A	0
Relative Mean Diff.:	0.0831375856609	N/A	0.00241747292182

Standard Error:	0.137290572049	0.0198481025066	0.0139417108724
Coef. of Variation:	0.0748750271678	N/A	0.0203234425161
Skewness:	0.659023703874	0.343836504641	-19.9657846841
Kurtosis:	2.09314113851	8.05420767419	459.196211652
Sum:	1483571.29979	-57.3502094512	555039
Sum Absolute:	1483571.29979	10953.0096899	555039
Sum Squares:	254902877.952	29698.4039581	35494129
Mean Square:	29356.5447371	3.42029298147	4087.77254405

Most under-estimated data:
X = 2386 Y = 341863 Z = 172.98
E = 160.13328587678 ID = 3092

Most over-estimated data:
X = 2393 Y = 341408 Z = 157.18
E = 172.91951216296 ID = 2649

Residual Regression at Validation Points: R = AX+BY+C

Fitted Parameters

	A	B	C
Parameter Value:	4.77516134803e-06	1.25573818401e-06	-0.447927814621
Standard Error:	1.93645741944e-05	2.25819452017e-05	7.68792988049

Inter-Parameter Correlations

	A	B	C
A:	1.000	-0.269	0.262
B:	-0.269	1.000	-1.000
C:	0.262	-1.000	1.000

ANOVA Table

Source	df	Sum of Squares	Mean Square	F
Regression:	2 0.038412994919	0.26285253292	0.13142626646	
Residual:	8680	29697.762314	3.42140118825	
Total:	8682	29698.0251666		

Coefficient of Multiple Determination (R^2): 8.85084215015e-06

Inter-Variable Correlation at Validation Points

	X	Y	Z	Estimated Z	Residual Z
X:	1.000	0.269	-0.799	-0.806	0.003
Y:	0.269	1.000	-0.454	-0.458	0.001
Z:	-0.799	-0.454	1.000	0.990	-0.136
E:	-0.806	-0.458	0.990	1.000	0.008
R:	0.003	0.001	-0.136	0.008	1.000

Rank Correlation at Validation Points

	X	Y	Z	Estimated Z	Residual Z
X:	1.000	0.273	-0.787	-0.798	-0.001
Y:	0.273	1.000	-0.503	-0.515	-0.002
Z:	-0.787	-0.503	1.000	0.969	-0.173
E:	-0.798	-0.515	0.969	1.000	0.010
R:	-0.001	-0.002	-0.173	0.010	1.000